THE DISRUPTION OF UNSTIRRED LAYERS IN VITRO AND ITS IMPACT ON THE DEVELOPMENT AND MAINTENANCE OF 3D SKIN MODELS

PANGILINAN, NEIL,DOMINIC,TAYAG

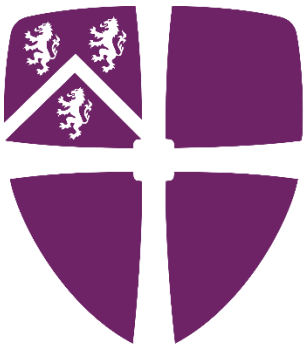

Durham University

DEPARTMENT OF BIOSCIENCES

THE DISRUPTION OF UNSTIRRED LAYERS *IN VITRO* AND ITS IMPACT ON THE DEVELOPMENT AND MAINTENANCE OF 3D SKIN MODELS

NEIL DOMINIC TAYAG PANGILINAN

A thesis submitted for the degree of MSc (By Research)

2022

Abstract

Full thickness skin models, generated *in vitro,* are now a common alternative to *ex vivo* human skin and animal tissue for testing new active compounds. Although skin models mimic the structure and physiology of both the dermis and epidermis, the culture conditions traditionally lack the dynamic fluid flow associated with vasculature *in vivo.* Additionally, *in vitro* static culture generates an unstirred water layer at the media-cell interface, which limits nutrient diffusion. In this study, I aimed to disrupt these unstirred layers by culturing Alvetex® Scaffold skin models in a dynamic bioreactor and subsequently investigating how model development and maintenance is affected. The results show that the time in which perfusion is introduced causes stark differences in model development. On the one hand, early perfusion leads to poor maturation of dermal models and a lack of stratification in the epidermal compartment of full thickness models. On the other hand, delayed perfusion leads to a thicker fibroblast surface layer and a thicker viable epidermis, indicating enhanced tissue development. In full thickness models cultured with delayed perfusion, proliferation of keratinocytes increased in the first week of culture, while early/mid differentiation was more prominent in the first 3 weeks. The barrier function of the delayed perfused models, as identified using trans-epidermal water loss (TEWL), did not change during model development and maintenance. A speed of 100 rpm was found to be suitable for skin models and increasing the stirrer speed led to greater shear stress, which negatively impacted cell morphology. Although this study was limited by great variability in models and reliance on qualitative analysis of relevant biomarkers, the importance of delaying perfusion as an optimisable factor for improving skin models was highlighted. Future work can be conducted, using a larger sample size, on identifying the precise time and speed of perfusion that would generate significant improvements in model structure, physiology, and function.

Table of Contents

List of Figures

Chapter I: Introduction and Literature Review

Chapter 2: Materials and Methods

Chapter 3: Results

Chapter 4: Discussion

List of Tables

Chapter I: Introduction and Literature Review

Chapter 2: Materials and Methods

Chapter 3: Results

Abbreviations

α-sma Alpha smooth muscle actin

AA Ascorbic acid

ALI Air-liquid interface

CAD-CAM Computer-aided design/computer-aided manufacturing

CFD Computational fluid dynamics

CO_2 Carbon dioxide

°C Degrees Celsius

DEJ Dermal-epidermal junction

DMEM Dulbecco's Modified Eagle Medium

ECM Extracellular matrix

EGF Epidermal growth factor

FBS Foetal bovine serum

GM-CSF Granulocyte-macrophage colony-stimulating factor

H&E Haematoxylin and Eosin

HDF Human dermal fibroblast

HDFn Human neonatal dermal fibroblasts

HEKn Human neonatal epidermal keratinocytes

HfKC Human foreskin keratinocytes

hEPSC Human epidermal stem cells

HKGS Human keratinocyte growth supplement

HuVEC Human umbilical vein endothelial cells

KGF Keratinocyte growth factor

L Litre

LSGS Low serum growth supplement

MMP Matrix metalloproteinase

M106® Medium 106

ms^{-1} Metres per second

µg Microgram

µL Microlitre

µm Micrometre

mL Millilitre

mM Millimolar

NCS Neonatal calf serum

PBS Phosphate buffered saline

PFA Paraformaldehyde

ROS Reactive oxygen species

RPM Revolutions per minute

SOP Standard operating procedure

TE Trypsin-EDTA

TEER Transepithelial electrical resistance

TEWL Trans-epidermal water loss

TIMP Tissue inhibitors of metalloproteinases

TGF-β Transforming growth factor beta

TN Trypsin neutraliser

Declaration

The work described herein was carried out in the Department of Biosciences at Durham University between October 2020 and September 2021. All of the work is my own, except where specifically stated otherwise. No part has been previously submitted for a degree at this or any other University.

Statement of Copyright

Acknowledgements

Firstly, I would like to give my sincere thanks to Professor Stefan Przyborski for recognising my potential to undertake postgraduate research and enabling me to pursue this opportunity in the first place. As a graduate who was keen to pursue a PhD degree, the Masters by Research opportunity has enabled me to refine my skills and adapt my attitude to an academic research environment. Over the course of the year at Durham University, Professor Przyborski has been a supportive and inspiring supervisor who has always guided me towards the right research direction. The outcome of this study is only made possible by the technology, concepts, and goals which have been strived for by Professor Przyborski himself.

While I was guided by Professor Przyborski at an administrative level, my mentors were the cornerstone for my day-to-day work in the laboratory. I would like to give thanks to both Dr Lydia Costello and Dr Henry Hoyle for always watching over my progress and being proactive in supporting me to reach my goals. The knowledge and experience of both mentors were beneficial in helping me craft my experiments and analyse them efficiently. They demonstrated great availability and were always swift to respond to any queries I had, regardless of whether it was in the lab or remotely. As a post-doctorate and PhD student (at the time), respectively, both mentors expressed qualities that would leave an impact on me, as an aspiring researcher.

Since my project was undertaken during the COVID-19 outbreak, there were also many challenges and limitations that were put in place, based on national regulations. I would like to thank the Przyborski group, as a whole, for taking me in as an additional member of the team and displaying a good team ethic despite the pandemic. Even with room occupancy limits and social distancing measures, the team were unflinching to help and continuously displayed a positive attitude towards working. By including me in lab responsibilities and lab meetings, the team has always made me feel included as a team player.

Lastly, I would like to give my thanks to my family who have been my emotional support during the course. Their words of encouragement and desire for me to have a bright future were the push I needed to succeed in this project.

Chapter I: Introduction and Literature Review

1.1 Introduction

As the largest organ, the skin forms the outermost layer, which covers the body, and is one of the most observable phenotypes of an individual. Therefore, the quality and appearance of skin is a physical aspect, which holds social and psychological value. In particular, the changes in appearance associated with ageing and skin diseases can be damaging (1,2). Research in cosmetics and drugs, which aim to improve skin quality, typically require the use of an appropriate platform for testing new compounds.

Whilst the use of *ex vivo* human and animal tissue has been a traditional approach for preclinical testing, *in vitro* skin models have become more widely used, based on the principles of tissue engineering (3,4). These models can be built from isolated cells using four components: a scaffold, cells, growth factors, and appropriate culture conditions. Skin models typically use 3D cell culture techniques, which mimic the *in vivo* conditions necessary for appropriate cell development, which enables them to be used as an alternative for testing new active compounds; this is possible as structure is a determinant of tissue function (5).

Skin models have been bioengineered successfully in the past using static culture, in which culture medium is replenished periodically during the culture duration. The 3D structure of models grown in static culture, as well as protein expression of relevant biomarkers, have been similar to that of skin (6–9). However, there is interest in developing skin models with an improved morphology, viability, and longevity. A major concern highlighted in previous studies regarding static culture is the development of unstirred layers in culture media, adjacent to the model. These unstirred layers insulate nearby cellular surfaces and slow down the movement of nutrients and waste; acting as a barrier to limit diffusion and exchange (10).

Generation of skin models in dynamic culture, with perfusion, is a potential solution for enhancing *in vitro* tissue development, in terms of structure and maturation. Unlike static culture, the skin models are grown in a dynamic environment whereby unstirred layers are disrupted through the use of a bioreactor. These devices or systems are designed to enable constant flow of media, which maintains an efficient diffusion gradient for nutrient and waste exchange. In more complex bioreactors, parameters impacting tissue health, such as pH and partial pressure of oxygen, can be monitored and controlled. These parameters can be monitored in real-time through the implementation of a feedback system (11). By

incorporating dynamic culture conditions and disrupting unstirred layers in 3D cell culture through the use of bioreactor technology, there is potential for generating skin models with greater resemblance to human skin, and enhanced viability and longevity.

1.2 The anatomy of skin

The skin is a complex multi-layered organ composed of the epidermis, dermis, and hypodermis. The outermost layer in contact with the external environment is the epidermis. This layer is mostly comprised of keratinocytes; however, melanin-producing melanocytes, and Langerhans cells can also be found (12). The epidermis is stratified, comprised of distinct layers: the *stratum basale*, *stratum spinosum*, *stratum granulosum*, *stratum lucidum*, and *stratum corneum*. These layers generate the structure of the epidermis from bottom-to-top respectively and are distinguished by varying keratinocyte morphology. The keratinocytes in each layer reflect a specific stage in differentiation as they migrate upwards through the epidermis; in each layer, the keratinocytes express specific biomarkers pertaining to its relative stage in differentiation (13).

The *stratum basale*, also known as the basal layer, is where basal keratinocytes reside. Basal keratinocytes typically have a round morphology lining the basement membrane at the foot of the epidermis and are highly proliferative (14). As this occurs, keratinocytes migrate to the *stratum spinosum* above, also known as the spinous layer or prickle cell layer. The keratinocytes in this layer are tightly packed and are named prickle cells, due to their "spiny" polyhedral morphology. This characteristic appearance viewed in histology can be attributed to the abundance of desmosomes present, which tightly link each of the prickle cells to another, and the shrinking of keratin filaments within the desmosomes during histological processing (15,16). In the *stratum spinosum*, proliferation is down-regulated, and keratinocytes undergo early differentiation; this is the start of a process called keratinization. A major difference which occurs between the *stratum basale* and the other layers within the epidermis, beginning with the *stratum spinosum*, is the type of keratin filament produced by keratinocytes. In the *stratum basale*, cytokeratins K5, K14, and K15 are produced, whilst in the other layers of the epidermis, cyto-keratins K1 and K10 are produced (17).

Above the *stratum spinosum* is the *stratum granulosum*, also known as the granular layer. The keratinocytes in this layer have a flat irregular morphology and are called granular cells due to the presence of intracellular basophilic lipid-containing keratohyalin granules (18). The keratinocytes in the *stratum granulosum* are in a mid-differentiation state and undergo

preparation for terminal differentiation as they are pushed upwards towards the *stratum corneum*. As the keratinocytes move from the *stratum granulosum* to the *stratum corneum*, they lose their nuclei and cytoplasmic organelles therefore forming fully keratinized corneocytes which reside on the surface of the skin (19). In thicker parts of the skin such as the soles of the feet, there is an additional thin layer present between the *stratum granulosum* and the *stratum corneum* known as the *stratum lucidum*.

Beneath the epidermis is the dermis, which is connected by the dermal-epidermal junction (DEJ). The DEJ, also known as the basement membrane, is a glycoprotein-rich zone which consists of many macromolecules such as fibronectins and laminins; these macromolecules interact with each other to form adhesion complexes between the lower epidermis and upper dermis, keeping the skin intact (20). Unlike the epidermis, the dermis is mostly composed of fibrous and elastic tissue and is vascularised. Furthermore, it is only comprised of two layers: the thin papillary layer and the bulk reticular layer. The papillary layer, in contact with the DEJ, is comprised of loose connective tissue. The abundant presence of capillaries in this layer is responsible for delivering nutrients to the dermis and the epidermis (21). Meanwhile, the reticular layer constitutes the majority of the dermis and is comprised of dense connective tissue. Within the reticular layer, fibroblasts secrete extracellular matrix, primarily collagen-I, collagen-III, and elastin (22,23). The reticular layer is not in contact with the epidermis, and rather, the hypodermis below, which is the deepest part of skin composed of adipose tissue and areolar connective tissue. Like the dermis above, the hypodermis is also vascularised. The three layers of skin are summarised in Figure 1 below, in terms of the types of cells and structures present. The latter are referred to as skin appendages, and have multiple functions relating to sensation, homeostasis, and lubrications; the appendages include nails, sweat glands, and hair-associated structures.

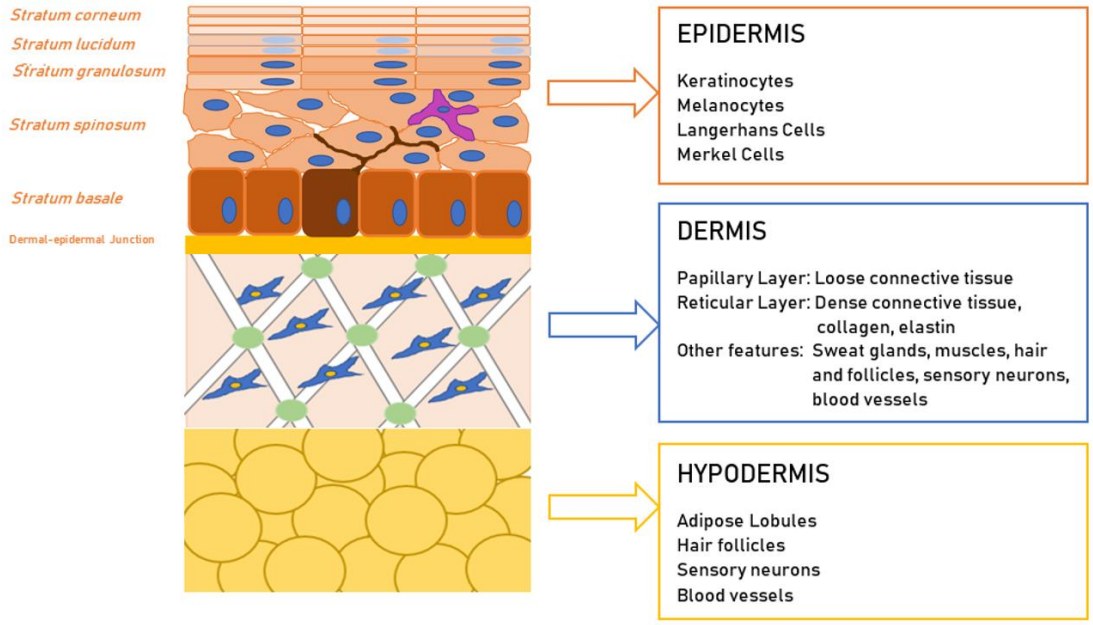

Figure 1: The Epidermis, Dermis and Hypodermis, and their respective constituents.
Adapted from Yousef, Alhajj and Sharma (12)

Whilst the primary function of skin is to be a barrier separating the internal and external environments of the body, each of the three skin layers have specific functions. Firstly, the epidermis has a barrier and regulatory function. The epidermis provides protection against the external environment by forming a physical barrier, which acts as a first line of defence against mechanical, chemical, ionising, and microbial factors. The *stratum corneum* is the major line of defence against each of the above factors as the aforementioned layer of thick keratinized corneocytes are in contact with the external environment where all of these factors can penetrate from. In addition, the epidermis regulates trans-epidermal water loss and is waterproof on the surface (13). The barrier function can also be attributed primarily to the keratohyalin granules in the *stratum granulosum,* which form an insoluble lipid barrier, and to a smaller extent, the desmosomes in the *stratum spinosum* (24). Secondly, the dermis beneath primarily has a support function. As this layer is mostly comprised of fibrous and elastic tissue, it provides strength and flexibility to the skin. Furthermore, as the dermis is vascularised, it plays a role in nutrient delivery and oxygenation of cells within this layer and the overlying avascular epidermis (25). Other roles of the dermis include sensation, and sweat and sebum production; these functions are attributed to the presence of nerve endings and glands, respectively (26). Lastly, the hypodermis has an insulation and structural support function.

1.3 Introduction to 3D cell culture for skin models

3D cell culture can be employed as a technique to produce *in vitro* skin models, which can replicate the multi-layered structure of skin. Traditionally, cell culture is conducted in 2D whereby a monolayer of cells is cultured. Whilst this is useful for fundamental studies in cell biology, it has limited applications for modelling skin as it generates a poor representation of *in vivo* conditions. When cells are cultured in 2D, the morphology of cells is flat as adhesion only occurs at the bottom of a cell culture flask; this can have implications on the structural and physiological behaviour of cells (27,28). 3D cell culture is an approach which mimics the complex 3D environment of cells *in vivo* and enables cells to benefit from multi-directional interactions in 3D, soluble gradients, steric hindrance of spreading, and a lack of imposed polarity (29).

3D cell culture can be conducted using spheroids, hydrogels, or scaffolds. Unlike the latter two, spheroids do not require the use of biomaterials to provide a 3D environment for cells to grow. Spheroids are spherical 3D aggregates of cells formed by the application of forces and, in some cases, the use of non-adhesive cell culture surfaces (30,31). One such technique for spheroid formation is the hanging drop approach which utilises surface tension and gravitational force (32). By stimulating self-assembly of cells into spheroids, 3D structures are created; such structures enable both nutrient delivery and oxygen via perfusion to a certain extent, depending on aggregate size (33).

For skin models, hydrogels and prefabricated scaffolds are used for 3D cell culture instead of spheroids, as a flat multi-layered tissue mimic is required. Hydrogels are the most common scaffold for 3D cell culture and are water-swollen polymeric networks which cells can be encapsulated in. Due to the high water content and the presence of pores, it is possible for hydrogels to mimic the extracellular matrix (ECM) generated by fibroblasts (34,35). Hydrogels are derived from either natural or synthetic materials. On the one hand, naturally-derived hydrogels such as collagen and chitosan generally elicit a better biological response for cell encapsulation purposes, but undesirably express poor mechanical strength and batch-to-batch variation (36,37). On the other hand, synthetic hydrogels such as polyethylene glycol display greater mechanical strength and stability at the slight expense of biocompatibility (38,39). Recent approaches in hydrogel development combine natural and synthetic materials to form organic-inorganic hybrid hydrogels which display both a good biological response and better mechanical properties (40). Whilst hydrogels are suitable 'scaffold' materials for 3D cell culture, hydrogel polymerisation through physical, chemical,

or light-cure approaches may affect cell viability (41,42). Moreover, most hydrogels are animal-derived, thus introducing inter-species differences and, as previously mentioned, batch-to-batch variation (43).

Prefabricated scaffolds are an alternative biomaterial, which are manufactured ready for use to create cultures with a more natural cellular morphology. Design parameters for these scaffolds generally include the biocompatibility of the material, the porosity, the thickness of the scaffold, and the incorporation of necessary nutrients or growth factors within the scaffold (44,45). Several commercial scaffolds exist, including CelluSponge™ and SeedEZ™, which are advertised to improve cell metabolism and growth. For this study, the commercially-available Alvetex® Scaffold is utilised. The Alvetex® Scaffold has a porous structure and is made from polystyrene, a similar material to tissue culture plasticware; this enables cell infiltration and attachment in a 3D environment. Proliferation and growth is facilitated in Alvetex® with improved cell-cell interactions, thereby mimicking the complexity of *in vivo* physiological behaviour and producing more representative tissue constructs. Previous work conducted with Alvetex® has successfully generated various 3D tissue models including skin tissue, airway mucosa, intestinal tissue and a model of neurite outgrowth (6,46,47). In the skin model, fibroblasts proliferate within the Alvetex® Scaffold and synthesise endogenous extracellular matrix (6).

All forms of 3D tissue culture mentioned above display different advantages and limitations. Figure 2 below summarises the options available for 3D cell culture of skin tissues.

Figure 2: The different techniques of 3D cell culture, respective examples, and their advantages and disadvantages. Adapted from Ryu et al., Ravi et al. and Fang and Englen (48–50)

1.4 *in vitro* skin models

Similar to human skin, tissue engineered skin models have a multi-layered structure, which represents the dermis and epidermis. For the dermal layer equivalent, fibroblasts are the primary cell type; whilst for the epidermal layer equivalent, keratinocytes are the primary cell type (51). The fibroblasts and keratinocytes used for skin models can be primary cells acquired from donor tissue, commonly from the human foreskin, or cell lines, such as HaCaT or TERT keratinocytes. Whilst these two cell types form the standard cellular composition of skin models, some studies in the literature have also reported skin models which include additional cell types depending on their specific application. For example, endothelial cells are used for mimicking skin vasculature (52), melanocytes are used for pigmentation studies (53), and adipose tissue is used for developing a hypodermis-like compartment (54).

In skin models, the structures of both layers differ; the epidermis has a differentiated and stratified structure, whereas the dermis has fibroblasts embedded in a matrix largely comprised of collagen (55). Traditionally, the epidermal compartment and the dermal compartment were generated independently as epidermal models and dermal models respectively. However, studies have shown that there is interplay, or "cross-talk", that occurs when fibroblasts and keratinocytes are cultured together which have a beneficial effect for *in vitro* skin models. In particular, the fibroblasts positively influence the viability, proliferation, and differentiation of the keratinocytes (56). Based on this knowledge, there has been interest during the last few decades in growing models which are multi-layered (57). Such models which have both a dermis and epidermis are called full-thickness skin models and require the co-culture of both fibroblasts and keratinocytes (6,55). Protocols for growing full thickness models can vary slightly depending on the scaffold, cell type, culture conditions, and culture time; however, the protocols usually follow the same development process in which a dermis is formed first followed by an epidermal compartment. An example of the process, which utilises Alvetex® Scaffold, is briefly outlined in Figure 3 below.

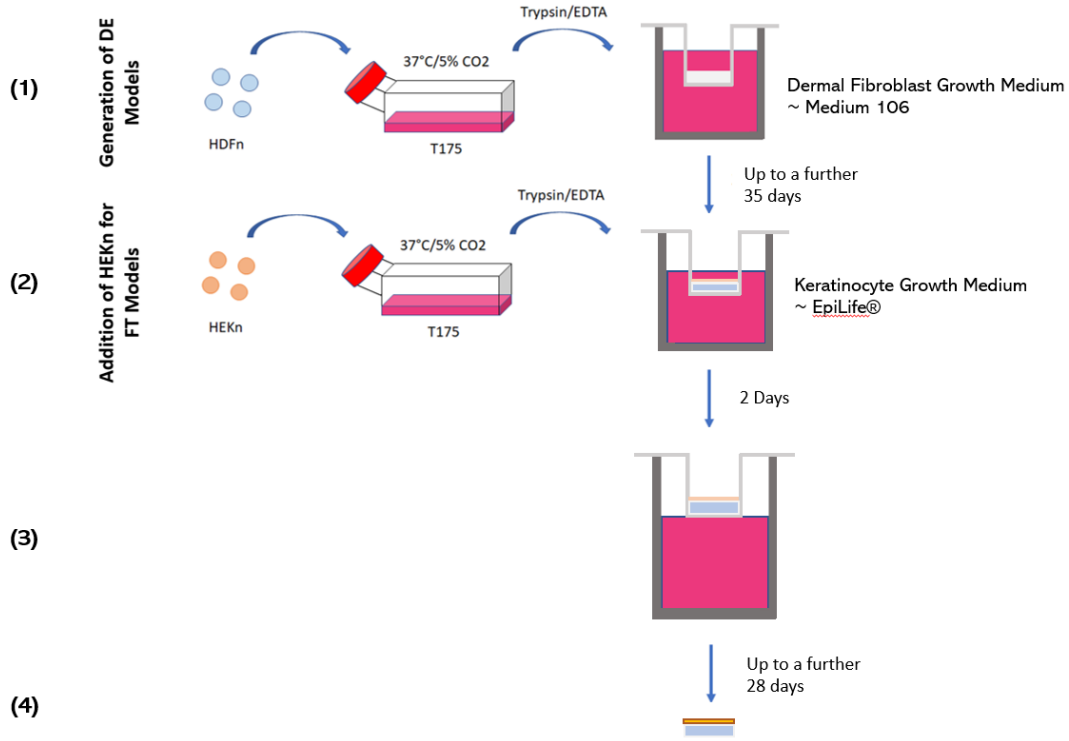

Figure 3: A standard protocol for generating a full thickness skin model using Alvetex®. [1] Fibroblasts are cultured in 2D and subsequently seeded onto Alvetex® scaffold. The model is supplemented with dermal fibroblast growth medium for up to 35 days; [2] Keratinocytes are cultured in 2D and subsequently seeded on top of the dermal compartment. The model is supplemented with keratinocyte growth medium and left in submerged culture for 2 days; [3] Model lifted to air-liquid interface (ALI) for up to 28 days; [4] Full thickness model is harvested for analysis. Adapted from Roger et al. (7)

Protocols for generating multicellular and multi-layered full thickness skin models begin with the generation of the dermal compartment, which is de-epithelialised. To create dermal models, primary fibroblasts or fibroblast cell lines are firstly acquired and cultured in 2D to proliferate. Once a suitable cell density is achieved, these cells are seeded into a scaffold and supplemented with media in submerged culture (7,8,58). The scaffold itself can act as the ECM, which surrounds cells and promotes cell-cell interaction, such as collagen hydrogels; however in some cases, endogenous ECM production can be stimulated by the addition of growth factors and supplements into synthetic scaffolds. One such growth factor is transforming growth factor beta (TGF-β) whose respective signalling pathway *in vivo* is important in healthy skin for ECM deposition. Additionally, TGF-β is usually upregulated *in vivo* within fibrotic skin; it affects fibroblasts by inducing excessive extracellular matrix deposition. Dermal fibroblasts exposed to TGF-β have been reported to express increased collagen-1 and fibronectin levels (59); these are two major proteins found in the extracellular

matrix within the dermis. The addition of TGF-β would therefore be beneficial in generating a mature dermal compartment in a shorter period of time.

Another supplement which is commonly used to improve dermal equivalents is ascorbic acid (AA). Similar to TGF-β, AA upregulates collagen secretion in fibroblasts to give rise to a well-developed extracellular matrix and a mature dermal equivalent. Collagen synthesis can be increased by up to 8-fold when exposing fibroblasts to AA (60), and thus it is essential to collagen formation in skin models.

Dermal models can be generated into full thickness models by subsequently seeding keratinocytes on top of the dermal compartment and producing a co-culture model (7). Unlike the dermal layer, the epidermal layer has a complex, stratified structure illustrated by varying levels of keratinocyte differentiation and keratinisation. Therefore, several considerations have to be made to replicate the epidermis' structure and physiology. Initially, the keratinocytes are subjected to submerged culture using low-calcium conditions to promote keratinocyte proliferation and induce formation of the *stratum basale* above the DEJ. However, after 2-3 days, the model must be raised to air-liquid interface (ALI) culture in high calcium conditions to achieve stratification, observed *in vivo* (61). The change to ALI and the 'calcium switch' also aids in regulating the change in protein expression within the epidermis; the most notable change is from the expression of keratin 5/14, upregulated in the basal layer, to keratin 1/10 upregulated in the suprabasal layer (62,63). This is necessary to produce a model representative of human skin. Calcium can be supplied to the keratinocytes by introducing it as a supplement in the media, along with other growth factors that aid in the development of the epidermal equivalent. The growth factors that can be supplemented include keratinocyte growth factor (KGF) and epidermal growth factor (EGF) which are usually synthesised by fibroblasts *in vivo,* as one of the cross-talk elements between fibroblasts and keratinocytes. On the one hand, KGF can induce hyperproliferation of basal keratinocytes and delay differentiation, which is significant for mediating epidermal growth. This can occur with the risk of crowding in the basal layer therefore leading to elongated basal keratinocytes (64). On the other hand, EGF has no significant effect on keratinocyte growth characteristics and morphology but can accelerate the rate of proliferation (65).

1.5 Nutrient delivery *in vivo* and its implications for *in vitro* models

When developing *in vitro* models, maintenance of cell metabolism is a major determinant for the success of tissue generation. Cells require the uptake of nutrients to respire, proliferate, grow, differentiate, and produce endogenous substances. However, cells must also remove the waste products that form due to cellular processes such as respiration. If the waste products are not expelled, they can accumulate within the cell and increase intracellular toxicity (66–69). The exchange of nutrients and waste therefore determines the viability of the cells in culture.

In 3D culture, the media is able to facilitate the exchange of nutrients and waste. However, in static conditions, the efficiency of exchange decreases over time due to the progressive loss of a diffusion gradient (70,71). This phenomenon is not representative of *in vivo* conditions whereby a specialised transport system exists. In humans, the vascular system and lymphatic system are responsible for the transport of nutrients and removal of waste.

The vascular system facilitates the transport of blood from the heart to different tissues, and vice versa. In skin, vasculature exists within the dermis and the hypodermis and is known as cutaneous vasculature. There are three major vasculature plexuses in skin which can be found from top to bottom: the superficial plexus, the deep plexus, and the subcutaneous plexus (25). The superficial plexus is situated at the top of the reticular layer of the dermis and arising from it are capillaries which extend towards the papillary layer, forming characteristic loops. These loops supply blood to the epidermis and form a large surface area for exchange, thereby improving the delivery of nutrients to keratinocytes and removing waste. Beneath the superficial plexus is the deep plexus which supplies blood exclusively to fibroblasts, hairs, and glands within the dermis. Lastly, the subcutaneous plexus extends from the base of the reticular layer of the dermis to the hypodermis, whereby it delivers blood to underlying adipocytes.

Although most cellular waste is transported away from cells via the veins in the vascular system, some are removed via the lymphatic system. This system is comprised of lymphatic vessels that carry excess fluid which have leaked out from capillaries. Likewise with blood vessels, lymphatic vessels can be found in the dermis and hypodermis. The vessels transport a fluid called lymph which primarily carry waste products and white blood cells and transport them to lymph nodes. Within these nodes, waste is filtered out and fluid is returned to the

vascular system, thereby maintaining fluid levels, and ensuring waste does not return to circulation (72).

The action of transport systems *in vivo* is dynamic as it enables continuous circulation of fluid to and from cells; in other words, the gradients for cellular exchange are maintained (73,74). One approach to mimic the dynamic nature of *in vivo* transport systems for *in vitro* models is to introduce perfusion. The concept of perfusion *in vitro*, is to initiate fluid flow and ensure cells receive the optimum nutrient diffusion rate. Perfusion of media has several functions which enable 3D culture systems to mimic *in vivo* conditions, as shown in Figure 4.

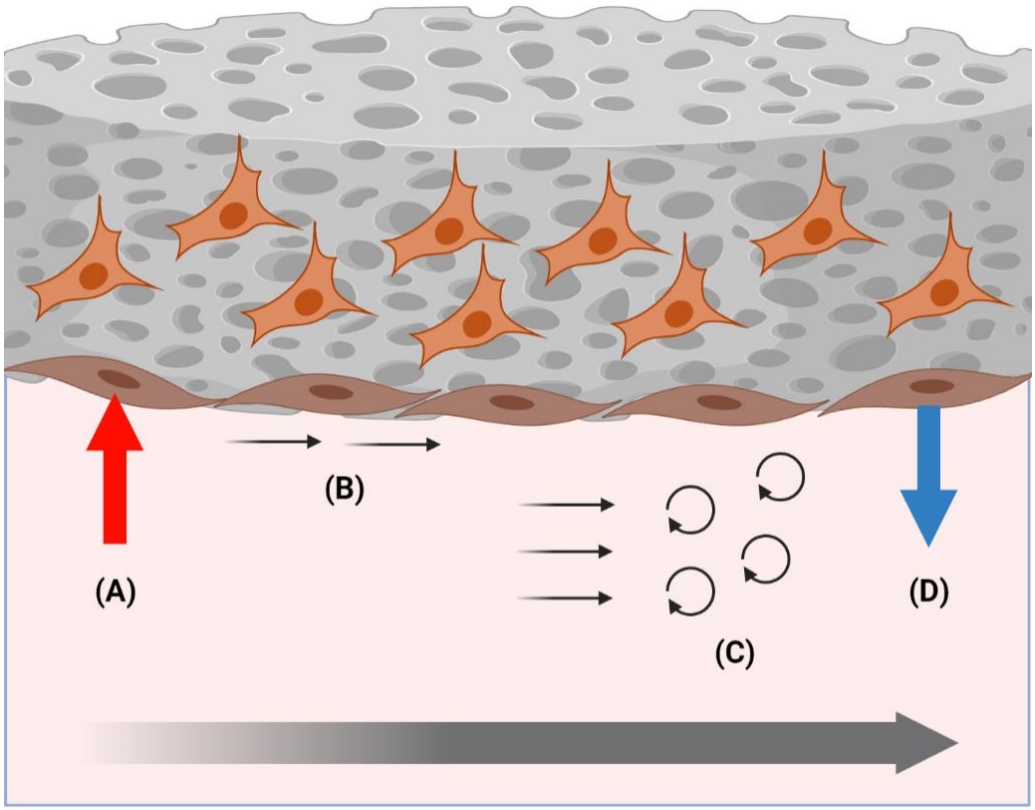

Figure 4: Functions of perfusion *in vitro*. (A) nutrient diffusion gradient into cells; (B) shear stress is a mechanical stimuli for cells; (C) fluid flow disrupts unstirred water layers; and (D) waste diffusion gradient into media

In skin models, it is the fibroblasts in the dermal compartment that are in contact with fluid flow, similar to *in vivo* vasculature. Fluid flow maintains concentration gradients, acts as a mechanical stimuli for fibroblasts, and disrupts unstirred layers in media, as shown in Figure 4 above. First, the dynamic movement of media ensures that fibroblasts are always in contact with fresh media and that waste does not accumulate adjacent to the cells. Second, fibroblasts in contact with the media are subject to mechanical stimuli, as a result of fluid

flow applying shear stress on the cells. The mechanical stimuli invokes physiological changes in fibroblasts which improve proliferation and alignment of secreted collagen (75). Lastly, and most importantly for this study, fluid flow disrupts unstirred layers that form adjacent to fibroblasts.

Unstirred layers are diffusivity barriers which form where mixing speed is not sufficient. This phenomenon is not exclusive to *in vitro* conditions, as it can be found *in vivo* in regions with poor stirring such as the human jejenum (76,77). However, this phenomena is more significant in static conditions where no mixing is observed, with unstirred layer thicknesses reaching at least 40-fold greater than *in vivo* (78). Over time, the thickness of the unstirred layer will continue to increase if sufficient mixing is not applied (79). Contrary to the name, unstirred layers are not stationary but rather express a slow laminar flow that impedes the bulk fluid flow (80). Therefore, concentration gradients can change due to the accumulation of nutrients and waste near this region (81). Due to low permeability, slow diffusivity, and solute accumulation, unstirred layers adjacent to cells are detrimental for 3D cell culture. Currently, there are no studies that investigate the effect of unstirred water layers on *in vitro* skin models.

1.6 The use of bioreactors to introduce perfusion

As static culture brings forth the problem of unstirred layers, there is an emergence in switching to dynamic culture to improve structure and function; this can be achieved using a bioreactor. Bioreactors are vessels or systems that enable cells to be cultured with continuous media flow, in controlled conditions. The use of a bioreactor provides greater control over parameters which may influence the efficiency of 3D cell culture, and the ability to monitor them in real-time. These parameters include mass transfer, oxygenation, and shear stress (82,83).

Within the bioreactor, the rate and direction of fluid flow is essential to regulate as it is a key factor which can impact mass transfer, oxygenation, and shear stress. Mass transfer is the delivery of nutrients and the removal of waste, while oxygenation is the delivery of oxygen to cells within the scaffold. By increasing the flow rate, mass transfer and oxygenation are optimised to improve cell viability (84). This optimisation can be attributed to improved diffusion gradients, and a reduction of unstirred liquid layers close to the cell surface which limit diffusion of oxygen and nutrients (85,86). However, by increasing flow rate, shear stress also increases which can be detrimental to some cells in contact with the media flow (87,88).

Therefore, a simulation of fluid flow is essential for deciding a suitable compromise between improved mass transfer and oxygenation, and low shear stress (83,89).

There are various types of bioreactors, which can be used for full thickness skin models. Bioreactor systems can be generated physically, but in recent years, they can also be designed using computer-aided design/computer-aided manufacturing (CAD-CAM) software, whereby its function can be digitally simulated and tested; this saves cost and time for development (90,91). Bioreactors developed in previous studies have so far been promising, as the culture of skin models within a bioreactor induced differences in epidermal thickness and protein expression in skin models, compared to static culture. The different types of bioreactors are shown in Table 1 below.

Table 1: Types of bioreactors for 3D cell culture. Adapted from Stephenson and Grayson, and Ahmed et al. (92,93).

Type of Bioreactor	Description	Diagram
Pumped Perfusion System	Media is pumped to and from a perfusion platform at a constant flow rate. Media can be recirculated or pumped to a waste reservoir. The platform for the scaffold has an inlet and outlet for media to be pumped across.	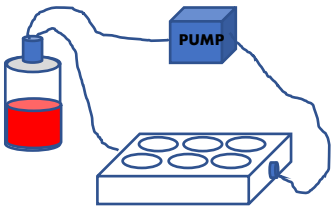
Stirred System	A magnetic stirrer at the bottom of the flask ensures that the culture medium is thoroughly mixed. In other cases, a physical motor-powered stirrer is present. Within these systems, there can either be suspension culture of aggregates, or a 3D scaffold fixed in place	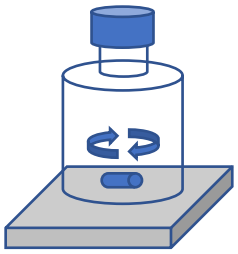
Rotary System	Media is mixed through rotation of a cylindrical flask. Cells in suspension are stimulated to form aggregates, by action of microgravity.	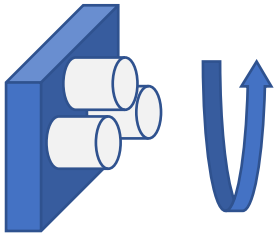

Rocking (Wave) System	A culture vessel containing media is placed on a rocking plate, which moves up and down on either side. Media flow is generated in a wave motion. Cells are either in suspension or seeded onto a scaffold fixed in place within the bag or flask	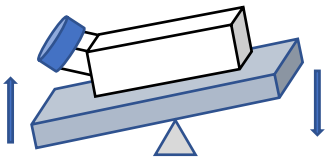
Microfluidic System	A miniaturised pumped perfusion system. Cells are cultured onto a miniature plate and supplemented with media through various channels fabricated within the plate.	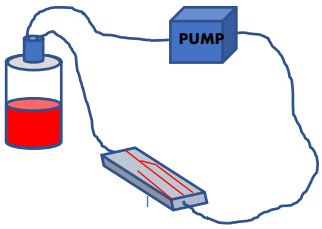

The choice of bioreactor depends on the application, cost, and scale of each study. For cells that require low shear stress, rotary systems are ideal (94). However, it is not ideal for skin models as it does not provide an ALI for improved keratinocyte differentiation (95). For small scale experiments with low installation costs and ease of use, spinner flasks and rocking systems are preferred (96). Whilst these systems provide good control of fluid flow direction, these systems are not preferred in complex tissue models which require intricate design: for example, the use of multiple perfusion channels. This can be achieved using pumped perfusion systems instead (94,97). In recent years, 3D microfluidic systems have been developed to miniaturise the scale of perfusion systems (98). These systems take into consideration optimised perfusion routes through intricate design and have been developed prior to this report as a means for creating models used in drug and inflammation testing (99).

1.7 Skin models grown in dynamic culture

In the past decade, some studies have investigated the effect of dynamic culture on the structure and physiology of different skin models; these studies and their subsequent findings are summarised in Table 2 below.

Table 2: 3D *in vitro* skin models developed with bioreactors, and observed effects compared to static culture.

Source	Model Developed	Type of Bioreactor	Scaffold/ Construct	Cell Source	Observed Effects of Bioreactor
(95)	Epidermal model	Rotating Cell Culture System (RCCS)	Spheroid	Human Epidermal Stem Cells (hEpSC)	• More keratinocytes grew around micro-carrier bead, based on histology • Increased proliferation compared to static culture, as shown by increased Ki-67 expression • Increased number of viable hEpSCs indicating improved cell viability • Decreased expression of involucrin suggesting that perfusion may inhibit terminal differentiation
(100)	Full-thickness skin model	Pumped Perfusion System	Collagen-Based hydrogel	Human Dermal Fibroblasts (HDF) Human Foreskin Keratinocytes (HfKC)	• Perfused models had a thicker *stratum corneum,* thinner dermis, and viable epithelium of same thickness, compared to static-grown models • Pumped perfusion increased expression of involucrin, claudin-1 and occludin, suggesting improved terminal differentiation and tight junction formation
(101)	Full thickness skin model	Pumped Perfusion System	Fibrin-based hydrogel	HDF HfKC Human Umbilical Vein Endothelial Cells (HuVEC)	• Perfused models had a stratified epidermis with a well-defined basal layer • The dermal compartment had evenly distributed fibroblasts and produced homogenous collagen type-I • The expression of vimentin, collagen type I, involucrin, and pan cytokeratin was clear

(102)	Full thickness model	Microfluidic Perfusion System	Skin-on-a-chip	HDF Immortalised human/TERT-1	• Perfused models displayed superior epidermal morphogenesis and a thick viable epidermis • Desmoglein-1, involucrin, loricrin and collagen type IV were significantly expressed • Comparable expression of KRT-10, filaggrin, integrin-β1, KRT-16 and collagen type I Confocal Raman Spectroscopy • Greater keratin intensity within *stratum corneum* • Thicker *stratum corneum*
(103)	Full thickness model	Microfluidic Perfusion System	Skin-on-a-chip	Human neonatal dermal fibroblasts (HDFn) Human neonatal epidermal keratinocytes (HEKn) HuVEC	• There was greater similarity to native skin tissue when the models were exposed to shear stress • A distinct basal layer of epidermis observed • A thicker epidermis was observed with dynamic stretching and perfusion (2.3-fold greater with 10% strain at 0.05HZ) • Increased cell densities in dermal layer in perfused conditions as observed with DAPI staining • Vascular channels only open in perfused conditions as observed with CD31 staining

The studies in Table 2 show that dynamic culture can have a major impact on the structure of skin models. In particular, dynamic culture enhanced the growth and maturation of the epidermal layer. This was evident in the epidermal model through the formation of a multi-layer of keratinocytes in dynamic culture compared to a monolayer in static culture (95). As for the full thickness models, this effect was observed through the acquisition of a thicker epidermis with improved stratification (101,102). Improved maturation of the epidermal layer with greater resemblance to *in vivo* skin was observed in all full thickness studies.

The studies in Table 2 also show that dynamic culture improves the structure of skin models. Generally, the incorporation of dynamic culture in full thickness models increased the expression of ECM proteins in the dermal compartment, tight junction markers in the DEJ, cell proliferation markers in the basal layer of the epidermal compartment, and keratinocyte terminal differentiation markers in the *stratum corneum* (100–102). Through these observations, it can be assumed that dynamic culture improved maturation of the dermal compartment through increased ECM deposition, influenced the formation of a defined DEJ, and improved the maturation of the epidermal compartment through better stratification, respectively. In the case of the epidermal model in rotary culture, the expression of the keratinocyte terminal differentiation marker involucrin dropped, thereby contradicting the positive effect of dynamic culture on biomarker expression. However, it can be suggested that this was due to a lack of ALI in that respective study which limited keratinocyte differentiation (95).

In the full thickness studies, dynamic conditions were implemented at different stages of the model development protocol. Helmedag et al. and Sriram et al. perfused the skin models in submerged culture during the development of the de-epithelialised dermal equivalent, whilst *Str*üver et al. and Mori et al. perfused the models during the air-lift culture of full thickness equivalents. On the one hand, models can be perfused during the generation of the dermal equivalent to potentially improve the maturation of the dermal compartment before seeding keratinocytes. In other words, perfusion of the dermal equivalent can potentially increase the rate of ECM deposition in a shorter period of time. It has previously been observed that perfusing the dermal compartment improves proliferation of human dermal fibroblasts and increase collagen production due to improved oxygenation (104). On the other hand, perfusion of the models at ALI can improve stratification stimulated by the ALI culture; this occurs as dynamic culture provides a continuous supply of nutrients and oxygen to keratinocytes, particularly in the basal layer, thereby improving viability and encouraging both proliferation and differentiation (105).

1.8 Conclusion

The generation of *in vitro* full thickness skin models, as animal-free alternatives for drug and cosmetic testing, has been promising. Previous studies have been successful in creating multi-layered skin models using biocompatible scaffolds and 3D cell culture, however they primarily use static conditions. The models generated from these studies have been found to resemble human skin, with regards to structure and function. However, a prominent issue

which occurs in static *in vitro* culture is that the thickness of the unstirred layer which forms is far thicker than *in vivo*. This can be detrimental to metabolic exchange, and therefore cell viability. Perfusion can potentially enhance the development of these models in terms of structure, maturation, viability, and longevity. By incorporating perfusion in culture with the use of a bioreactor, there is a window for refinement with full thickness models to maximise resemblance to *in vivo* skin, necessary for improving accuracy in subsequent drug testing.

1.9 Project overview

The overall aim of this project is to investigate how the disruption of unstirred layers affects the development and longevity of skin models generated using Alvetex®. To achieve the disruption of unstirred layers, perfusion will be incorporated in 3D culture using in-house bioreactor technology. It is hypothesised that characterisation and evaluation of dynamically cultured human skin models, in contrast to statically generated models, will provide a greater understanding on the significance of culture conditions for generating models with greater resemblance to *in vivo* skin. Furthermore, based on the literature, it can be hypothesised that an enhanced full thickness skin model will be generated in dynamic conditions due to increased ECM deposition in the dermal compartment, improved stratification and maturation of the epidermal layer, and increased cell viability in both layers.

Within the scope of this project, the following hypotheses are proposed:

1. Disruption of unstirred layers, caused by perfusion of the models, can improve the structure of the dermal compartment and the deposition of ECM proteins
2. Disruption of unstirred layers, caused by perfusion of the models, can improve the development of full thickness models, in terms of structure, physiology, and function
3. Disruption of unstirred layers, caused by perfusion of the models, can improve the longevity of full thickness models, in terms of structure, physiology, and function
4. The speed of media mixing, when disrupting unstirred layers, can influence the development and maintenance of full thickness models

1.9.1 Project objectives

First, it is hypothesised that the disruption of unstirred layers will improve the structure and ECM deposition of Alvetex®-based dermal models. Dynamic culture will be achieved using a low-cost magnetic stirrer-based bioreactor developed in the Przyborski lab. The bioreactor

will be used to investigate enhanced development of a mature dermal compartment in submerged culture, through assessment of changes in ECM deposition.

For the initial phase of this project, dermal models will be generated and characterised in both static and perfused conditions. The objectives are as follows:

- Generate dermal models in 3D cell culture, using Alvetex® scaffold technology and develop a novel protocol for perfusion. Models will be grown in static or perfused conditions.
- Harvest the dermal models for subsequent analytical processing:
    - Histological analysis: Models will be stained with Haematoxylin and Eosin (H&E). The cross-section of the dermal model will be observed to identify any changes in the structure, arrangement, and thickness of the dermal layer.
    - Immunofluorescence analysis: Changes in ECM protein deposition will be detected by staining models with antigen-specific antibodies. Collagen-I and Collagen-III will be analysed.

Second, it is hypothesised that full thickness models in dynamic culture will also have an improved structure, physiology, and function compared to models grown in static culture, due to the disruption of unstirred layers. This can be beneficial for model development and longevity. In terms of structure, the epidermal compartment grown in perfusion is expected to display greater stratification. In terms of function, it is expected that epidermal layer will have greater proliferation and early, mid, and terminal keratinocyte terminal differentiation. Additionally, it is predicted that the trans-epidermal water loss will be reduced in perfused models, as barrier properties are enhanced.

To assess the effects of dynamic culture on the stratification and expression of keratinocyte differentiation markers, the bioreactor is most suited to be implemented during the ALI. However, several considerations must be made when using the magnetic stirrer-based bioreactor:

- Mixing speed – This must be minimised to avoid media spillage onto the top of the model
- Evaporation of growth medium – The volume of growth medium in the bioreactor must be regularly observed for any evaporation, and replenished if necessary

- Degradation of growth factors – Growth factors such as KGF and AA in growth medium will degrade over time. Therefore, growth medium must be replaced twice a week.
- Media Volume – This must be optimised to ensure that mixing speed and evaporation did not negatively affect the model

With these considerations in mind, the objectives are as follows:

- Generate full thickness models in 3D cell culture, using Alvetex® scaffold technology and develop a novel protocol. Models will be grown in static or perfused conditions at the ALI.
- Harvest the dermal models for subsequent analytical processing:
    - Histological analysis: H&E staining will be used to observe the cross-section of the full thickness models and identify changes in the structure and thicknesses of epidermal compartments.
    - Biometric Analyses: ImageJ software will be used to quantify epidermal thickness
    - Immunofluorescence (IF) analysis. IF will be used to analyse the distribution of biomarkers in the model: (A) Ki67 to analyse basal keratinocyte proliferation; (B) K14/K10 to analyse early and mid-differentiation of keratinocytes; and (C) filaggrin to analyse keratinocyte terminal differentiation
    - Trans-epidermal water loss (TEWL) analysis: Trans-epidermal water loss will be analysed as a measure of barrier function

Lastly, it is hypothesised that increasing the speed of perfusion would negatively affect the development of full thickness models, as literature links perfusion speed to increased shear stress.

The objectives are as follows:

- Generate 14 day full thickness models in 3D cell culture, using Alvetex® scaffold technology. Models will be grown in perfused conditions at the ALI, with varying stirrer speeds.
- Harvest the full thickness models for subsequent analytical processing:

    - Histological analysis: H&E staining will be used to observe the cross-section of the full thickness models and identify whether the models display any changes in structure or physiology due to stirrer speeds.
- If significant observations are made, proceed to conduct further analysis.

Chapter II: Materials and Methods

2.1 Introduction

In this study, a variety of scientific techniques were used to generate and characterise both dermal and full-thickness skin equivalents. Firstly, to generate skin equivalents, 2D and 3D cell culture techniques were used. Secondly, to characterise skin equivalents, the main techniques used were histological and immunofluorescence techniques. Characterisation of skin equivalents was also achieved using other analytical techniques, such as epidermal thickness and trans-epidermal water loss measurements. This chapter aims to outline all of the main techniques used, and the methodology applied.

2.2 Alvetex® technology for 3D skin models

Alvetex® was employed in this study as a scaffold for generating 3D skin models. It is a commercialised polystyrene-based scaffold for 3D culture, which is available in three formats: Scaffold, Strata, and Polaris. The difference in the type of Alvetex® primarily refers to the porosity and void size of the scaffold. For the generation of the dermal equivalent, Alvetex® Scaffold is routinely used due to its higher porosity and larger void size of 42µm, which enables the fibroblasts to infiltrate and reside within the scaffold. The Alvetex® Scaffold used is shown in Figure 5.

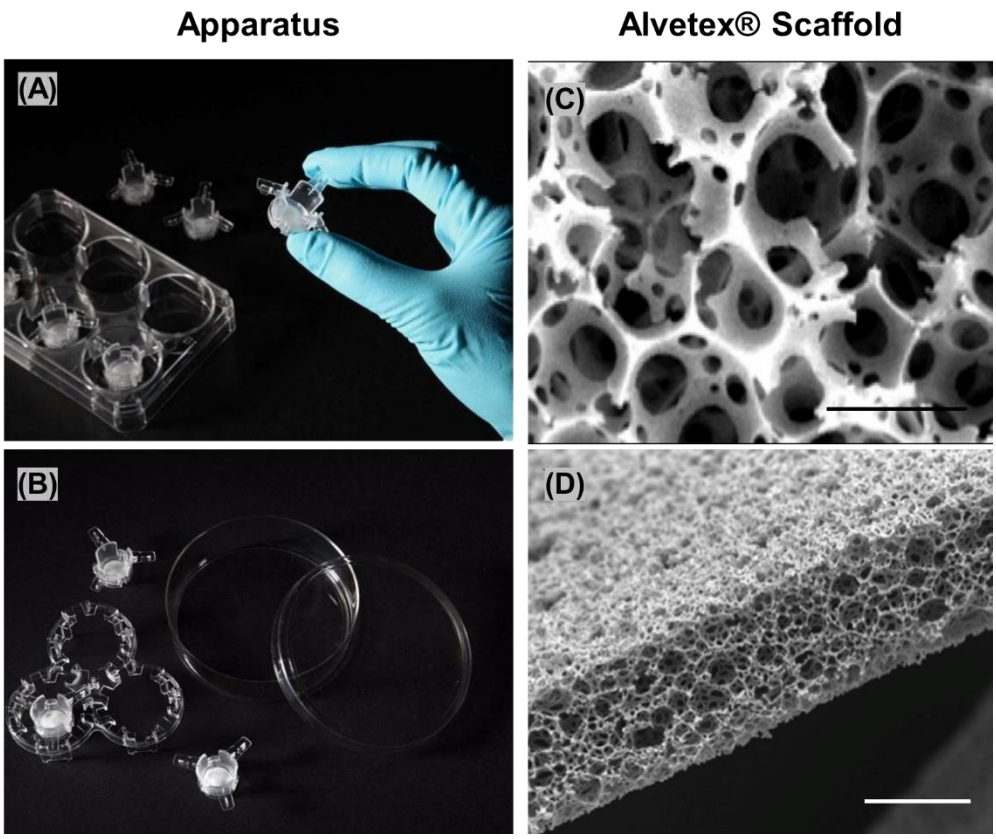

Figure 5: Alvetex® Scaffold for 3D cell culture. (A) Alvetex® 12-well inserts can fit into standard 6 well plates. (B) Deep dish with a holder that can hold three Alvetex® inserts at various heights, the medium setting is suitable for ALI culture. (C-D) Electron scanning microscopy images of Alvetex scaffold at high and low magnification. Scale: (C) = 10 µm; (D) = 200 µm. Images courtesy of Reprocell Europe.

The Alvetex® scaffold has a thickness of 200µm, which ensures that the seeded fibroblasts are able to efficiently acquire nutrients and exchange waste from the supplied media, through a shorter nutrient diffusion distance of 100µm or less. This is beneficial as increased efficiency in nutrient and waste exchange improves the long-term viability of the cells. Fibroblasts encapsulated in the scaffold are able to produce their own endogenous extracellular matrix, without addition of exogenous matrix proteins, to form the dermal equivalent.

2.3 A magnetic stirrer-based bioreactor for incorporating perfusion

As this project aims to investigate the development and longevity of skin models as a consequence of disrupting unstirred layers in media, perfusion must be introduced to continuously mix the media. Whilst the use of traditional well plates and deep petri dishes to generate skin models have been the gold standard for effectively generating skin models in static conditions, there is a greater variability in the literature on what apparatus is used to introduce perfusion. In this study, an in-house magnetic stirrer-based bioreactor is used to introduce perfusion, as it is low-cost, small scale and purpose-built for Alvetex® inserts. Based on literature, microfluidic systems and pumped perfusion systems are the most common approaches for skin models; the use of a magnetic stirrer for skin models is scarcely, if not, documented. The apparatus for the bioreactor used to disrupt unstirred layers is shown below in Figure 6. Alvetex® skin models can be placed on top of the bioreactor stand (Figure 6E), and media can be supplied beneath the model. To operate the bioreactor vessel, the whole apparatus must be carefully placed on a magnetic stirrer with adjustable speeds, whereby an electromagnetic field will cause the stirrer within the vessel to spin.

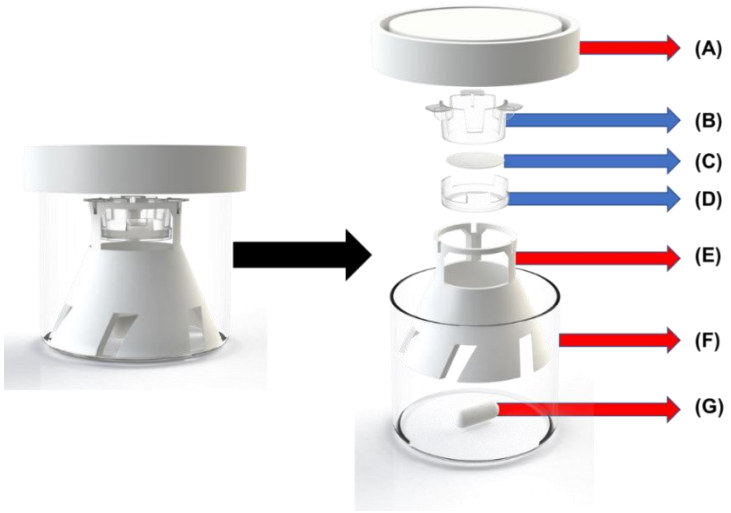

Figure 6: Components of the in-house magnetic stirrer bioreactor. (A) Lid; (B) Alvetex® 12-well insert body; (C) Alvetex® Scaffold; (D) Alvetex® Scaffold insert base; (E) Stand for Alvetex® insert; (F) Bioreactor vessel; (G) Magnetic stirrer bar. The blue components are commercially available, and the red components have been designed in-house.

2.4 Cell culture

2.4.1 Commercially available cells and their maintenance in 2D

In this study, cell lines were purchased and used for generation of skin equivalents. In this project, human dermal fibroblasts (HDFn) and human epidermal keratinocytes (HEKn) were used. Initially, these cells were grown in 2D culture before switching to 3D culture.

2.4.1.1 Human neonatal dermal fibroblasts (HDFn)

Human neonatal dermal fibroblasts (HDFn, ThermoFisher, Loughborough, UK) were used in the generation of dermal compartments in both dermal and full-thickness skin equivalents. For dermal equivalents, HDFn were maintained in defined Dulbecco's Modified Eagle Medium (DMEM, ThermoFisher), supplemented with non-heat treated foetal bovine serum (FBS, ThermoFisher), L-glutamine (ThermoFisher), 10 µg/mL gentamicin (Thermofisher), and 0.25 µg/mL amphotericin B (ThermoFisher), following the supplier's instructions. For full-thickness skin models, HDFn were maintained in defined medium 106 (M106®) (ThermoFisher), supplemented with low serum growth supplement (LSGS, Thermofisher), 10 µg/mL gentamicin (ThermoFisher) and 0.25 µg/mL amphotericin B (ThermoFisher), following the supplier's instructions. The supplemented media will be referred to as complete DMEM and complete M106®, respectively. HDFn were maintained in T175 flasks with 25 mL complete DMEM or complete M106® and incubated at 37 degrees Celsius (°C) and 5% carbon dioxide (CO_2) in a humidified environment.

Passage 4 or 5 HDFn were revived from vials in Synthafreeze, at 150°C. Vials of HDFn were thawed in a pre-heated 37°C water bath and transferred to warm complete DMEM or warm complete M106®. The cells were seeded at a cell density of $5x10^5$ in T175 flasks, containing 25 mL of respective media used. Media was changed the day after revival to remove the cryopreservative, and media was changed every 2-3 days until an 80% HDFn confluency was achieved. Growth and morphology of the HDFn population in 2D culture was periodically observed after 1, 3, and 7 days using phase contrast microscopy, described in Section 2.7.1. The expected growth of HDFn under a phase contrast microscope over 1 week is shown in Figure 7 below.

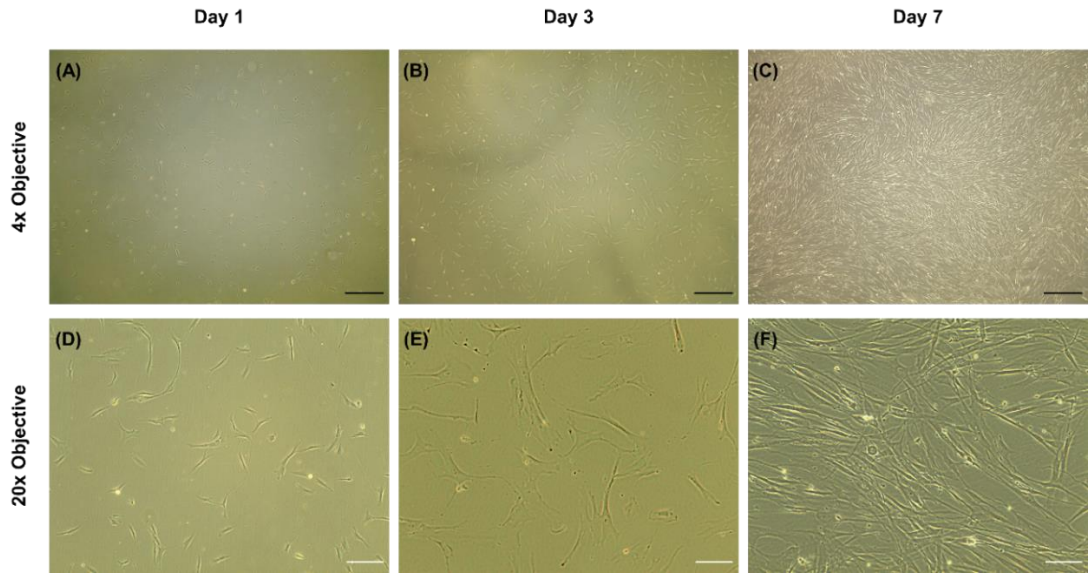

Figure 7: Phase contrast micrograph images of neonatal human dermal fibroblasts (HDFn) grown in 2D culture over 1 week. (A-C) Growth of HDFn at day 1, 3, and 7 using 4x objective. By day 7, confluency is at approximately 90%. (D-F) Growth of HDFn at day 1, 3, and 7 using 20x objective. Over time, the morphology of the fibroblasts become more elongated and spindle shaped. Scale: (A-C) = 500 µm, (D-F) = 100 µm.

2.4.1.2 Human neonatal epidermal keratinocytes (HEKn)

Human neonatal epidermal keratinocytes (HEKn, ThermoFisher, Loughborough, UK) were used in the generation of dermal compartments in full-thickness skin equivalents. HEKn were maintained in defined EpiLife® medium (ThermoFisher), supplemented with human keratinocyte growth supplement (HKGS, ThermoFisher), 10 µg/mL gentamicin (ThermoFisher) and 0.25 µg/mL amphotericin B (ThermoFisher), following the supplier's instructions. The supplemented media will be referred to as complete EpiLife®. HDFn were maintained in T175 flasks with 25 mL complete EpiLife® and incubated at 37°C and 5% CO_2 in a humidified environment.

Passage 3 HEKn were revived from vials in liquid nitrogen, at 150°C. Vials of HEKn were thawed in a pre-heated 37°C water bath and transferred to warm complete EpiLife®. The cells were seeded at a cell density of $5x10^5$ in T175 flasks, containing 25 mL of complete EpiLife®. Media was changed the day after revival to remove the cryopreservative, and media was changed every 2-3 days until an 80% HEKn confluency was achieved. Growth and morphology of the HEKn population in 2D culture was periodically observed after 1,3, and 7 days using contrast phase microscopy. The expected growth of HEKn under a phase contrast microscope over 1 week is shown in Figure 8 below.

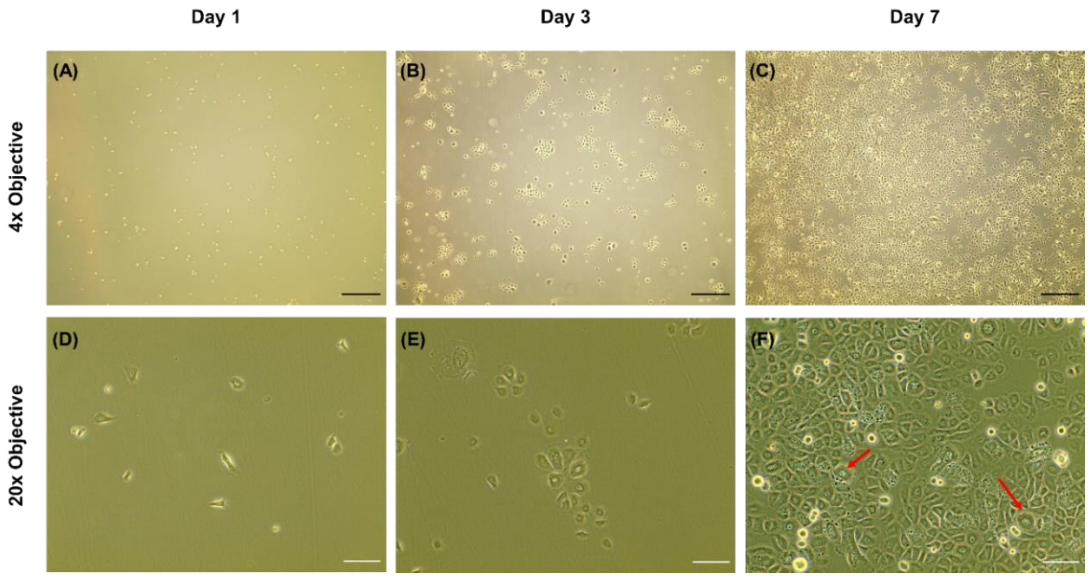

Figure 8: Phase contrast micrograph images of neonatal human epidermal keratinocytes (HEKn) grown in 2D culture over 1 week. (A-C) Growth of HEKn at day 1, 3, and 7 using 4x objective. By day 7, confluency is at approximately 80%. (D-F) Growth of HEKn at day 1, 3, and 7 using 20x objective. Over time, the morphology of the keratinocytes become rounder, forming clusters. Some HEKn begin to differentiate and grow much bigger over time. Scale: (A-C) = 500 µm, (D-F) = 100µm.

2.4.2 Generation of dermal skin equivalents

Dermal skin equivalents were generated using a detailed standard operating procedure (SOP) developed in-house. This is illustrated in Figure 9 below:

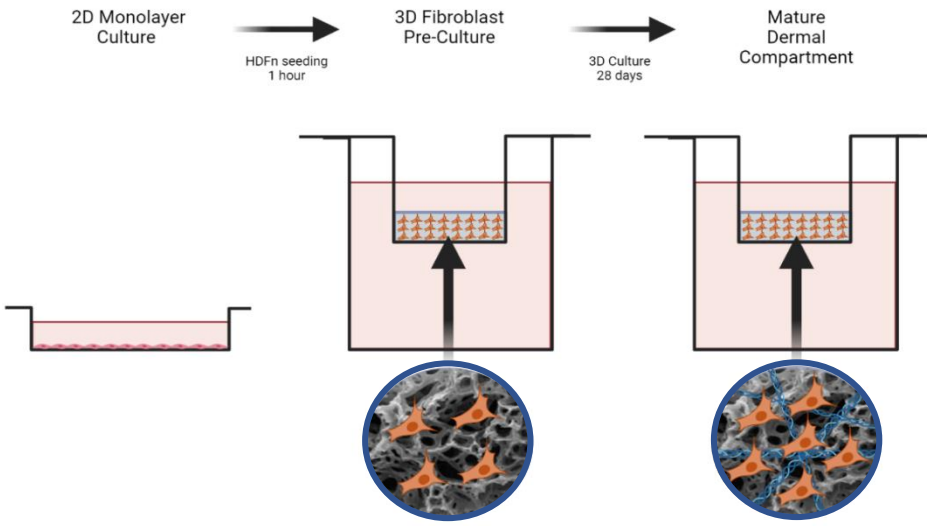

Figure 9: Methodology for the generation of a dermal equivalent. HDFn are expanded in 2D monoculture for a week and are acquired using trypsin-EDTA (TE). The resulting HDFn in suspension are then seeded into the Alvetex® scaffold at $5x10^5$ cell density. An hour after seeding, complete M106® supplemented with TGF-β and AA is added to the model. A mature dermal equivalent, with increased fibroblast population and ECM deposition, is formed after 28 days of 3D culture.

2.4.2.1 Preparation of Alvetex® Scaffold

Dermal skin equivalents were generated using Sterile Alvetex® scaffold 12-well inserts (200µm, 36-40µm pore polystyrene membrane, Reprocell, Europe, Sedgefield, UK). The inserts were pre-treated before use to induce hydrophilicity, by being washed in 70% ethanol for 5 minutes and subsequently washed in phosphate buffered saline (PBS) for an additional 5 minutes. Once treated, the inserts were submerged in complete DMEM until cell seeding.

2.4.2.2 Retrieval of HDFn using enzymatic passaging

Passage 4 or 5 human neonatal dermal fibroblasts (HDFn) were grown in T175 until 80% confluency. HDFn were acquired by enzymatic passaging. This was achieved through aspiring the complete DMEM in the T175 flask, gently washing the cells once with sterile 1x PBS (ThermoFisher), and carefully rinsing the cells with 5 mL 0.025% trypsin-EDTA (TE, ThermoFisher), diluted at a 1:10 ratio with sterile versene. The TE-rinsed HDFn were incubated for 2-5 minutes, at 37°C, 5% CO_2 and 95% humidity, until the cells had fully detached from the surface of the T175 flask. Once cells were detached, the TE was neutralised by adding 5 mL trypsin neutraliser solution (TN, ThermoFisher), and the resulting cell suspension was transferred to a 50 mL falcon tube. The T175 flasks were further rinsed

with an additional 5 mL TN twice and was added to the falcon tube. The cell suspension was centrifuged at 200 g for 5 minutes, to acquire a pellet of HDFn at the bottom of the falcon tube. The supernatant was aspirated, and the pellet was gently resuspended in 1 mL fresh complete DMEM.

2.4.2.3 Cell counts and cell seeding

Using a micropipette, 20 µL of the cell suspension was transferred to a microcentrifuge tube (Eppendorf, Hamburg, Germany) and diluted 1:10 with trypan blue. The number of viable cells was determined using a haemocytometer, and the concentration of the cell suspension was adjusted with fresh DMEM to the desired level for seeding the models.

The treated Alvetex® inserts were transferred to sterile 6-well cell culture plates and HDFn were gently seeded onto the top of the Alvetex® inserts, at the appropriate cell density provided in the protocol ($5x10^5$/100 µL). The cells were incubated at 37°C and 5% CO_2 in a humidified environment for 1 hour to allow the HDFn to adhere to the Alvetex®. After 1 hour, the cells were submerged in complete DMEM, supplemented with 5 ng/mL TGF-β and 100 µg/mL AA. The generated dermal equivalents were incubated at 37°C and 5% CO_2 in a humidified environment for 14-28 days. Media was replaced every 3-4 days, and inserts were transferred to new 6-well plates after the first media change, and 2 weeks after dermal equivalent generation.

2.4.3 Generation of full-thickness skin equivalents

Full-thickness skin equivalents were generated using a detailed SOP developed in-house. As these skin equivalents require both a dermal and epidermal compartment, a dermal equivalent is generated first, as outlined in Section 2.4.2. However, for full thickness skin equivalents, the media used to grow HDFn was changed from DMEM to M106®. Furthermore, the dermal compartment had to be grown for at least 28 days to ensure that it was mature to support the development of the epidermal compartment. The protocol for generating full thickness skin equivalents is outlined in Figure 10 below.

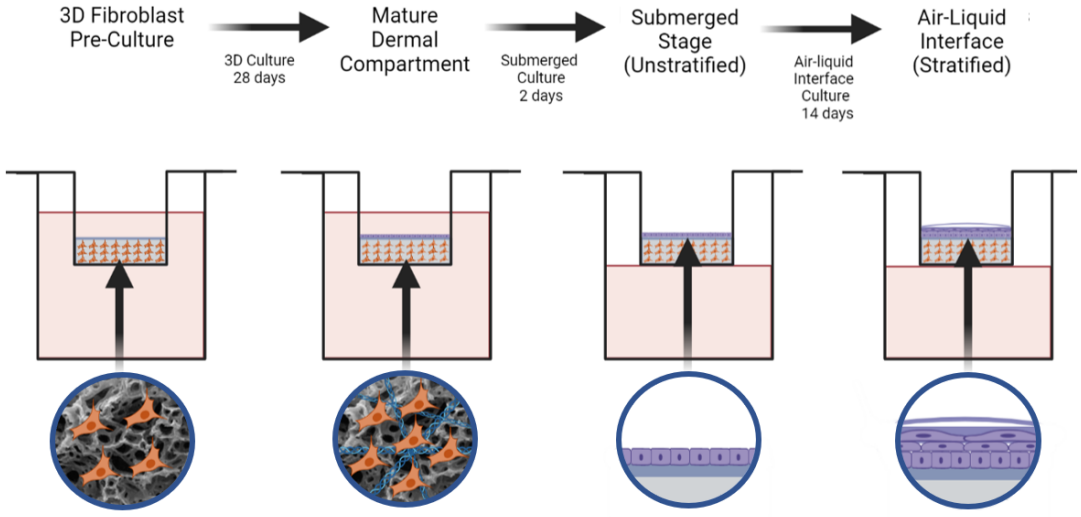

Figure 10: Methodology for the generation of a full thickness model. A mature dermal compartment is firstly formed. HEKn are seeded onto the top surface of the dermal compartment and the model is supplemented with complete Epilife® (with low calcium) in submerged conditions for 2 days. This promotes keratinocyte adhesion and basal layer formation. After 2 days, the full thickness model is raised to the ALI and supplemented with complete Epilife® (with high calcium) for 14 days to promote stratification of the epidermal compartment.

2.4.3.1 Seeding of keratinocytes onto the surface of the dermal compartment

Human epidermal keratinocytes (HEKn) at Passage 3 were grown in T175 flask. Upon reaching 80% confluency and ensuring that HEKn were not differentiated, HEKn were acquired by detaching the cells from the surface of the T175 flask, by enzymatic passaging. The process for acquiring a cell suspension is identical to Section 2.4.2.2 with the only difference being the media used, which is Epilife® for HEKn. Upon acquiring a cell suspension, a cell count was performed in the same fashion as Section 2.4.2.3 and the concentration of the cell suspension was altered respectively. For HEKn, the cell seeding density as outlined by the protocol was $1.3x10^6$ per model in 100-300 µL. The dermal equivalents which were previously generated were transferred to a new 6-well plate, and gently, HEKn were seeded onto the upper surface of the mature dermal compartment at the given density. The newly generated full-thickness models were incubated at 37°C and 5% CO_2 in a humidified environment for 2 hours to allow the HDFn to adhere onto the surface. Afterwards, the models were submerged in Epilife®, supplemented with 10 ng/mL KGF (ThermoFisher), 140µM calcium chloride ($CaCl_2$, Sigma Aldrich, Dorset, UK), and 100 µg/mL AA, and incubated at 37°C and 5% CO_2 in a humidified environment for 2 days.

2.4.3.2 Air-liquid interface culture of full thickness skin models

After 48 hours, the full thickness models were transferred from submerged culture to ALI culture. The models were transferred to either a deep Petri dish containing an Alvetex® well insert holder (Reprocell Europe), or an Alvetex® well stand custom-built for the in-house bioreactor used in study; the former is for models which are subjected to ALI in static conditions while the latter is for models subjected to perfusion during ALI. Before proceeding to supply the model with media, the upper surface of the models was aspirated to ensure that the epidermal surface was dry for ALI culture. When using the deep-well apparatus, up to 3 models were left to rest on the medium height setting, and 35 mL of Epilife®, supplemented with 10 ng KGF, 1.64 mM $CaCl_2$, and 100 µg AA, was added to the Petri dish. When using the bioreactor apparatus, the well stand, holding just 1 full thickness model, was placed within the glass bioreactor vessel and 88 mL of Epilife®, supplemented with 10 ng KGF, 1.64 mM $CaCl_2$, and 100 µg AA, was added to the vessel. Media was replaced every 3-4 days, with the deep-well apparatus having a full media change and the bioreactor apparatus having a half-media change (44 mL). The full-thickness models were cultured at the ALI for 7-28 days before harvesting.

2.5 Fixation and post-processing techniques

2.5.1 Fixation and embedding

For this study, fixation was achieved through the use of paraformaldehyde (PFA), and embedding was achieved through the use of paraffin wax. Models that were ready to be harvested were removed from their inserts by unclipping them from the insert holder. The models were washed in 5mL PBS twice prior to fixation, and submerged in 4% PFA (Sigma Aldrich) diluted in PBS for overnight fixation at 4°C. The following day, the models were washed in PBS for 10 minutes and sequentially dehydrated using ethanols of increasing concentrations: 30%, 50%, 70%, 80%, 90%, and 95%, for 10 minutes each. For the final step of dehydration, the models were submerged in 100% ethanol for 30 minutes at room temperature, or overnight at 4°C. Upon successful dehydration, the models were transferred to tissue processing cassettes and placed in a beaker of Histoclear II (ThermoFisher) for 30 minutes within a fume hood. After 30 minutes, half of the Histoclear II was poured out and replaced with molten paraffin wax, ensuring that a 1:1 ratio was achieved. The models in Histoclear II: wax solution were incubated at 60°C in a convection oven for an additional 30 minutes. Subsequently, the Histoclear II: wax solution was poured out fully and replaced with

100% molten paraffin wax. The models submerged in wax were incubated at 60°C, for 1 hour. The models were removed from the cassettes and cut in half across their diameter using a scalpel. Molten wax was poured onto plastic moulds and once the wax at the base began to solidify, the cut samples were embedded upright, with the flat side touching the base of the mould. The wax blocks were left to solidify overnight in room temperature prior to subsequent sectioning.

2.5.2 Sectioning

The paraffin wax blocks were removed from the plastic moulds and sectioned using a rotary manual microtome (Leica RM2125RT), fitted with MB DynaSharp microtome blades (ThermoFisher). The microtome was set to generate 5µm-thick transverse sections to use for histological or immunofluorescence analysis. The transverse sections were carefully placed on the surface of a 37°C water bath using forceps and the samples were mounted onto charged SuperFrost Plus microscope slides (ThermoFisher). The glass slides were placed on a 30°C heat rack and left to dry overnight for further processing.

2.6 Analytical techniques

2.6.1 Histological analysis - Haematoxylin and Eosin (H&E)

The paraffin wax sections were deparaffinised in Histoclear I for 5 minutes, and subsequently placed in 100% ethanol for 2 minutes. The sections were then rehydrated by placing the slides in ethanols of decreasing concentration for 1 minute each: 95% ethanol, 70% ethanol, and distilled water, respectively. Afterwards, the sections were stained with Mayers Haematoxylin for 5 minutes, followed by a wash in distilled water for 30 seconds. To ensure that nuclei appeared blue during imaging, the haematoxylin-stained sections were submerged in alkaline alcohol for 30 seconds. Prior to staining with eosin, the sections were sequentially rehydrated in 70% ethanol and 95% ethanol for 30 seconds each. The rehydrated sections were stained with eosin for 30 seconds, and subsequently subjected to further dehydration: twice in 95% ethanol for 10 seconds then twice in 100% ethanol for 15 and 30 seconds, respectively. The H&E-stained sections were placed in Histoclear I two times, for 3 minutes each, until they were ready for mounting with a coverslip. The sections were mounted with a coverslip using Omni-mount (Scientific Laboratory Supplies Ltd., Nottingham, UK) and slides were imaged under a brightfield microscope, as described in Section 2.7.2.

2.6.2 Biometric analysis of epidermal thickness

Brightfield microscopy images displaying the histology of full-thickness models were opened on ImageJ image processing software. The scale of the images were set using the software. Using the *line* tool, a vertical line was drawn from the base of the epidermis to the top of the viable epidermis. The thickness of the epidermis at the point where the line was drawn was automatically measured by the software using the *Analyze > Measure* tool. Additional measurements were taken by drawing another four lines along the length of the epidermis in each image. Based on five measurements per image, an average thickness was calculated. Three images were used for each condition.

2.6.3 Immunofluorescence analysis

The paraffin wax sections were deparaffinised in Histoclear I for 15 minutes, followed by sequential rehydration in 100% ethanol, 95% ethanol, 70% ethanol, and PBS respectively, for 5 minutes each. The slides were then transferred to a pre-heated black insulated box containing citrate buffer (pH 6.0, Sigma Aldrich), in a 95°C water bath. The sections were incubated in citrate buffer for 20 minutes to enable antigen retrieval. After 20 minutes, the slides were left to cool at room temperature for 5 minutes. Slides were encircled with a hydrophobic pen and covered with 200µl blocking solution, comprised of 20% neonatal calf serum (NCS, Sigma Aldrich) diluted in 0.4% Triton-X-100 diluted with PBS, for 1 hour. The rings ensured that the blocking buffer was evenly distributed and in contact with the sample during blocking. Concurrent with the blocking process, the required primary antibodies were diluted in the original blocking buffer solution; the appropriate dilutions are shown in Table 3. After 1 hour, the samples were incubated with 200µl primary antibody solution, and left overnight in the humidity chamber at 4°C.

Table 3: Primary antibodies for immunofluorescence (ICC/IF), with their respective supplier, species, and dilution for application.

Antibody	Supplier	Product Code	Species	Dilution
Collagen-I	Abcam	Ab34710	Rabbit	1:100
Collagen-III	Abcam	Ab7778	Rabbit	1:100
Ki-67	Abcam	Ab16667	Rabbit	1:100
Alpha smooth muscle actin (α-sma)	Abcam	Ab5694	Rabbit	1:100
Cytokeratin-10 (K10)	Abcam	Ab76318	Rabbit	1:100
Cytokeratin-14 (K14)	Abcam	Ab7800	Mouse	1:100
Filaggrin	Abcam	Ab17808	Mouse	1:100

The following day, the slides were washed three times in PBS, for 10 minutes each, to remove excess primary antibody. Secondary antibodies and Hoescht solution was diluted in blocking buffer solution, using the dilutions shown in Table 4, and 200µl of this secondary antibody solution was added to each sample.

Table 4: Secondary antibodies for immunofluorescence (ICC/IF), with their respective supplier and dilution for application.

Antibody	Supplier	Product Code	Dilution
Donkey Anti-Rabbit IgG Alexa Fluor® 488	ThermoFisher	A-21206	1:1000
Donkey Anti-Mouse IgG Alexa Fluor® 488	ThermoFisher	A-11001	1:1000
Donkey Anti-Rabbit IgG Alexa Fluor® 594	ThermoFisher	A-21207	1:1000
Donkey Anti-Mouse IgG Alexa Fluor® 594	ThermoFisher	A-21203	1:1000

The samples were left to incubate for 1 hour at room temperature in the humidity chamber. Excess secondary antibodies were removed by washing the slides again three times with PBS, for 10 minutes each. A coverslip was mounted onto the slides using Vectashield mounting medium (Vector Laboratories, Peterborough, UK) and nail varnish was applied to the edges of the coverslip. The slides were covered and stored at 4°C until imaging with a laser confocal microscope, as described in Section 2.7.3.

For each batch of samples stained, an additional slide was stained as a negative control. Unlike samples, the negative control was not stained with primary antibodies, but rather, blocking solution. The negative control was stained with secondary antibodies as normal. The negative control was used as a reference for post-imaging comparisons. Ideally, the negative control should only emit blue fluorescence, in this case, DAPI stain; biomarkers investigated should not appear in the negative control. A typical example is shown in Figure 11.

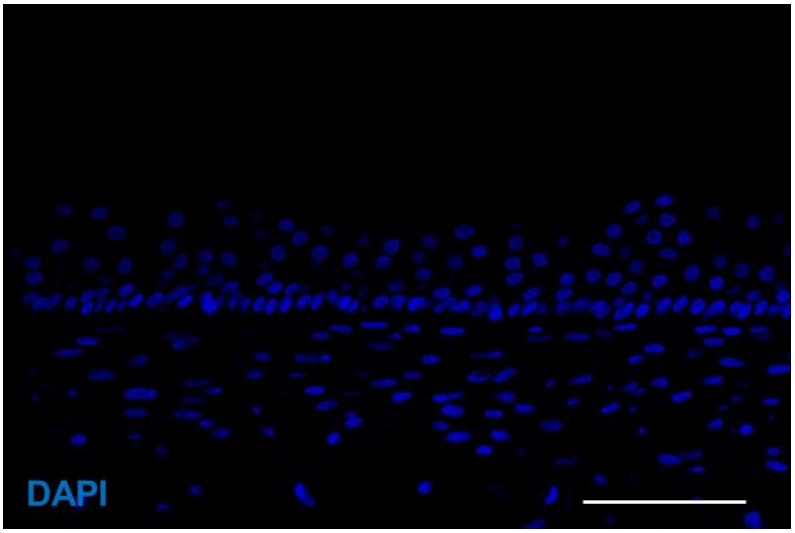

Figure 11: Negative control for immunofluorescence. Only blue fluorescence, showing DAPI, can be observed. Scale: 100 µm

2.6.4 Quantification of Ki-67 positive cells

For Ki-67 immunofluorescence experiments, three images were taken for each model condition. The triplicate images were loaded onto ImageJ image processing software and the *Cell Counter* plugin was utilised to count the number of keratinocytes in the basal layer of the epidermal compartment and the number of Ki-67 positive cells, respectively. The numbers acquired were transferred to Excel (Microsoft, Albuquerque, New Mexico, United States) and an average percentage of Ki-67 positive cells per condition was calculated, as an indicator of proliferation. The resultant averages were transferred to Prism 5.0 (San Diego, California, United States) statistical software to generate graphs and conduct statistical analysis, as described in Section 2.8.

2.6.5 Trans-epidermal water loss

For full-thickness models, trans-epidermal water loss (TEWL) was measured using a vapometer (Delfin Technologies, Kuopio, Finland) prior to fixation and embedding outlined in Section 2.5.1. Upon unclipping the models from the insert holder, the bottom surface of the models were wet with PBS, to prevent the models from drying, and placed on a flat sterile surface. The vapometer was carefully lowered on top of the model vertically until the nozzle was in contact with the top surface of the model. Measurements were digitally acquired in $g/m^{2}/h$ after 3-10 seconds of contact. Three repeats were taken for each model. After use, the adaptor was removed and washed in 70% ethanol overnight at 4°C.

2.7 Microscopy

2.7.1 Phase contrast imaging

For maintenance of 2D-culture of fibroblasts and keratinocytes, the surface of T175 culture flasks were imaged using EVOS® XL Core phase contrast microscope (ThermoFisher). Images were acquired using the x4 and x20 objective.

2.7.2 Brightfield imaging

Histology samples of dermal equivalents and full thickness models stained with H&E were imaged using a Leica ICC50 high definition camera mounted to a Leica microscope. Images were taken using x4, x20, and x100 objective, with the latter requiring oil immersion. Images were captured using the LAS EZ 3.4 imaging software (Leica Microsystems, Wetzlar, Germany), and afterwards processed using the ImageJ software.

2.7.3 Confocal fluorescence imaging

Immunofluorescence samples of dermal equivalents and full thickness models were imaged using the Zeiss 880 confocal laser scanning microscope with Airyscan (Carl Zeiss AG, Oberkochen, Germany). Imaging was performed using the x20 Plan Apochromat DIC II objective lens with filters for DAPI, 488nm, and 594nm. Images were captured using the Zeiss Zen Black software, and afterwards processed using the ImageJ software.

2.8 Statistical techniques

Using Graphpad Prism 5.0, the statistical significance of quantitative results was assessed by applying relevant statistical tests. For this study, two-way ANOVA was used on datasets, where applicable, with Tukey' post-hoc test. The statistical differences of a dataset are graphically represented as: ns = P>0.05, * = P<= 0.05, ** = P<= 0.01, *** = P<=0.0001.

2.9 Fluid modelling

Computational fluid dynamics (CFD) analysis was conducted using Fluent 19.2 software (Ansys, Canonsburg, PA, USA). The geometry of the bioreactor system was designed using Solidworks 2018 (Dassault Systèmes, Vélizy-Villacoublay, France) and meshing was performed on Fluent 19.2. The fluid flow simulation had the characteristics of an incompressible and isothermal fluid. The dynamic viscosity was set to 1.003 gm^{-1} and a

constant density of 998.2 kgm^{-3} was applied. Analysis was conducted on the XY plane for vector and contour application, and on a specified ZX plane for calculations of shear stress and flow rate. Calculations were taken using a function calculator within the software.

Chapter III: Results

3.1 The effect of perfusion on dermal models

3.1.1 Generation of dermal models

Whilst the overall goal of the study is to identify the effect of perfusion on full thickness models, which are more representative of skin, it is necessary to appreciate that the formation of an epidermal compartment is highly dependent on the presence of a mature dermal compartment. If the dermis is not mature, the keratinocytes could fall through the Alvetex® scaffold and infiltrate the dermal compartment. Therefore, the initial stage of this study aims to address the effect of perfusion on the development and maintenance of a mature dermal compartment. Previous literature have shown that dynamic culture can improve fibroblast proliferation and ECM deposition (104), so it is hypothesised that perfusion can improve maturation.

3.1.1.1 Delayed perfusion enhances fibroblast proliferation and ECM deposition

The effect of perfusion on the development of dermal equivalents was investigated. The dermal equivalents were grown in 3 different conditions over the 4 week period: the standard protocol of 4 weeks static, 2 weeks static followed by 2 weeks perfused, and 4 weeks perfused (Figure 12). Three models for each condition were sectioned and analysed. By investigating dermal equivalents grown with delayed perfusion and early perfusion, I aimed to investigate whether perfusion is more suitable during the start of the culture where initial adhesion of fibroblasts is still occurring, or when an established fibroblast layer has already formed. For preliminary studies investigating dermal equivalents, DMEM was used instead of M106® due to the increased dermal maturation.

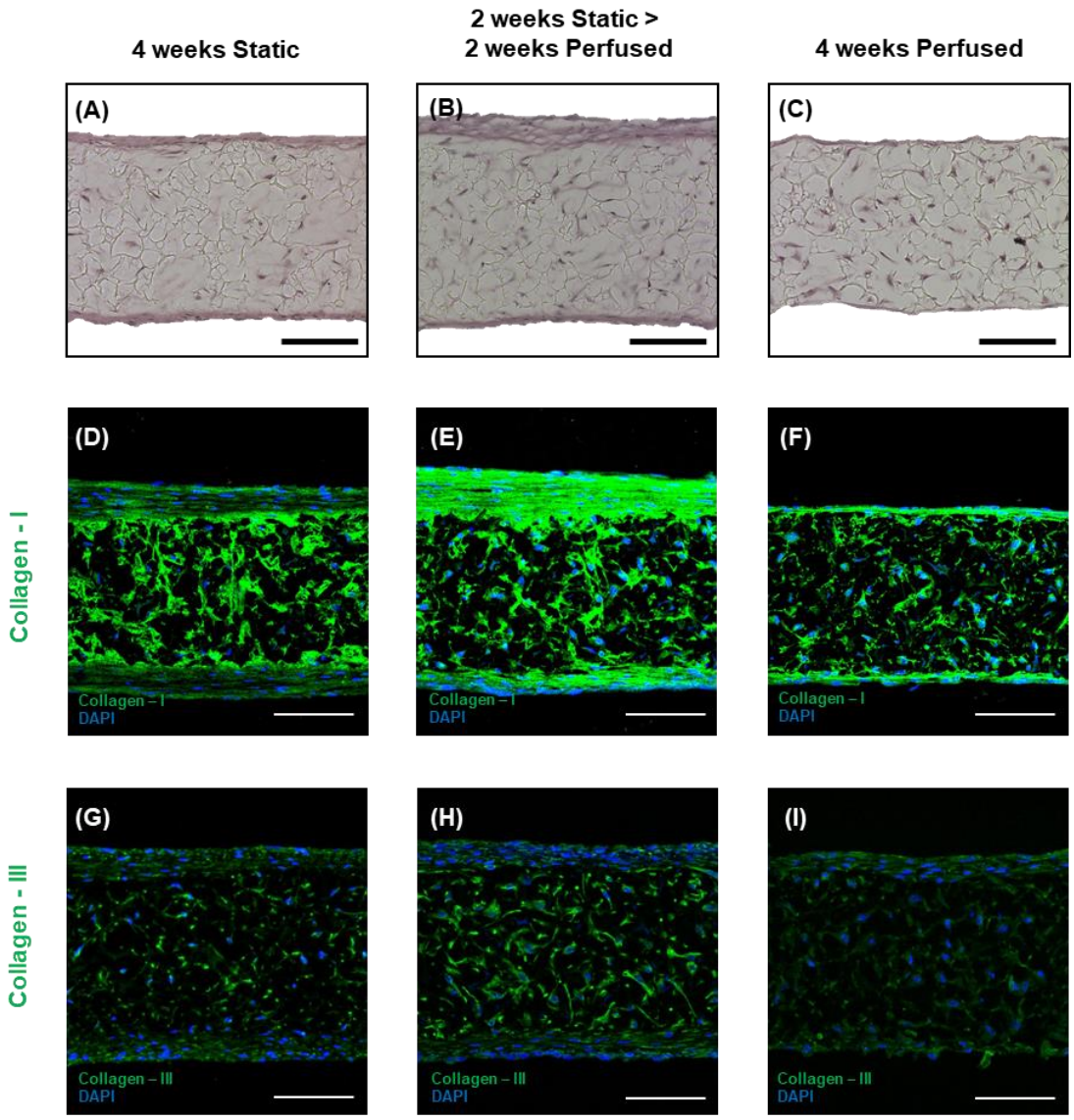

Figure 12: Histological and immunofluorescence analyses of 4-week dermal equivalents grown in varying conditions. (A-C) Histological analyses. (D-F) Collagen-I immunofluorescence images. (G-I) Collagen-III immunofluorescence. Arro images Scale bars: 100 µm.

The histological analysis in Figure 12 shows that delayed perfusion has a beneficial effect on the structure of the dermal equivalent, while early perfusion is detrimental. On the one hand, initially growing a dermal compartment in static and switching to perfusion later in culture increases the thickness of the fibroblast layer which forms on the surface of the Alvetex® Scaffold (Figure 12B). On the other hand, perfusing the dermal equivalent from the start of culture yields a dermal compartment that has a significantly thinner fibroblast surface layer (Figure 12C). Based on the histology, it was assumed that fibroblast proliferation was

improved by delayed perfusion, and thus hypothesised that ECM deposition would also be improved in this condition. To confirm this, immunofluorescence of the two prominent ECM proteins deposited by fibroblasts, collagen-I and collagen-III, was analysed in a qualitative manner.

Consistent with the improved structure observed in histology, dermal equivalents grown with delayed perfusion displayed a greater presence of both collagen-I and collagen-III (Figure 12E, 12H). Dermal equivalents grown in full perfusion displayed a weaker presence of collagen-I and III (Figure 12F, 12H). When comparing both collagen types, the presence of collagen-I appears greater than collagen-III, which could suggest that early perfusion has a more significant effect on collagen-III expression. However, quantitative conclusions cannot be drawn from immunofluorescence.

Comparing the three conditions above, it was clear that early perfusion was detrimental to the development of dermal compartments, and thus it would be of greater interest to further investigate the beneficial effect of delayed perfusion. The protocol parameters for delayed perfusion such as the feeding regime and the culture duration time were further optimised.

3.1.1.2 Half media changes are the optimal feeding regime during perfusion

In the previous experiment, the feeding regime during perfusion was half media changes every 3 to 4 days. The following experiment investigated whether another feeding regime, such as periodic addition of supplements, termed media spiking, improved fibroblast proliferation and ECM deposition alongside delayed perfusion. As DMEM has been demonstrated to successfully support an epidermis in the full thickness skin model after 2 weeks in static conditions, this time-frame was used for future experiments. For this experiment, there were three experimental conditions: 2 weeks static, 1 week static to 1 week perfused with half media changes, and 1 week static to 1 week perfused with media spiking. Three models for each condition were sectioned and analysed. It was decided that early perfusion would not be investigated for 2 weeks dermal equivalents as it did not produce a suitable dermis at 4 weeks (Figure 12). The outcome of this experiment is shown in Figure 13.

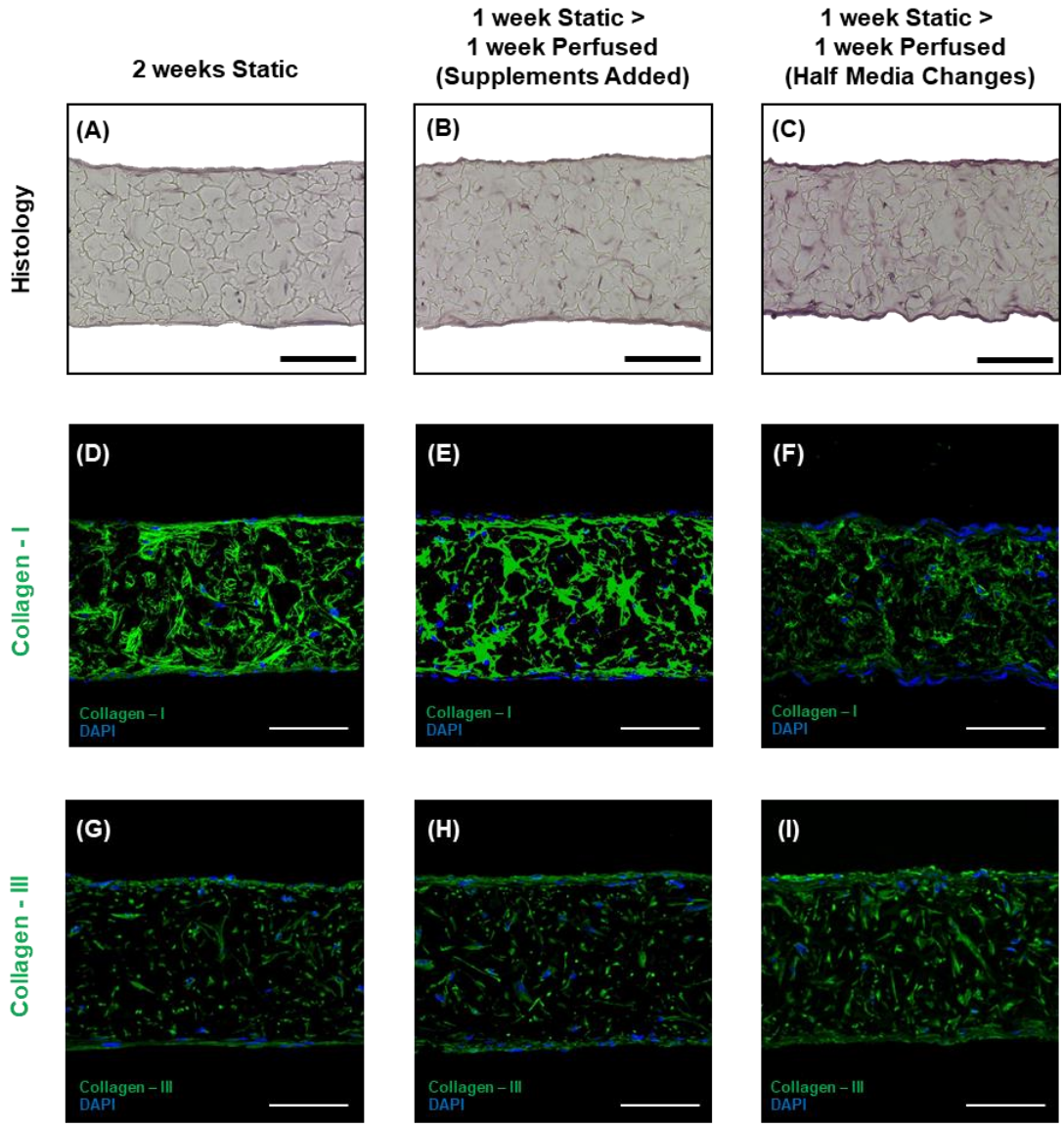

Figure 13: Histological and immunofluorescence analyses of 2-week dermal equivalents grown in varying conditions. (A-C) Histological analyses. (D-F) Collagen-I immunofluorescence images. (G-I) Collagen-III immunofluorescence images. Scale bar: 100 µm.

The histology in Figure 13 shows that the half-media change may be a more superior feeding regime during perfusion than media spiking due to the apparent increased numbers within the Alvetex® Scaffold and on the surface (Figure 13C). Similar to the previous experiment, immunofluorescence of collagen-I and collagen-III was observed. The hypothesis made, based on histology, was that the half media change regime would express greater ECM deposition. The immunofluorescence analysis showed that the presence of Collagen-III was slightly greater with half media changes than with media spiking (Figure 13I); however, the

presence of collagen-I appeared to be greater with media spiking (Figure 13E). Therefore, the observations imply a change in ECM composition rather than an increase in overall ECM deposition.

From the initial experiments above, it is clear that the disruption of unstirred layers caused by perfusion has an effect on the development of dermal equivalents, whether it be beneficial in the case of delayed perfusion, or detrimental in the case of early perfusion. However, this was investigated during the development of dermal equivalents; therefore, the effect of perfusion was determined using mature dermal equivalents.

3.1.2 Increasing the speed of perfusion is detrimental to the integrity of the dermal equivalent

The previous experiments showed that delayed perfusion improved the development of dermal equivalents and formed mature models. Based on this observation, it can be hypothesised that perfusion will also have a beneficial effect on the maintenance of mature dermal equivalents, which have been fully developed in static beforehand. To investigate this, mature dermal equivalents were generated for 28 days in static culture then moved to perfusion for an additional 5 days. For this experiment, another parameter was introduced which could affect the fibroblasts in the dermal equivalent: stir speed. Previously, dermal equivalents were perfused at a stirrer speed of 100 revolutions per minute (rpm). Based on previous literature, speed of perfusion has been shown to affect fibroblast adhesion and proliferation (104). Stir speeds were investigated on dermal equivalents grown for 28 days rather than dermal equivalents grown at shorter time points due to improved stability of mature models.

Mature dermal equivalents were cultured for 28 days in static conditions then cultured for an additional 5 days at different stir speeds (Figure 14). Likewise, three models for each condition were sectioned and analysed. The histology of the models were subsequently viewed to observe differences in the model structure and fibroblast morphology, as shown in Figure 14.

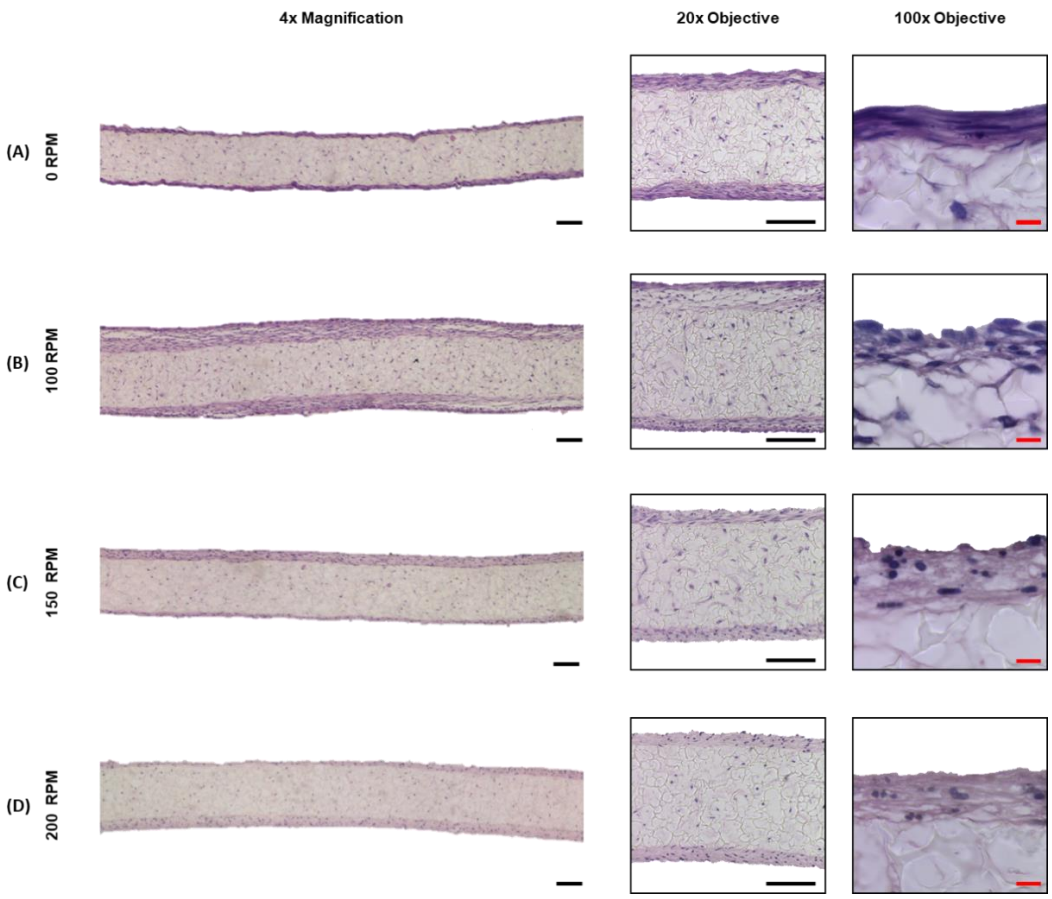

Figure 14: Histological analysis of mature dermal equivalents subject to different stirrer speeds for an additional 5 days. Stir speeds used: (A) 0 rpm; (B) 100 rpm; (C) 150 rpm; (D) 200 rpm. Scale: 4x and 20x objective = 100 µm, 100x objective = 10µm.

Mature dermal equivalents, cultured using different stir speeds, express differences in fibroblast surface layer and fibroblast morphology. In static conditions (Figure 14A), the mature dermal equivalent maintains a thin but dense fibroblast surface layer, with the fibroblasts maintaining their typical elongated morphology. When incorporating perfusion at the standard 100 rpm speed previously used, the fibroblast surface layer thickens, consistent with previous results (Figure 14B). When using a higher magnification, it can be observed that the fibroblasts still look healthy, with an elongated morphology. Moreover, perfusion at 100 rpm does not damage the integrity of the dermal equivalent. Models perfused at higher speeds have a very thin fibroblast surface layer and the fibroblasts begin to lose their elongated morphology (Figure 14C, 14D). At 150 rpm, some of the fibroblasts have adopted to a rounder nuclear morphology, while at 200 rpm, almost all of the fibroblasts have lost their elongated morphology. The change suggests that the fibroblasts are not healthy at faster stirrer speeds.

In summary, dermal compartments can be grown at a stirrer speed of 100 rpm if perfusion is implemented after a delay. Early perfusion appears to be detrimental to the thickness of the dermal compartment, when compared to both the static control and the delayed perfused compartments. Thus, for the remainder of this study, only delayed perfusion was investigated. Additionally, in terms of media feeding regime for models subjected to mixing, there is no clear advantage observed between half media changes and media spiking. With regards to stirrer speed, 100 rpm remains to be optimal for following experiments, when contrasting with higher stirrer speeds investigated.

3.2 The effect of perfusion on full thickness models

Upon identifying that delayed perfusion at 100 rpm improved the development of the dermal equivalent, the next stage of this study was to investigate the effect of perfusion on epidermal development in a full thickness model. As delayed perfusion improved fibroblast proliferation and ECM deposition, it is possible that an improvement in epidermal development would also be observable due to fibroblast and keratinocyte cross-talk. In the following experiments, perfusion was implemented at the ALI, since previous literature has shown that this has benefitted full thickness skin models through the generation of thicker viable epidermis and increased expression of differentiation markers (100–102). Additionally, it is a well-established protocol (7).

Likewise with the dermal equivalents, the effect of perfusion on full thickness models was investigated at the pre-maturation stage and the post-maturation stage, to assess how development and longevity is affected. The standard ALI duration for developing a mature full-thickness model with a stratified epidermis was 14 days. Cells were grown for periods of 7 – 28 days to assess the effects of perfusion on both maturation and longevity. The experimental conditions for full thickness models at the ALI were as follows: static in a deep dish, static in the bioreactor vessel, early perfusion, and delayed perfusion. Similar to above, in each experiment, three models were grown for each condition. However, some models experienced failure during development and only 2 repeats could be acquired for sectioning and analysis.

3.2.1 Development of full thickness models

3.2.1.1 Delayed perfusion increased the epidermal thickness during full-thickness model development

Full thickness models were grown for 7 or 14 days at the ALI. The observed histology of 7 and 14 day models are shown in Figure 15.

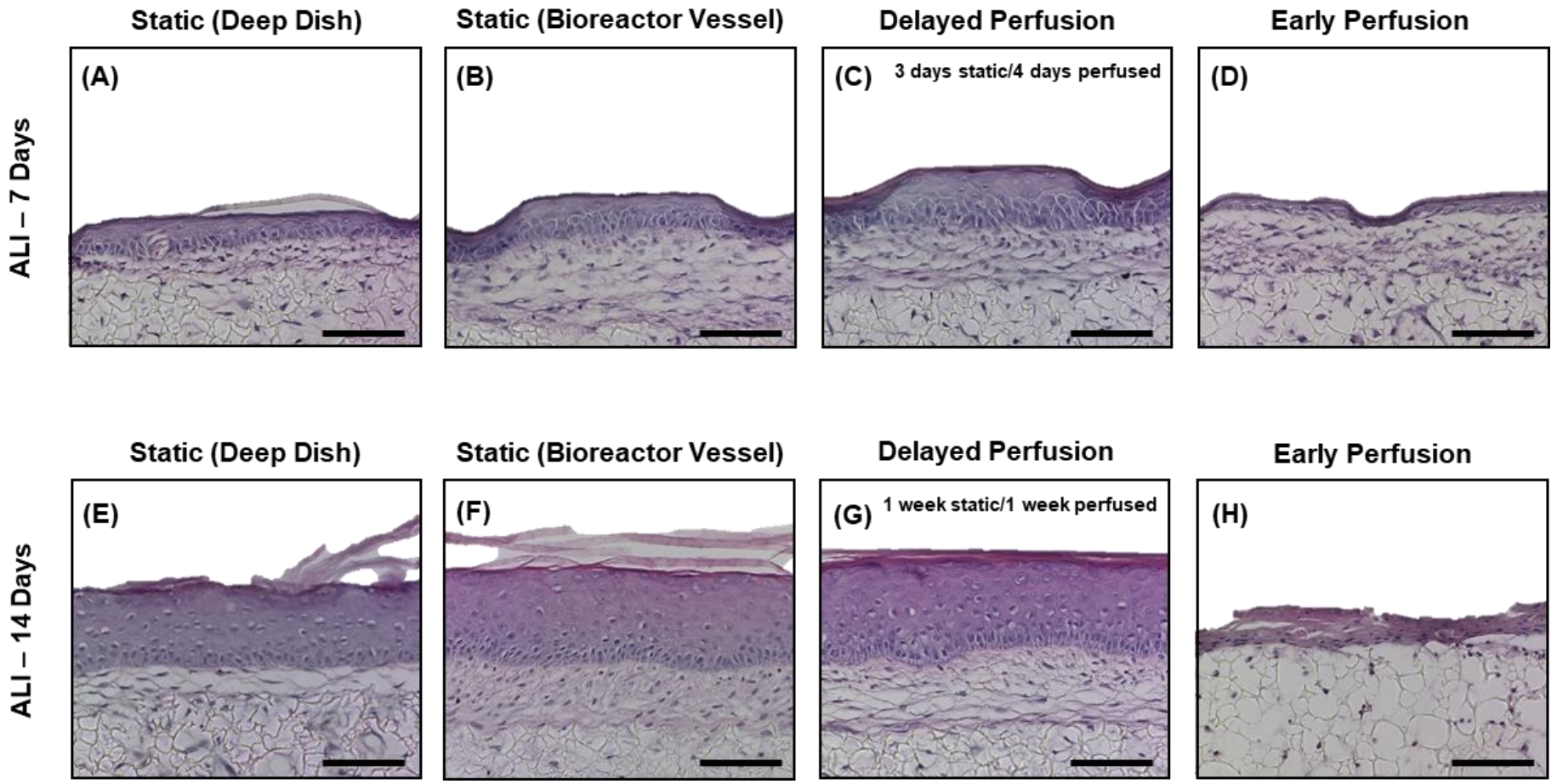

Figure 15: Histological analysis of full thickness models grown at the air-liquid interface (ALI) in varying conditions after 7 and 14 days. (A) 7 days static in deep dish; (B) 7 days static in bioreactor vessel; (C) 3 days static, 4 days perfused; (D) 7 days perfused; (E) 14 days static in deep dish; (F) 14 days static in bioreactor vessel; (G) 7 days static, 7 days perfused; (H) 14 days perfused. Scale: 100µm.

The standard protocol of using static culture in the deep dish (Figure 15A, 15E) produced a stratified epidermal compartment. The models cultured in the bioreactor vessel displayed a thicker epidermis compared to the static control, which suggests that increased media volume has a beneficial effect on epidermal development (Figure 15B, 15F). In addition, when incorporating delayed perfusion, the increase in epidermal thickness is amplified further, and the basal keratinocytes show greater organisation and alignment (Figure 15C, 15G). Therefore, delayed perfusion is shown to have a positive effect on the development of full thickness models.

However, early perfusion does not favour epidermal development based on the histology (Figure 15D, 15H). In 7 day ALI models with early perfusion, the epidermal compartment is significantly thinner than the other conditions. After 14 days in perfusion, the epidermal compartment completely fails as no stratification can be observed, and the epidermis detaches from the dermal compartment. This suggests that full thickness models subjected to early perfusion do not show longevity past 7 day ALI culture.

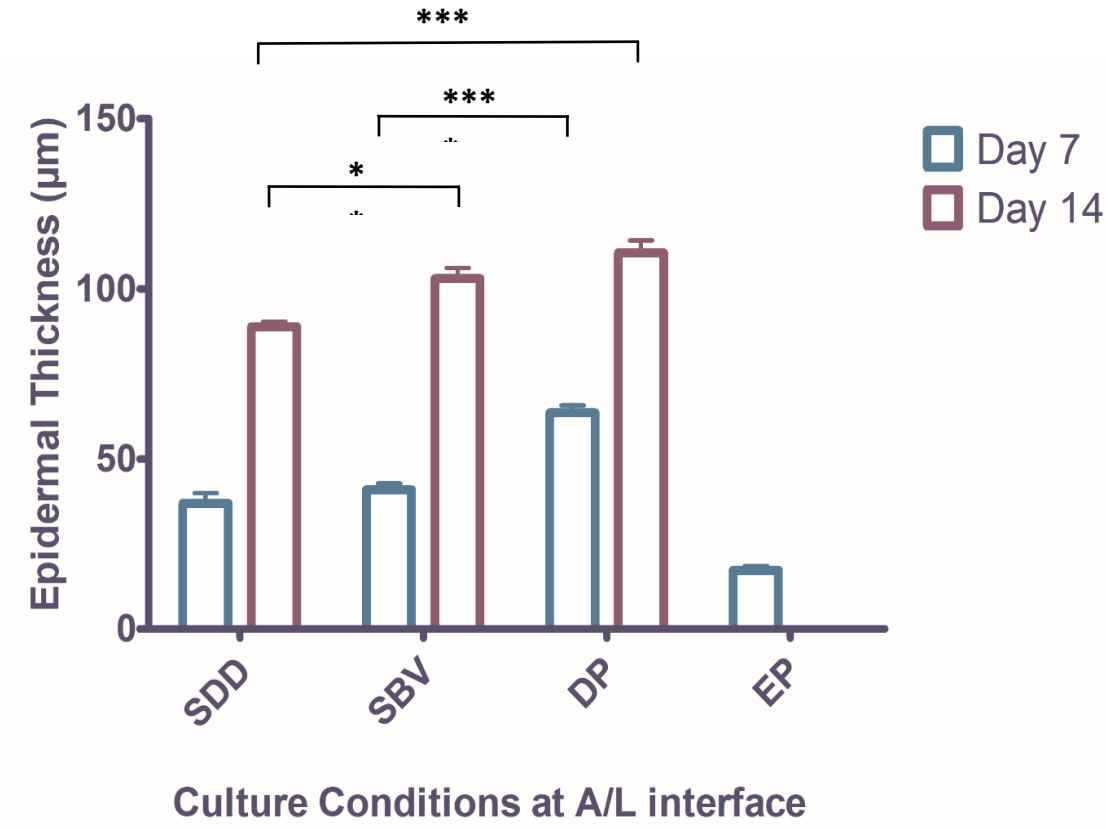

Figure 16: Biometric analysis of epidermal thickness of full thickness models grown in varying conditions at the air-liquid interface (ALI) after 7 and 14 days. (Data represent mean +- SD, number of replicates = 3, number of measurements per replicate = 5). SDD = Static in deep dish, SBV = Static in bioreactor vessel, DP = Delayed perfusion, EP = Early perfusion. Statistical differences are denoted as: ns = P>0.05, * = P≤0.05, ** = P≤ 0.01, *** = P≤0.01, **** = P≤0.0001

Figure 16 confirms the qualitative differences in epidermal thicknesses made from Figure 15. For 7 day ALI full thickness models, there is no significant difference observed between the static controls cultured in the deep dish and bioreactor vessel. However, there is a very significant difference between the static models in the bioreactor vessel and delayed perfusion (P≤0.0001). This suggests that delayed perfusion is the main factor improving epidermal thickness. For 14 day ALI models, there is no significant difference between the static in the bioreactor vessel and delayed perfusion. Instead, there is a significant difference between the two static controls (P≤0.01). This suggests that the increased media volume improves epidermal development over a longer ALI culture duration. A significant difference can also be found between static in the deep dish and delayed perfusion (P≤0.0001) which confirms that the combination of delayed perfusion and increased media volume improves epidermal thickness over time.

3.2.1.2 Delayed perfusion increases proliferation in full thickness models during full thickness model development

It can be hypothesised that the increased epidermal thickness demonstrated in Figures 15 and 16 are attributed to the effect of delayed perfusion on increased proliferation. To understand whether the rate of proliferation in the basal layer of the epidermal compartment influenced epidermal thickness, immunofluorescence analysis of Ki67, a marker of proliferation, was conducted. The Ki67 immunofluorescence and quantification of Ki-67 positive cells in 7 and 14 day ALI full thickness models are shown in Figure 17.

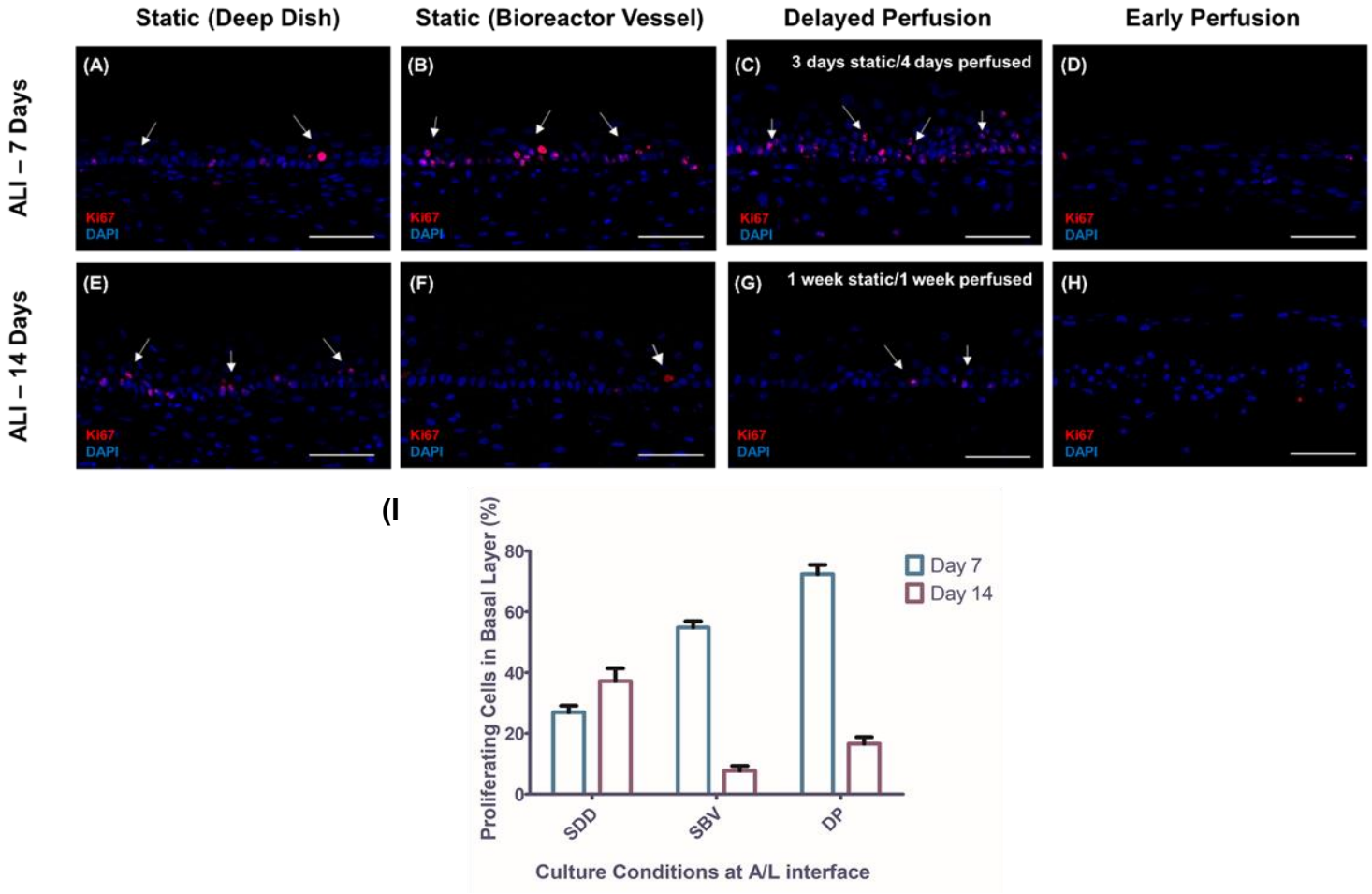

Figure 17: Ki-67 analyses of full thickness models grown for 7 and 14 days ALI culture in different conditions. (A-H) Immunofluorescence analyses. (A) 7 days static in deep dish; (B) 7 days static in bioreactor vessel; (C) 3 days static, 4 days perfused; (D) 7 days perfused; (E) 14 days static in deep dish; (F) 14 days static in bioreactor vessel; (G) 7 days static, 7 days perfused; (H) 14 days perfused.Ki-67 positive cells are found in the basal layer of the epidermal compartment. Arrows show Ki-67 positive cells. Scale: 100µm (I) Quantitative analysis. Early perfused models was excluded as there was no significant expression in the basal layer. SDD = Static Deep Dish, SBV = Static Bioreactor Vessel, DP = Delayed Perfusion (Number of replicates = 2, Number of measurements per replicate = 3).

The rate of basal keratinocyte proliferation is affected by increased media volume and delayed perfusion, as shown in Figure 17, however, it is dependent on the duration of ALI culture. Comparing all conditions, the static control in the deep dish is shown to have consistent proliferation between 7 (Figure 17A) and 14 (Figure 17E) days ALI. Immunofluorescence analysis of 7 days ALI models show that the number of Ki-67 positive cells greatly increase when increasing media volume and incorporating delayed perfusion, with 72.4% of the total cells in the basal layer undergoing proliferation (Figure 17B, 17C). On the other hand, there are very few Ki-67 positive cells in 14 day ALI models grown with increased media volume and delayed perfusion, compared to the traditional static condition (Figure 17F, 17G); where the percentage of proliferative cells drops below 20%. Early perfused models, which did not form viable epidermal compartments, did not express Ki-67 positive cells and did not show a distinct basal layer.

The Ki-67 data suggests that delayed perfusion at the ALI influences the rate of proliferation. The increased epidermal thickness in models grown with delayed perfusion, observed in Figure 15 may be caused by an increase in proliferation for the first 7 days of ALI. However, proliferation does not seem to be the major determinant of increased epidermal thickness beyond that duration. Therefore, early, mid, and terminal differentiation was also analysed.

3.2.1.3 Delayed perfusion affects early-mid differentiation of keratinocytes during full thickness model development

Since Section 3.2.1.2 identified that delayed perfusion does not improve proliferation post-7 days ALI, it was hypothesised that improvements in epidermal thickness may be attributed to delayed perfusion stimulating changes in differentiation. K10 and K14 was observed as markers for early/mid differentiation, whilst filaggrin was observed for terminal differentiation. As early perfused models at 14 days ALI had a detached epidermal compartment, it was excluded from further analyses.

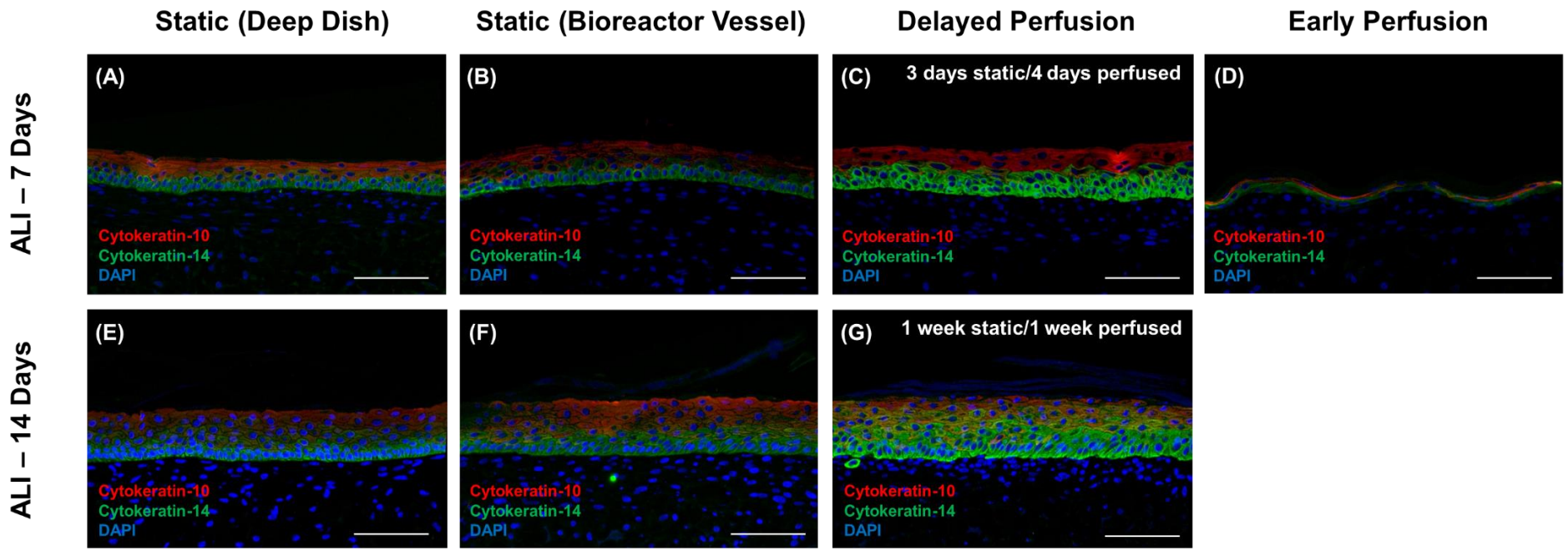

Figure 18: Cytokeratin-10 and cytokeratin-14 immunofluorescence analyses of full thickness models grown for 7 and 14 days ALI culture in different conditions. (A) 7 days static in deep dish; (B) 7 days static in bioreactor vessel; (C) 3 days static, 4 days perfused; (D) 7 days perfused; (E) 14 days static in deep dish; (F) 14 days static in bioreactor vessel; (G) 7 days static, 7 days perfused. Scale: 100µm

Figure 18 shows that delayed perfusion increases the expression of K14 during the development of full thickness models. In both static controls, the expression of K10 and K14 remain similar despite an increased epidermal thickness in the static bioreactor vessel condition based on distribution within the epidermal compartment, and to an extent, intensity. For models grown with delayed perfusion, the intensity of K10 is also similar to the other conditions, but K14 is shown to have a more intense fluorescence (Figure 18C, 18G). The increased intensity for K14 is consistent for both 7 and 14 days ALI culture and suggests that delayed perfusion does have a profound effect on the early differentiation of keratinocytes. Additionally, K14 is usually found strictly in the basal layer of the epidermal compartment as a marker for early differentiation. In the models cultured with delayed perfusion, K14 is highly expressed beyond the basal layer, particularly with the 14 days ALI culture (Figure 18G). Based on the K14 observation, it is possible that the keratinocytes above the basal layer are undergoing hyperproliferation. Although early perfusion did not yield a thick epidermal compartment, there is evidence of some differentiation (Figure D).

Upon identifying that early differentiation was improved by delayed perfusion, terminal differentiation was subsequently observed, as shown in Figure 19. Based on literature, it was hypothesised that perfusion would improve terminal differentiation (100).

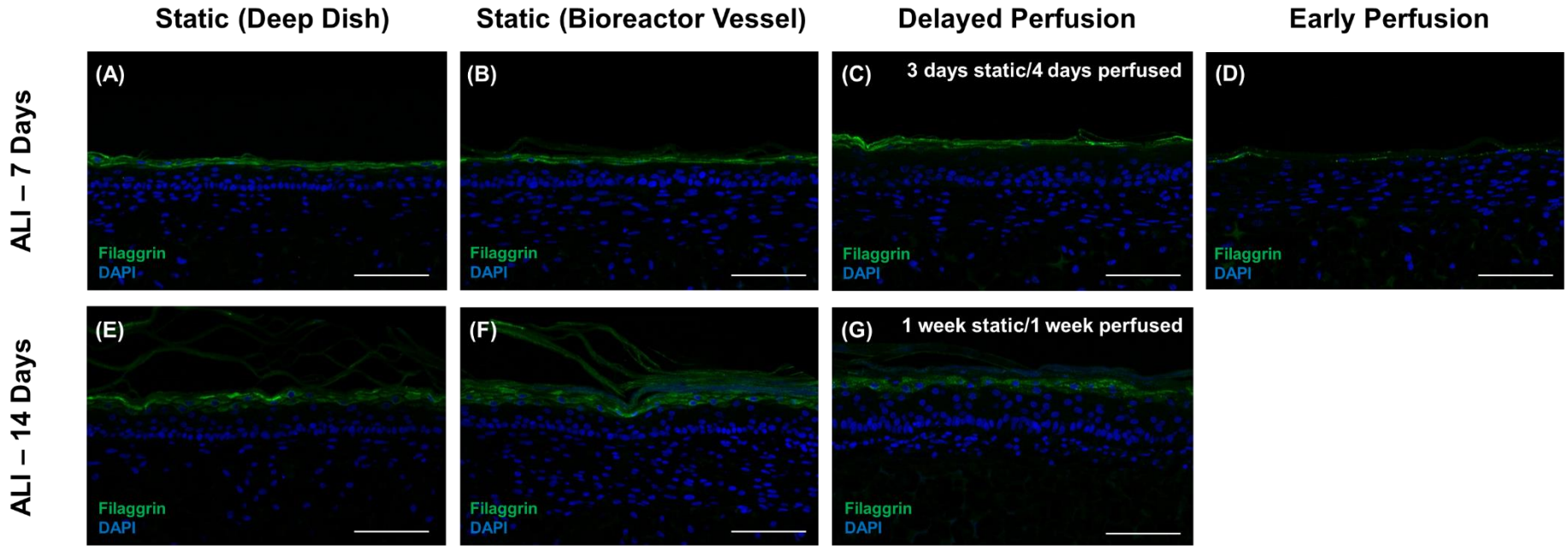

Figure 19: Filaggrin immunofluorescence analysis of full thickness models grown at the air-liquid interface (ALI) in varying conditions after 7 and 14 days. A) 7 days static in deep dish; (B) 7 days static in bioreactor vessel; (C) 3 days static, 4 days perfused; (D) 7 days perfused; (E) 14 days static in deep dish; (F) 14 days static in bioreactor vessel; (G) 7 days static, 7 days perfused. Scale: 100 µm

Contrary to the literature, terminal differentiation of full thickness models was not affected by delayed perfusion, as shown in Figure 19. All conditions expressed filaggrin, which is indicative of the epidermal barrier, however perfusion did not affect filaggrin staining. All conditions express filaggrin layers that are approximately 2 layers thick, which is expected for the granular layer. Although it may appear that the filaggrin band is thicker in the static bioreactor vessel condition at 14 days (Figure 19F), it may be that the staining observed in the stratum *corneum* is non-specific. The height of the filaggrin layer differs between all conditions but this occurs due to differences in epidermal thicknesses and cannot be correlated with any changes in terminal differentiation; the height corresponds to the position of the *stratum granulosum* in each model.

So far, the effect of perfusion on the structure and physiology of the epidermal compartment have been analysed. However, the effect of perfusion on function has yet to be understood. Therefore, the barrier function was analysed by measuring TEWL.

3.2.1.4 Early perfusion is not beneficial to the barrier function of the epidermis during full-thickness model development

The barrier function of the 7 and 14 day ALI models was observed by measuring TEWL. The average measurements for the TEWL of 7 and 14 day ALI models are shown in Figure 20.

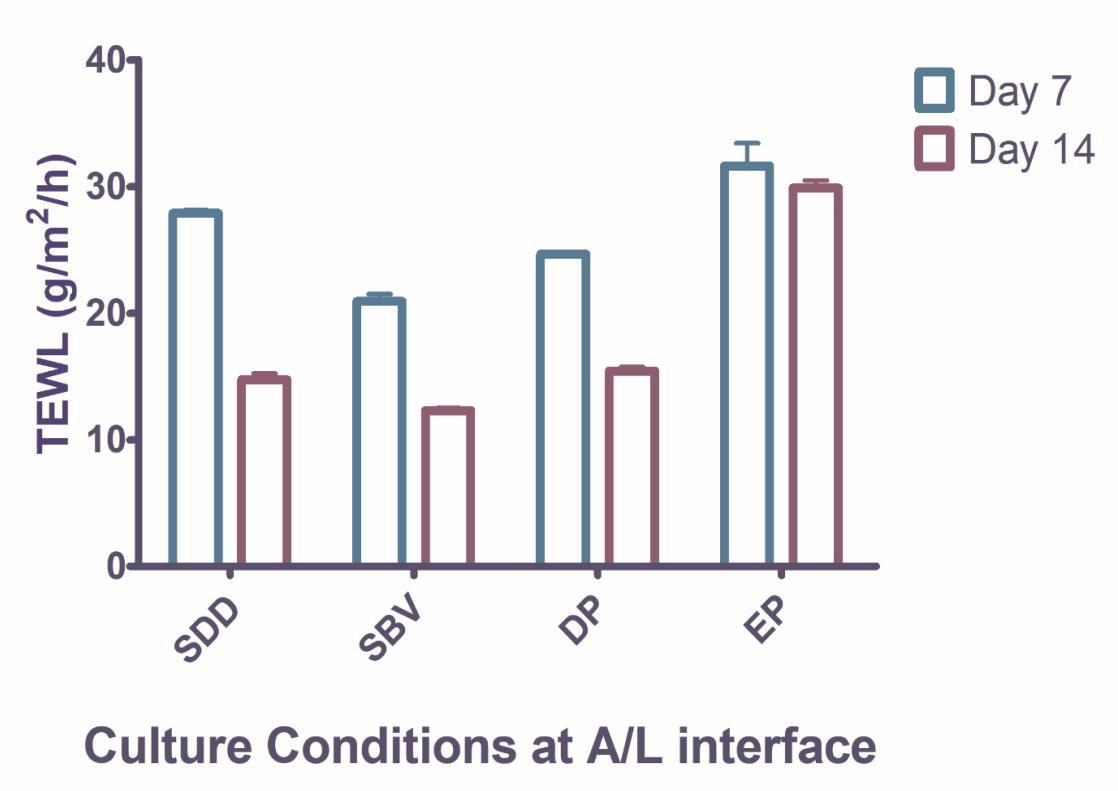

Figure 20: Biometric analysis of trans-epidermal water loss (TEWL) of full thickness models grown in varying conditions at the air-liquid interface (ALI) after 7 and 14 days. Data represent mean +- SD, number of replicates = 1, number of measurements per replicate = 3). SDD = Static in deep dish, SBV = Static in bioreactor vessel, DP = Delayed perfusion, EP = Early perfusion.

The TEWL measurements indicate that early perfusion is detrimental to barrier function. Early perfused models, which have been subjected to perfusion for a longer duration of time, have a TEWL measurement of 30 $g/m^2/h$, which is significantly higher than the other conditions and indicative of a poor barrier. The poor barrier function of perfused models is expected based on the histological and terminal differentiation analyses performed previously. In contrast, models grown in static within the bioreactor vessel have the lowest TEWL values at 7 and 14 days, indicating that increased media volume improves TEWL. Generally, Day 14 TEWL values are lower than Day 7 TEWL values, with delayed perfusion having slightly higher TEWL than the static bioreactor; however, it is still within a physiological range. This is expected as there would be a more mature barrier after a longer duration of epidermal development. In all of these descriptions, it is difficult to draw any true conclusions between the static deep dish and perfused models - it is better to compare the perfused models to the static bioreactor to determine the effect of perfusion alone.

Using the 7 and 14 day ALI models, it was possible to observe the effect of perfusion on structure, physiology, and structure of full thickness models that are still in the development stage. Similarly to the studies on dermal equivalents, delayed perfusion is identified to be the best condition for improving the development of skin models, as it improved the epidermal thickness, short-term proliferation, and early differentiation. As delayed perfusion improved development, the next stage was to identify whether perfusion improved the longevity of full thickness models.

3.2.2 Longevity of full thickness models

The longevity of full thickness models refers to the duration that models are able to maintain a viable epidermis in which keratinocytes proliferate and differentiate efficiently. The ALI culture duration can be extended to investigate the effect of perfusion on longevity rather than development. It was hypothesised that delayed perfusion would improve longevity of the models, in addition to development. As the epidermis failed after day 14 in early perfused models, only models grown with delayed perfusion were observed in this part of the study.

3.2.2.1 Delayed perfusion maintains increased epidermal thickness at 21 days ALI but fails to improve longevity at 28 days ALI

Full thickness models were grown for 21 and 28 days ALI culture to assess longevity. The histology of these models are shown in Figure 21.

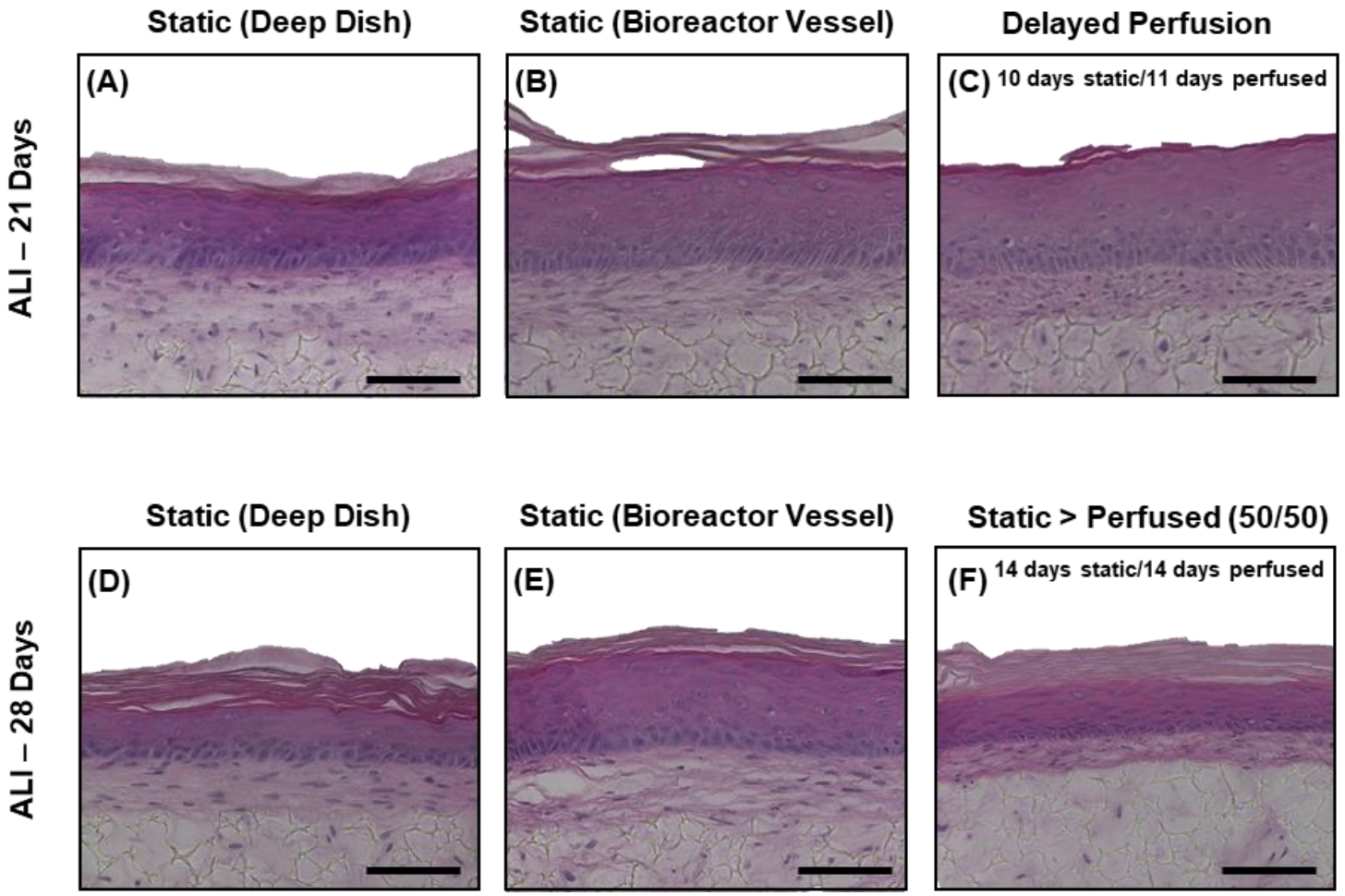

Figure 21: Histological analysis of full thickness models grown at the air-liquid interface (ALI) in varying conditions after 21 and 28 days. (A) 21 days static in deep dish; (B) 21 days static in bioreactor vessel; (C) 10 days static, 11 days perfused; (D) 28 days static in deep dish; (E) 28 days static in bioreactor vessel; (F) 14 days static, 14 days perfused. Scale: 100 µm

The histology in Figure 21 shows that increased media volume and delayed perfusion improve the thickness of the viable epidermis at 21 days ALI, but only increased media volume maintains similar thickness at 28 days ALI. At 21 days ALI, both static (Figure 21B) and perfused models (Figure 21C) grown in a bioreactor vessel generate a thicker epidermis than the traditional static deep dish control. However, at 28 days ALI, only the static in the bioreactor vessel condition produces models that are able to maintain a thick epidermis (Figure 21E). Delayed perfusion fails to maintain the thickness observed at 21 days ALI, and the viable epidermis appears similar to the traditional static control by 28 days ALI (21F). Further insight into epidermal thickness was conducted using quantitative measurements as shown in Figure 22 below.

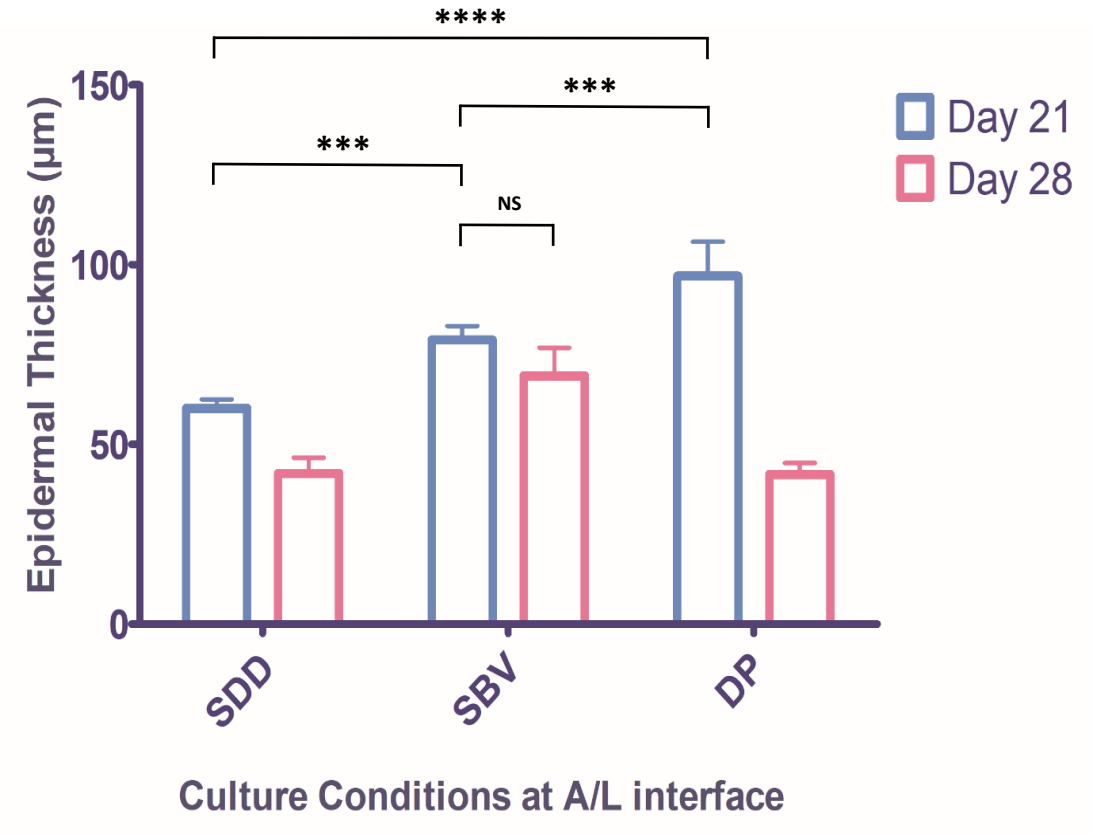

Figure 22: Biometric analysis of epidermal thickness of full thickness models grown in varying conditions at the air-liquid interface (ALI) after 21 and 28 days. (Data represent mean +- SD, number of replicates =3, number of measurements per replicate = 5). SDD = Static in deep dish, SBV = Static in bioreactor vessel, DP = Delayed perfusion, EP = Early perfusion. Statistical differences are denoted as: ns = P>0.05, * = P<= 0.05, ** = P<= 0.01, *** = P<0.01, **** = P<=0.0001

The measurements in Figure 22 shows that delayed perfusion has the thickest viable epidermis at 21 days ALI. At this time point, there is a significant difference between each condition, with increased media volume and delayed perfusion showing a beneficial effect on epidermal thickness. However, at day 28, the static deep dish condition and the delayed perfusion condition shows a drastic difference from their day 21 counterparts. Both of these conditions display a thinner epidermis than the static bioreactor vessel condition, but it can still be classed as a good epidermis based on previous in-lab results (~40-50µm). Unexpectedly, there is no significant difference in epidermal thickness when grown in the static bioreactor vessel condition from 21 to 28 days. From these measurements, it can be suggested that delayed perfusion is only beneficial for the maintenance of full thickness models up to 21 days, and increased media volume in static conditions is preferred for longer maintenance post-21 days.

3.2.2.2 Delayed perfusion does not improve or maintain proliferation of keratinocytes in long-term mature full thickness models

Based on the histology in Section 3.2.2.1, it was hypothesised that there would be greater proliferation at day 21 in all conditions than at day 28. Additionally, it was expected that models grown in delayed perfusion would have greater proliferation, accounting for improved epidermal thickness at day 21, while the static bioreactor vessel condition would maintain improved proliferation at day 28. The immunofluorescence and quantitative measurements for proliferation are shown in Figure 23.

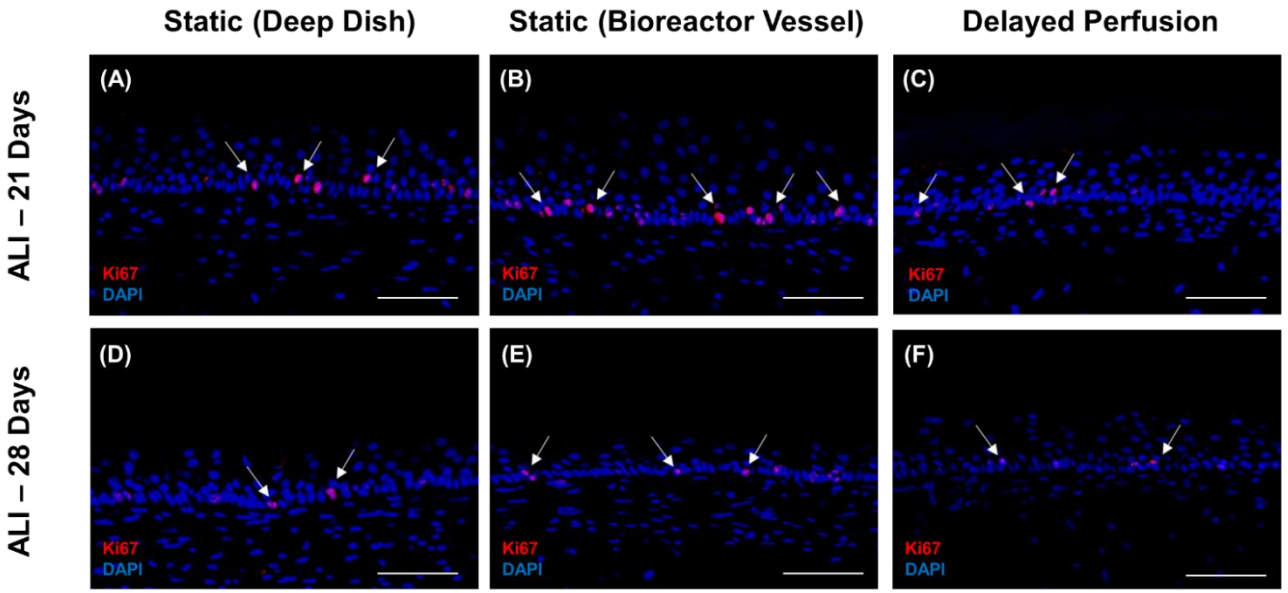

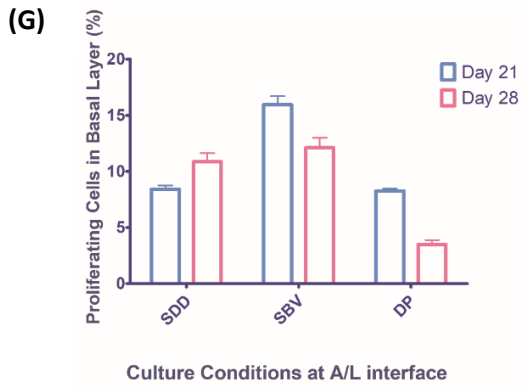

Figure 23: Ki-67 analyses of full thickness models grown for 21 and 28 days ALI culture in different conditions. (A-H) Immunofluorescence analyses. Arrows show Ki-67 positive cells. Scale: 100 µm (I) Quantitative analysis. A graph of the percentage of Ki-67 positive cells in the basal layer of the epidermis. SDD = Static Deep Dish, SBV = Static Bioreactor Vessel, DP = Delayed Perfusion (Number of replicates = 2, Number of measurements per replicate = 3).

The immunofluorescence shows that delayed perfusion does not improve proliferation at both day 21 and day 28. The static bioreactor vessel condition is shown to have the greatest number of Ki-67 positive cells in the basal layer, suggesting that it is the optimal condition for maintaining proliferation. Based on observations, at day 21 and day 28 respectively, proliferation in models grown with delayed perfusion is similar to that in the static deep dish condition. The quantitative measurements give further clarity on the differences between conditions at different time points. It can be confirmed that the proliferation in delayed perfused models is similar to the static deep dish control, however, differences can be observed at day 28. In the latter time point, delayed perfusion is detrimental to maintaining proliferation as the rate is much lower than both static conditions; additionally, proliferation is shown to increase in the static deep dish control. This can be characterised by the observation that the rate of proliferation from both static controls at day 28 are more than double that of models subjected to delayed perfusion.

3.2.2.3 Delayed perfusion improves early, mid, and terminal differentiation of mature full thickness models at 21 days culture but has minimal impact at 28 days

As the increased epidermal thickness caused by delayed perfusion was not correlated with increased proliferation, it was hypothesised that increased thickness was correlated to improved differentiation. Firstly, early/mid differentiation was analysed as shown in Figure 24.

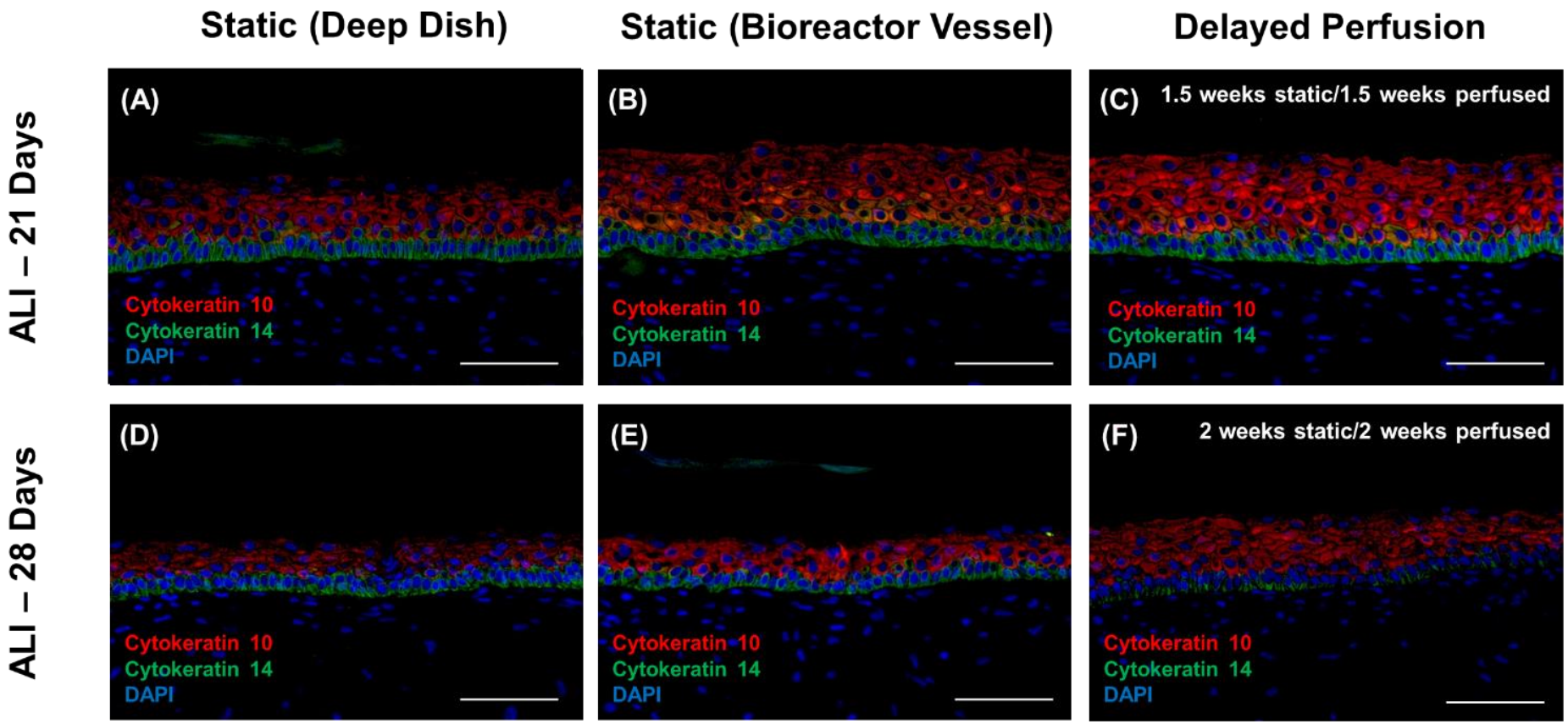

Figure 24: Cytokeratin-10 and cytokeratin-14 immunofluorescence analyses of full thickness models grown for 21 and 28 days ALI culture in different conditions. Scale: 100µm

Analysis of K10 and K14, as shown in Figure 24, shows that both biomarkers are highly expressed in models grown with delayed perfusion at day 21, and appear to be less expressed by day 28. At day 21, all conditions express a clear K10 and K14 expression. The localisation of K14 is consistent and is present in the basal layer, while K10 is expressed above the basal layer. The models grown for 28 days in the static deep dish and delayed perfusion conditions show that the expression of K10 and K14 may be significantly downregulated compared to their day 21 compartments; however further research needs to be undertaken. Interestingly, for day 28 models grown with delayed perfusion, the fluorescence of K14 is almost completely absent which suggests that early differentiation ceases earlier with perfusion (23F). The expression of K10 and K14 is consistent for both time points in models grown in a static bioreactor vessel (23B, 23E). The early/mid differentiation immunofluorescence shows greater correlation with the histology and epidermal thicknesses described in Section 3.2.2.1, compared to the proliferation analysis in Section 3.2.2.2. Therefore, it can be suggested that in terms of longevity, the effects of delayed perfusion are more correlated with differentiation. For further analysis, terminal differentiation was also observed, as shown in Figure 25 below.

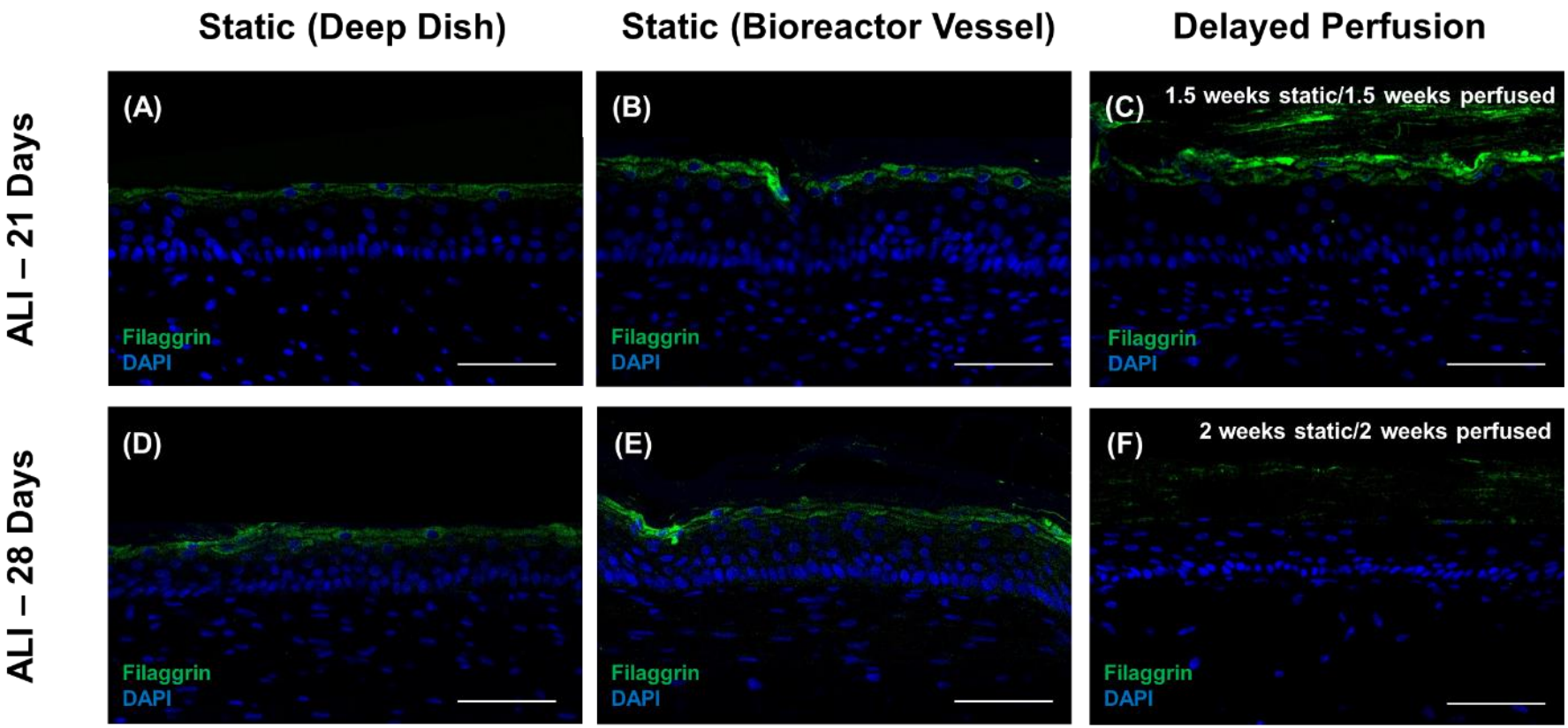

Figure 25 Filaggrin immunofluorescence analysis of full thickness models grown at the air-liquid interface (ALI) in varying conditions after 21 and 28 days. Scale: 100um

As shown in Figure 25, delayed perfusion greatly upregulates filaggrin expression at day 21, but is almost unobservable by day 28. Between conditions at day 21, increased media volume and delayed perfusion both contribute to improved thickness of the filaggrin band in the *stratum granulosum* at day 21, with the latter producing the thickest band of filaggrin. At day 28, the thickness of filaggrin bands are maintained in both static conditions (21D, 21E), but no band can be observed in the delayed perfusion condition (21F). Traces of filaggrin can still be observed at day 28 in the *stratum corneum* but is faint and discontinuous. The trends of terminal differentiation are comparable to that of early/mid differentiation and suggests that delayed perfusion may not bring any benefits for long term maintenance of full thickness models post-21 days.

3.2.2.4 Delayed perfusion greatly increases TEWL at day 28

After identifying the physiology of long-term full thickness models in different conditions, the barrier function of these models was also investigated. For longer term models, a thicker *stratum corneum* would generally be expected, and this would correlate with increased resistance to TEWL. The filaggrin bands observed in Section 3.2.2.3, as a marker for terminal differentiation, are a foundation for providing a hypothesis on barrier function. It was hypothesised that at day 21, the barrier function of delayed perfused models would be improved, in line with increased filaggrin band thickness. However, based on previous TEWL results with short term full thickness models, it can be suggested that perfusion may have a negative effect due to slightly higher TEWL values. The TEWL measurements are shown in Figure 26.

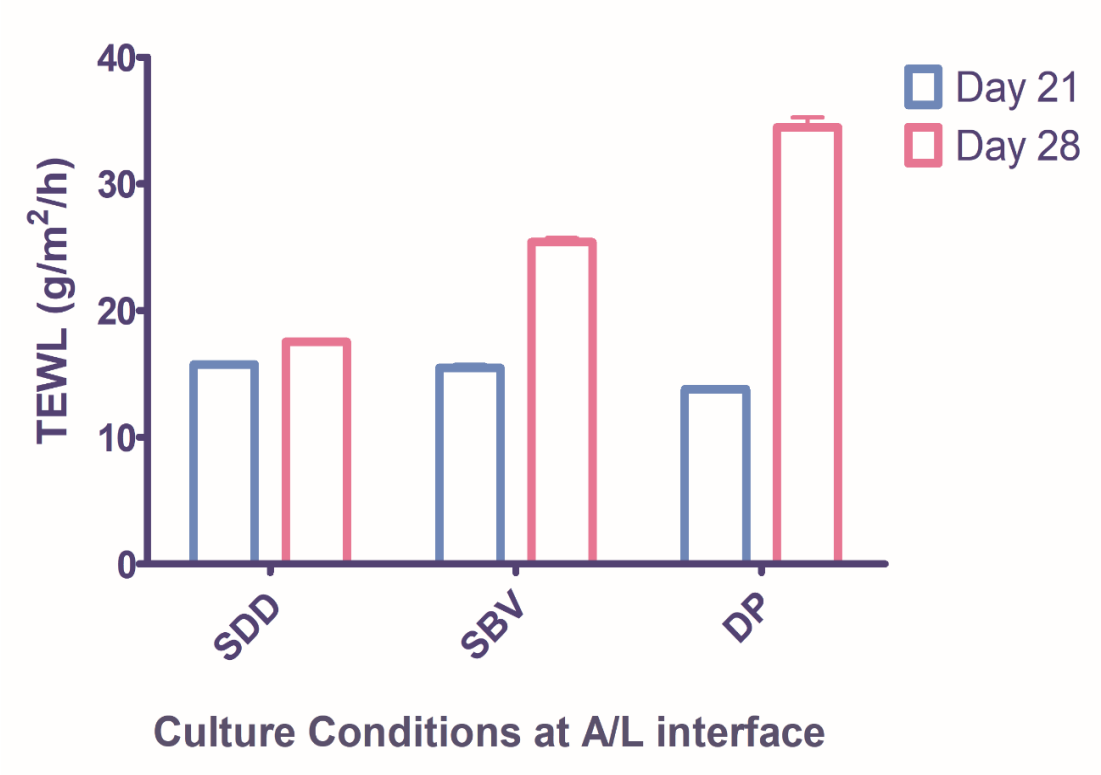

Figure 26: Biometric analysis of trans-epidermal water loss (TEWL) of full thickness models grown in varying conditions at the air-liquid interface (ALI) after 21 and 28 days. Data represent mean +- SD, number of replicates = 1, number of measurements per replicate = 3). SDD = Static deep dish, SBV = Static bioreactor vessel, DP = Delayed perfusion, EP = Early perfusion.

The TEWL of all conditions, as shown in Figure 26, were similar at day 21, in the range of 10-20g/m^2/h. However, at day 28, there is a drastic difference between all conditions, with delayed perfusion displaying the greatest TEWL at approximately 34.5g/m^2/h. The increased TEWL in the day 28 delayed perfusion model may be correlated with absence of filaggrin in Figure 25. Comparing all conditions in general, the static deep dish condition is the most consistent at maintaining TEWL between day 21 and day 28. This can be correlated to a similar filaggrin thickness and maintained stability between time points found in the previous section.

Based on the above analyses, it can be concluded that delayed perfusion is beneficial to the maintenance of mature full thickness models, in terms of epidermal thickness and differentiation, for culture durations up to 21 days. After 21 days, delayed perfusion is observed to have a poor barrier function, but not entirely detrimental as model morphology is still maintained.

3.2.3 The effect of perfusion speed at the ALI

When investigating the effect of perfusion on short-term and long-term full thickness models, a speed of 100 rpm was used. In Section 3.2.1.1, it was found that early perfused models at 100 rpm all failed by 14 days, therefore it is of interest to investigate early perfusion at a lower speed such as 50 rpm. The hypothesis is that with a lower perfusion speed, early perfusion will yield similar beneficial effects as delayed perfusion. No literature can be found pertaining to the effect of speed in stirrer-based bioreactors, but there are some which exist in rotary systems. These studies suggest that lower stirrer speeds can aid development in skin-related cell studies (106). Moreover, it has been identified that a slower speed which is amplified later in culture shows improved keratinocyte development (95). It can therefore be hypothesised that a lower slow speed will induce lower shear stress, thus improving keratinocyte adhesion and proliferation.

3.2.3.1 Early perfusion, regardless of stir speed, fails to develop a stratified epidermal compartment

Full-thickness models were generated using the standard protocol, with 14 days at the ALI. However, the conditions were varied at the start of the ALI, and these are as follows: (A) 14 days static deep dish; (B) 14 days perfused at 50 rpm; (C) 14 days perfused at 100 rpm; and (D) 7 days perfused at 50rpm to 7 days perfused at 100 rpm. The histology of these models are shown in Figure 27.

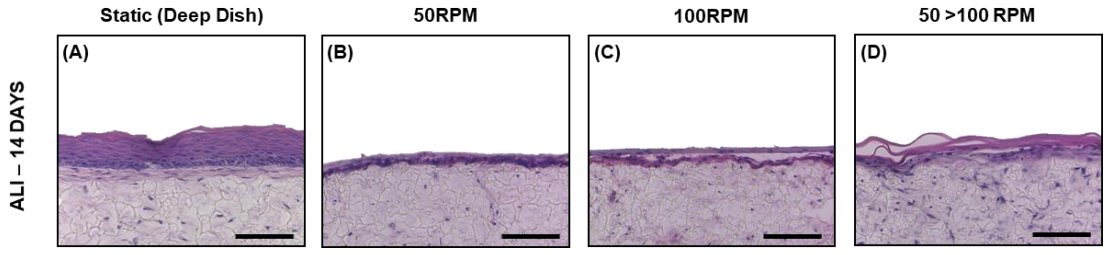

Figure 27: Histological analysis of early perfused full thickness models grown at different stirrer speeds for 14 days air-liquid interface (ALI) culture. The static control produced a stratified epidermal compartment (A), but early perfused models did not, regardless of stirrer speed (B-D). Scale: 100 µm.

The histology in Figure 27 shows that early perfusion is detrimental to the development of a stratified epidermis, regardless of stirrer speed. From all experimental conditions, only the static control produced a stratified epidermis reminiscent of *in vivo* skin. The early perfused models, regardless of stirrer speeds, formed a thin layer of keratinocytes on the surface of the dermal compartment. With higher stirrer speeds, the thin keratinocyte layer detaches which implies that this layer can be easily displaced by perfusion. It can be concluded based on these findings that delayed perfusion is the only condition in which perfusion improves the development and maintenance of full thickness models.

The above experiments demonstrate the effect of disrupting unstirred layers *in vitro* on the development and maintenance of skin models. To explain how perfusion and stirrer speeds may potentially impact skin models, the final part of this study investigates the CFD within the bioreactor.

3.3 Fluid modelling of the perfusion apparatus

It was hypothesised based on literature that perfusion speed impacted the disruption of unstirred layers, but also increased shear stress on adjacent cells. Therefore, in addition to analysis of *in vitro* models, this study also looked at the fluid mechanics which occurred within the bioreactor apparatus used in this study. For this experiment, there were four fluid modelling files used which were adjusted to take into account ALI culture and different stirrer speeds. Using Fluent 19.2 software, fluid modelling files of the bioreactor apparatus at 50, 100, 150, and 200 rpm environments were analysed.

3.3.1 Direction of flow is consistent for all stirrer speeds, but the range in velocity increases as stirrer speed increases

Using Fluent 19.2, vectors were applied to investigate the direction of flow of fluid and contours were applied to investigate velocity in the XY plane of the bioreactor apparatus, as shown in Figure 28. The vectors show that fluid is circulated in a similar motion regardless of stirrer speed. Fluid is moved in an upwards and outwards motion from the base of the vessel's inner region, where the magnetic stirrer is situated, to the outer edges of the vessel. As fluid is moved upwards, the fluid is subsequently drawn back inwards towards the base of the Alvetex and forced to steeply flow downwards back towards the stirrer. This cycle is then repeated. Using this information, paired with velocity contours, it can be observed that the range of velocity increases as stirrer speed is increased. The contours show that the speed of fluid flow is most intense at both ends of the magnetic stirrer and decreases as fluid

moves upwards and outwards. When the fluid is drawn inwards and reaches contact with the Alvetex® Scaffold, the intensity of the velocity contour pushing the fluid downwards increases again; the intensity of which depends on how fast the stirrer speed is.

While the contours and vectors give an implication of how fluid flow and stirrer speed are connected in the apparatus used, it does not give a clear indication of how these findings actually affects the cells in the model. Therefore, calculations were conducted to investigate the shear stress at the surface of the models in contact with the media and identify the flow rates of the perfusion systems at different speeds; the latter of which would be relevant to comparing with perfused systems in past literature.

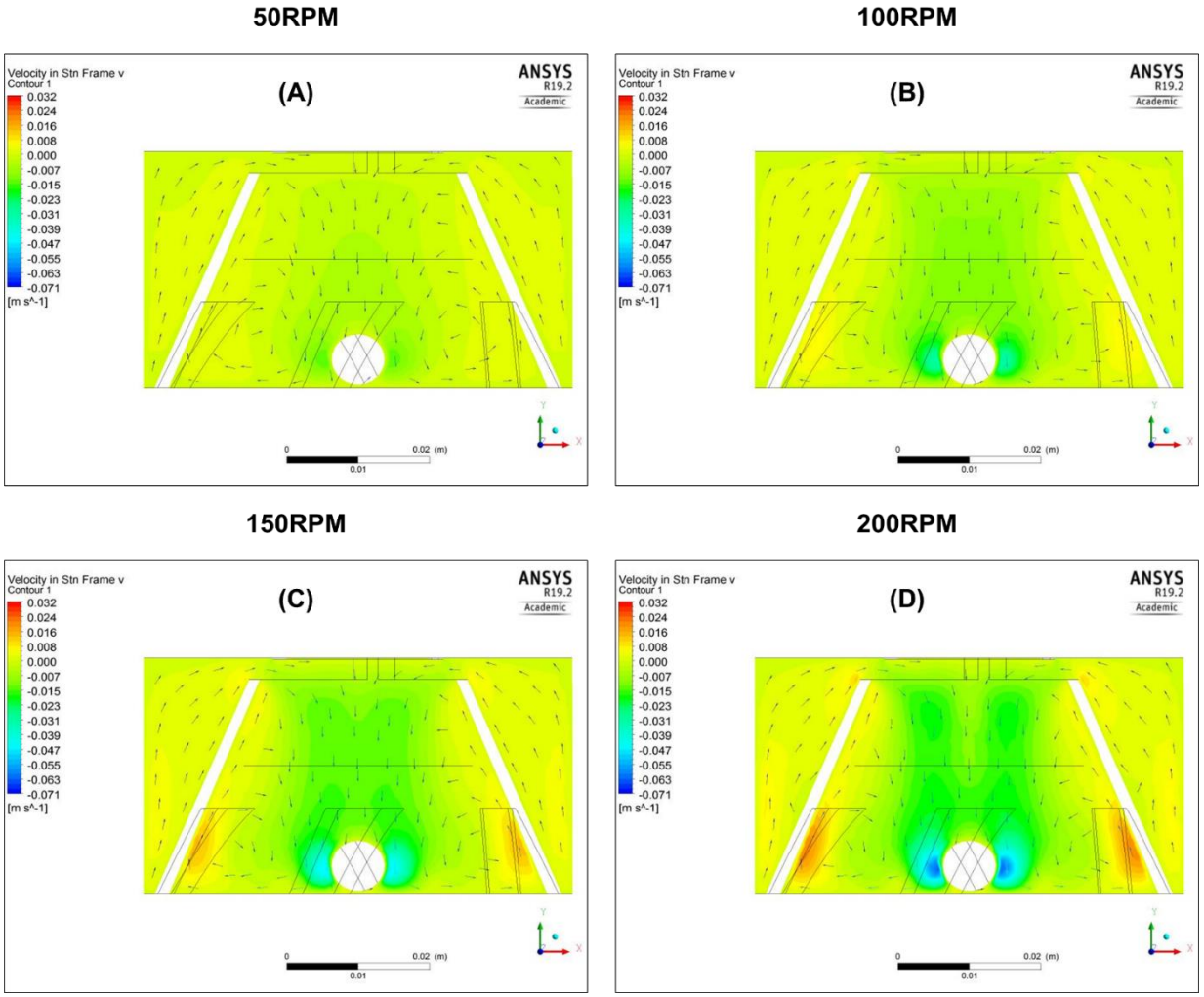

Figure 28: Velocity contours and fluid flow vectors for the bioreactor apparatus at the air-liquid interface (ALI), at different speeds. The direction of fluid flow is similar for all conditions. However, the velocity contours become more intense with higher speeds, particularly in (D). Scale is given on the diagram

3.3.2 Shear stress and flow rate increased with increasing stirrer speed

The function calculator in Fluent 19.2 was used to calculate shear stress and flow rate, independently, where the fluid moves adjacent to the surface of the Alvetex® Scaffold. This would give an estimation of the above parameters where fluid is closest to the cells. Table 5 below shows that shear stress increases as stirrer speed increases. As speed is raised by increments of 50 rpm, the resultant increase in shear stress is exponential. The greatest increase in shear stress is between 150 rpm to 200 rpm whereby the increase in shear stress is ~0.019Pa, compared to ~0.003Pa between 50 rpm and 100 rpm. The difference in shear stress between 50 rpm and 200 rpm is significant, as it is approximately 22-fold. Additionally, in Table 6, it can also be observed that flow rate also increases as stirrer speed increases by increments of 50 rpm. The difference in flow rate between 50 rpm and 200 rpm is approximately 9-fold. From the calculations, the increase in shear stress is the most significant consideration to make. As shear stress is detrimental to the fibroblasts, maintaining lower stirrer speeds at 50 rpm and 100 rpm seems more reasonable to use due to higher increases in shear stress with 150 rpm and 200 rpm.

Table 5: Shear stress calculations for the fluid-substrate interface during air-liquid interface (ALI) perfusion at different stirrer speeds.

Stirrer Speed (RPM)	Shear Stress (Pa)
50	0.00125871
100	0.00401156
150	0.00797487
200	0.0265924

Table 6: Flow rate calculations for the fluid-substrate interface during air-liquid interface (ALI) perfusion at different stirrer speeds.

Stirrer Speed (RPM)	Flow Rate (ms^{-1})
50	0.00331503
100	0.0102955
150	0.0188827
200	0.0298979

Chapter 4: Discussion

In this section, the phenomenon observed in this study when Alvetex® Scaffold dermal and full thickness models are grown in dynamic culture using our novel magnetic stirrer-based bioreactor will be discussed. By disrupting the unstirred media layers that form in static culture, it was anticipated that perfusion of the models through media mixing would improve the development and maintenance of skin models. In hindsight, I observed changes in the structure, physiology, and function of the models. Additionally, by investigating parameters which may influence model development and maintenance, a link between stirrer speed, shear stress, and model quality was identified.

4.1 Incorporation of fluid flow in dermal models

3D *in vitro* skin models have previously been established as potential replacements for ex vivo human and animal tissue, in fields such as basic skin research, cosmetic development, and drug testing studies. However, ongoing research on how to optimise these models is crucial. In this study, I aimed to improve the development of full thickness skin models through dynamic culture, which could remove diffusion-limiting unstirred layers and enable cells to be perfused, similar to *in vivo* vasculature. Initially, it was found that *in vitro* dermal compartments were influenced by dynamic culture in terms of structural development, ECM deposition, and nuclear morphology.

4.1.1 Initial adhesion of fibroblasts is hindered by shear stress

During the development of dermal compartments, a thicker surface layer of dermal fibroblasts was formed under the influence of delayed perfusion (Figure 12). On the contrary, early perfusion led to a thinner fibroblast layer. Ideally, a mature dermal compartment which will be brought forward for full thickness model generation requires a stable fibroblast layer which can uphold the epidermal compartment and prevent infiltration of keratinocytes into the dermal compartment. From the results acquired, the fibroblast layer in models grown with early perfusion does not appear to be mature due to it being thinner than the static control. Therefore, it was hypothesised that if keratinocytes were to be seeded above the dermal compartment, it would be likely that the basal layer of the epidermis would not form continuously due to keratinocyte infiltration (7).

A thinner fibroblast layer in early perfused models suggest that newly seeded fibroblasts cannot adhere as well to the Alvetex® scaffold when exposed to fluid flow. This lack of

adhesion hinders the growth of the initial fibroblast layer that forms, as most human cells depend on anchorage-based adhesion for proliferation (107). Based on histology, the surface fibroblast morphology appears to be healthy, which suggests that they are not stressed by early exposure to fluid flow; this asserts that instability may be the key issue. There is a possibility that early perfusion can facilitate the formation of a thicker fibroblast layer but, due to instability, the fibroblast layer is disrupted and detached from the scaffold. In literature, this phenomenon has previously been discussed as "cell wash-out", in which dynamic culture increases shear stress on adjacent cells and may displace them from the substrate (108).

On the contrary, if dermal equivalents are firstly grown in static conditions and later perfused, the resultant fibroblast layer is thick. Fibroblast growth in static, prior to perfusion, seems to be necessary for generating an improved surface for a dermal compartment. The rationale behind initial static growth is to ensure that fibroblasts are given more time to adhere to the scaffold and stabilise with the absence of fluid flow and shear stress. Previous cell studies have adopted the methodology of their work, based on this rationale, to ensure cell adhesion to the substrate and semi-confluency, before applying delayed perfusion (109). In this study, the development of a thicker fibroblast surface layer suggests that cell wash-out has been minimised. Through initial static culture, the initial fibroblast layer is stabilised before perfusion is applied, and proliferation is stimulated afterwards.

Based on these findings, the disruption of unstirred layers during delayed perfusion can improve the structure of the dermal compartment. However, it is worth noting that delayed perfusion may not only affect surface fibroblasts, but also the fibroblasts encapsulated within the scaffold. Therefore, ECM deposition by fibroblasts within the scaffold was subsequently investigated.

4.1.2 Mechanotransduction stimulates ECM deposition and media feeding regime affects the composition of ECM proteins in the matrix

The primary ECM proteins, collagen-I and collagen-III, analysed in Sections 3.3.1.1 and 3.3.1.2, appear to be greatly expressed within the dermal compartment after delayed perfusion, based on immunofluorescence. Based on these results, it is assumed that the disruption of unstirred layers in media after initial fibroblast growth in static conditions improves ECM deposition; however it cannot be confirmed without quantitative analysis. This observation is expected as dynamic culture stimulates collagen-producing cells, such as

fibroblasts, to synthesise new collagen proteins and form their own ECM within the scaffold space (110). The distribution of collagen-I and collagen-III within the scaffold is shown to be well dispersed within the scaffold amidst the fibroblasts, therefore mimicking the continuous ECM matrix found *in vivo*.

Dynamic flow of media, as incorporated in this study, can stimulate ECM production in the dermal compartment through mechanotransduction. The presence of shear stress can trigger either intracellular signalling pathways or gene transcription in cells. On the one hand, intracellular signalling affects processes such as migration, proliferation, and differentiation; while on the other hand, gene transcription can lead to the production of matrix metalloproteinases (MMPs), their inhibitors (TIMPs), and ECM proteins themselves (111,112). Due to the complexity of the response to shear stress, interplay between the two may also occur. In the case of gene transcription, it was previously identified that dynamic culture conditions led to changes in the genes of dermal fibroblasts associated with cell-cell adhesion, ECM production, and ECM organisation; however, only less than 25% of the genetic profile altered was specific to skin itself (113). Fibroblasts were also found to be sensitive to mechanical stresses; studies have shown that shear stress, osmotic pressure, and tension all induce effects on fibroblasts in terms of their structure and physiology (114–116). Therefore, the increase in ECM deposition observed due to delayed perfusion may be the result of changes in gene transcription caused by mechanotransduction, and increased sensitivity. A summary of how shear stress affects cells is shown in Figure 29.

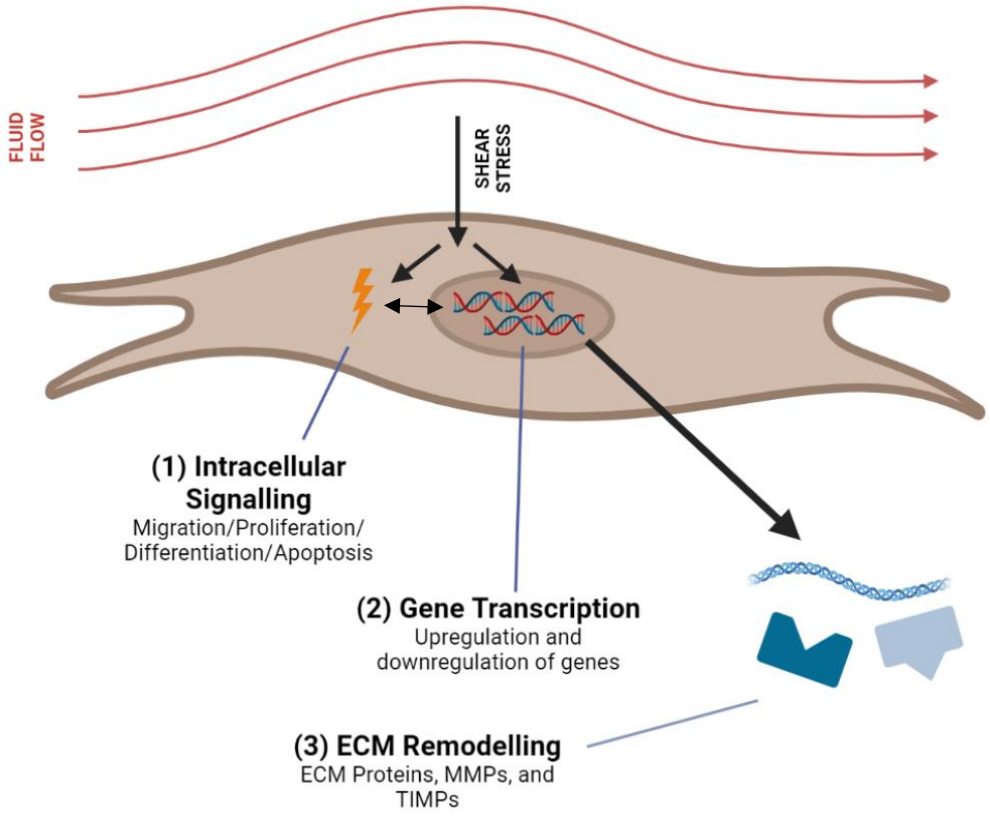

Figure 29: Mechanotransduction in cells. External stresses can either cause changes in intracellular signalling (1) or gene transcription (2). Interplay can also occur between (1) and (2). The latter influences the production of ECM proteins, MMPs, and TIMPs. Adapted from Pfenniger et al. (111).

When applying delayed perfusion, the media feeding regime within the bioreactor vessel was also found to impact ECM deposition. Feeding regime is important to consider when culturing cells, as it determines how nutrients are replenished within the 3D culture system. In this paper, two approaches were investigated: media spiking and half media changes. The former refers to the periodical addition of exogenous proteins into the culture medium, while the latter refers to the replacement of half the volume of media in the system with fresh complete medium. Both techniques enable exogenous growth factors in the system to be replenished, as they may either deplete or degrade over time. The latter is a potential issue when growing 3D skin models, as some exogenous growth factors may generate by-products that have adverse effects on cells. In particular, there is a concern that the by-products of AA (dehydro-ascorbate, oxalate, and threonate) may be detrimental (117). Dehydro-ascorbate has been found to induce stress signalling in some cell types (118), oxalate has cytotoxic properties (119), and threonate may impact cell signalling pathways (120). However, the extent to which these by-products have an effect on fibroblast cultures

have not been previously studied. By assuming this potential risk, it was predicted that half media changes would be advantageous over media spiking as it partially accounts for the removal of degraded growth factors.

However, there was no clear feeding regime that led to significant improvements on ECM deposition, based on immunofluorescence analysis (Figure 13). Generally, a dermis with a good distribution of both collagen-I and collagen-III was formed in both feeding regime conditions. Although the images show that the presence of collagen-III is greater with half media changes, and the presence of collagen-I is greater with media spiking, this cannot be validated without quantitative analysis such as Western Blot. If feeding regime did have an effect on ECM composition, as shown by the immunofluorescence images, there could be some biological implications caused by an increase or decrease in a certain type of ECM protein. For example, studies on the relative levels of collagen-III have validated its relevance for development and wound healing; its deficiency or absence can have adverse effects (121,122). However, the mechanisms for this phenomenon are not clear. One plausible reason may be due to differences in cell density between models, rather than the feeding regime itself. In 2D culture, it has been reported that high density skin fibroblasts tend to express a greater proportion of collagen-III to collagen-I (123); however, this is unexplored in 3D culture. If a link were to be formed between cell density and the feeding regime in 3D, half media changes supply fresh media that has thoroughly mixed exogenous growth factors, while media spiking does not; this could lead to variances in growth factor uptake which is necessary for proliferation. Further studies should quantitatively analyse the amount of each ECM protein, through Western Blot, to clarify this observation.

4.1.3 Increasing shear stress changes the nuclear morphology of fibroblasts and may have implications on cell morphology

The stirrer speed of the bioreactor was also shown to influence the development of the dermal compartment, in particular, nuclear morphology of the fibroblasts. In H&E, haematoxylin stains the nucleus of fibroblasts, and Figure 14 shows stark differences in nuclear morphology based on perfusion speed; static and 100 rpm maintained fibroblasts' elongated oval-shaped nuclear morphology while higher speeds caused fibroblasts to adopt a rounder morphology. In most cases, changes in nuclear morphology can be attributed to apoptosis, as nuclear degradation occurs early in apoptotic cells (124). However, as the largest organelle in mammalian cells, nuclear morphology can also be affected by external stresses which propagate from focal adhesions, through the cytoskeleton, and to the nucleus

(125). Primarily, stresses have been observed to induce changes in nuclear reorganisation or gene transcription (126). For fibroblasts, changes in gene transcription is significant as it can be associated to nuclear deformation (127). However, the nucleus should not bear the full extent of external stresses due to the presence of laminins which stabilise nuclear morphology (128). Therefore, the nucleus should experience minor changes in morphology, compared to the cell body itself. Further studies could investigate changes in the cell body morphology by performing immunofluorescence analysis of vimentin, which is a mesenchymal marker that strongly stains fibroblasts embedded in paraffin. The use of this stain would be useful for observing changes in cell shape under stress and would be more informative compared to analysing just the nucleus.

By investigating the effects of dynamic culture on the dermal compartment, it was identified that the time-based implementation of perfusion in culture, media feeding regime, and speed of media mixing were three parameters that need to be regulated during its development. Firstly, delayed perfusion has been identified to be beneficial compared to early perfusion and this is significant for future perfusion-based studies. However, the ideal time of implementation was not identified in this study. Secondly, media feeding regime was found to potentially affect ECM deposition but cannot be clarified based on qualitative immunofluorescence observations alone. Lastly, a stirrer speed of 100 rpm was identified as a suitable speed for maintaining a thick fibroblast layer for subsequent keratinocyte seeding; despite this, it may not be the optimal speed as the range of speeds investigated were broad, at 50 rpm increments.

4.2 Incorporation of fluid flow in full thickness models

Following the observations made on the dermal compartment, the impact of early and delayed perfusion on the epidermal compartment of full thickness models was investigated. In this case, perfusion was implemented at the start of the ALI culture or halfway through, following 4 week static growth of the dermal compartment. As previous full thickness model studies incorporated perfusion at the ALI, this was the most beneficial approach for investigating changes in the epidermal compartment (100,103).

4.2.1 Early perfusion hinders the development of the epidermal compartment in full thickness skin equivalents

The application of shear stress directly after cell seeding negatively impacted the downstream development of an epidermal compartment. In previous observations with

dermal compartments, early perfusion did not completely prevent the development of a fibroblast cell layer, as it was still structurally observed, albeit thinner than in static. In the case of epidermal compartment development, similar outcomes were observed, as day 7 histology showed a functional, but underdeveloped, epidermal layer (Figure 15D). The model was functional as stratification can be observed, and the localisation of K10 and K14 corresponded with the epidermal layers in which their presence was expected (Figure 18D). Previous studies have shown that K14-expressing keratinocytes appear only in the basal layer, while K10-expressing keratinocytes are found across the bulk of the viable epidermis, above the basal layer (7,52). Comparing the effect of early perfusion on dermal and epidermal compartments, it is clear that early perfusion is detrimental, but not to a critical extent. However, as the day 14 epidermis began to break apart and was not stratified (Figure 15H), it can be assumed that poor development due to early perfusion can lead to time-based failure of an *in vitro* epidermal compartment.

It may be the case that initial adhesion of keratinocytes to the dermal compartment is also affected due to dynamic culture, which leads to poor downstream development. However, unlike the fibroblasts in dermal compartments, the keratinocytes in the epidermal compartments are not in contact with the culture medium. Therefore, the poor development of newly seeded keratinocytes cannot directly be associated with cell wash-out. The effect of media mixing on keratinocytes is likely to be indirect through the fibroblasts themselves; this phenomenon was previously mentioned in Section 1.4 as fibroblast and keratinocyte cross-talk.

The *in vitro* attachment of keratinocytes is highly dependent on the fibroblast layer upon which they are seeded. As mentioned previously, the fibroblast surface layer of the dermal compartment must be structurally mature, with sufficient ECM deposition, to form a distinct DEJ. Keratinocytes do not attach directly to the fibroblasts themselves, but rather to laminins, which are connected to ECM proteins deposited by fibroblasts (129). The resulting basement membrane between the epidermis and dermis not only connects the two layers, but also plays a significant role in cell signalling. Therefore, ECM deposition is crucial to keratinocyte attachment. Figure 30 below shows how keratinocytes attach to the dermal compartment, with keratinocytes and fibroblasts both producing components of the DEJ.

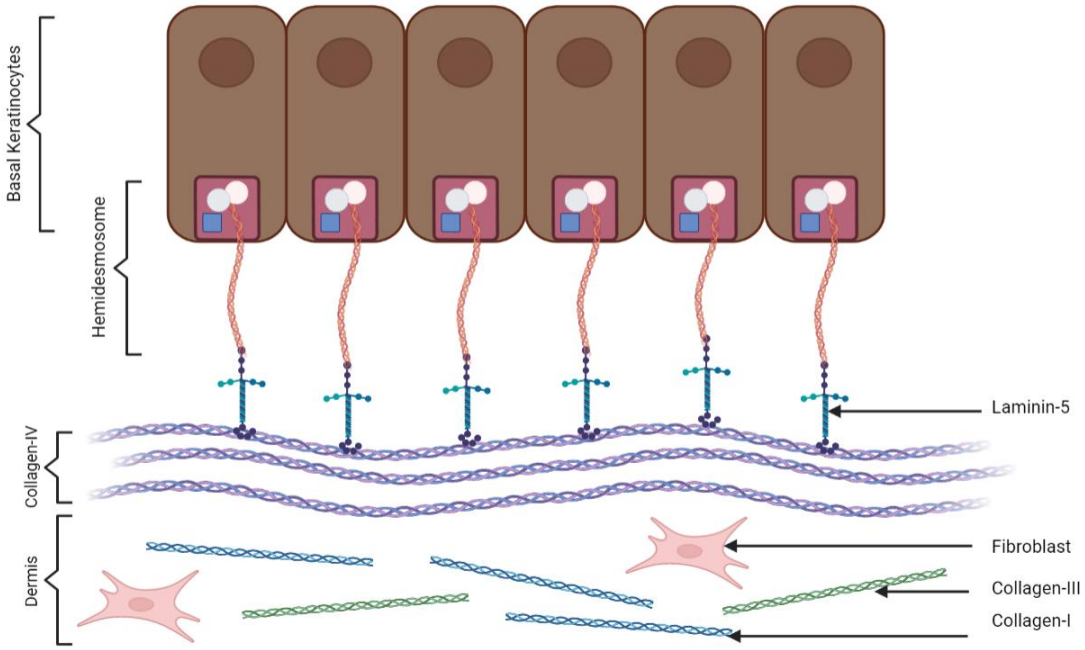

Figure 30: Schematic to show the attachments that occur at the dermal-epidermal junction (DEJ). Hemidesmosome consists of plectin, integrin α6β4, BP230, and collagen-XVII. The hemidesmosome attaches to laminin-5, which is connected to collagen-IV situated above the dermis. Adapted from Tasanen et al (130).

The major protein of attachment at the DEJ is collagen-IV; however, some studies on keratinocyte attachment have identified that the rate of attachment increases in the presence of collagen-I and fibronectin (131–133). The poor epidermal development observed in this study may be caused by variations in ECM deposition stimulated by shear stress. Although collagen-IV was not investigated in this study, the immunofluorescence analysis of collagen-I and collagen-III showed that sufficient ECM deposition was occurring; however, compositions cannot be clearly determined without quantitative analysis. As it was ensured that all dermal compartments were grown similarly for all conditions (28 days static) and ECM proteins were sufficiently identified, the ECM composition is not likely to be the dominant reason for poor epidermal formation in early ALI perfused models.

Another hypothesis for the poor epidermal development could be due to the initial wetting of the epidermal surface. Unlike the poor early perfusion results acquired in this study, Strüver et al. successfully generated a stratified epidermis despite perfusing at the start of the ALI culture. The major difference which contributes to this is that Strüver et al. utilised an enclosed perfusion platform with a specific orifice which ensured that only the bottom of the model was able to come into contact with the media. Therefore, it was impossible for

any media to spill outside of the enclosed platform and potentially wet the upper epidermal surface (100).

When generating epidermal compartments, the ALI is essential, as the keratinocytes need to be exposed to air on its surface. In humans, the epidermal surface is exposed to the atmosphere, which consists of 21% oxygen. If keratinocytes are in culture with <21% oxygen at its surface, the keratinocytes will experience limited growth and differentiation (134). If keratinocytes are grown in submerged culture, the distribution of keratins produced become imbalanced and subsequent growth does not lead to a stratified epidermal structure. It is reported that over time, high molecular weight keratins are lost if no ALI is generated (135). In this study, it was ensured that the top surface of the dermal compartment remained dry and in contact with air, to ensure an effective ALI. However, through media stirring, it is possible that media may spill onto the top surface. If perfusion is applied at the start of the ALI, the keratinocytes are at risk of becoming wet before they have stabilised to the ALI. This would therefore reduce the rate of oxygen required by the keratinocytes and restrict initial growth and differentiation.

Based on histology, the models generated in early perfused ALI conditions were thin and unstratified; thus, it can be assumed that early ALI perfusion affects the proliferation and differentiation of keratinocytes, respectively. Immunofluorescence analysis confirmed that keratinocyte proliferation was indeed scarce (Figure 17D,H), but early and mid-differentiation patterns were still consistent of a functional epidermal compartment (Figure 18D). Assuming that the issue lies in keratinocyte and fibroblast cross-talk, it has been reported that both proliferation and differentiation of an epidermal compartment highly depends on the presence of fibroblasts. Keratinocyte proliferation is stimulated by certain cytokines expressed by fibroblasts, such as pleiotrophin, stromal cell-derived factor 1, and granulocyte-macrophage colony-stimulating factor (GM-CSF); these cytokines take part in paracrine signalling processes which help regulate proliferation (136,137). As previously mentioned, shear stress is a significant contributor to changes in gene expression within fibroblasts. It may be that the low keratinocyte proliferation of early ALI perfused models is attributed to the downregulation of certain cytokines in fibroblasts, the response of undifferentiated keratinocytes to cytokine concentrations, or the upregulation of proinflammatory cytokines causing a negative response (138). Likewise, keratinocyte differentiation is also regulated by fibroblast-expressed cytokines, including GM-CSF which has a double regulatory function (137). In literature, most co-cultures of fibroblasts and keratinocytes develop a stratified epidermis, to varying extents, and only when fibroblasts

are absent do significant changes occur. In this case, the morphology of keratinocytes become irregular, distinct epidermal layers are not formed, and keratinocytes at different stages of differentiation overlap with each other (139). Although exogenous growth factors such as KGF are supplemented to all models in all conditions, the differences in epidermal morphology, keratinocyte proliferation, and keratinocyte differentiation between models is likely to be attributed to changes in cell signalling within the models. This can be tested further by investigating changes in phosphorylation in keratinocytes, such as the ERK1/2 pathway (140).

In an attempt to understand whether stirrer speed also affected the failure of the epidermal compartment in early perfused models, a lower stirrer speed was investigated. Figure 27 shows that regardless, if stirrer speed is halved during early ALI perfusion, the epidermal compartment still does not undergo stratification; only a thin keratinocyte layer is formed. As previously mentioned, this can occur due to accidental wetting of the epidermal surface during ALI. Additionally, as it was observed that 50 rpm models remained intact above the dermal compartment, while 100 rpm models showed detachment and dissociation, adhesion is therefore a key issue to consider when implementing dynamic culture early in ALI and increasing the stirrer speed. Poor adhesion may occur due to the effect of shear stress on ECM protein deposition (such as collagen-I, collagen-IV, and fibronectin), which keratinocytes rely on for adhesion. While it was expected that using an initial slower speed and increasing it over time could also improve keratinocyte development, based on a previous study (95), this was not the case. It is possible that the lower stirrer speed used in this study (50 rpm) needed to be reduced further to <25 rpm, as Lei et al. utilised. However, it was regarded that the very low speeds in Lei et al.'s rotary system were due to the design and nature of the models grown in those systems; they were not reflective of full thickness models grown in our novel magnetic stirrer-based bioreactor systems. To clearly demonstrate that early perfusion completely fails to form a viable epidermal compartment, regardless of stirrer speed, further studies should investigate stirrer speeds <50 rpm.

4.2.2 Improved epidermal thickness in delayed perfusion models may be influenced by increased circulation of growth factors and the presence of mechanical stimuli

In previous literature, perfusion has generally been regarded to improve 3D *in vitro* skin models, as it enables constant nutrient delivery to cells, similar to *in vivo* vasculature, and introduces relevant forces and stresses, experienced *in vivo*, to otherwise static systems (100). While this study identified that early perfusion to full thickness models was

detrimental, delayed perfusion generated similar benefits to those reported in literature. It can be assumed that stability of the basal epidermal layer needs to be established first before perfusion can improve development. Our attempt to introduce fluid flow, disrupt unstirred layers, and apply relevant forces to an existing model grown in static conditions (6) has strong implications for future optimisation of these models.

The disruption of diffusion-limiting unstirred layers at the media-cell interface and continuous exchange of nutrients and waste through media mixing, was hypothesised to improve the structure and physiology of the full thickness models in this study. Through delayed perfusion, these objectives were achieved, and this is reflected in an improved epidermal compartment, observed during its standard 14 day development. Noticeably, a thicker viable epidermis was observed in delayed perfused models at day 7 and day 14, maintaining a stratified structure with distinct layers of different keratinocyte morphologies (Figure 15C,G). Moreover, basal keratinocytes had greater organisation and were vertically aligned. The thicker viable epidermis observed with delayed perfusion reflects the observations by Sriram et al. and Mori et al. when perfusing *in vitro* full thickness models (102,103). Naturally, the development of the epidermal compartment relies on several factors such as the ALI (58), growth factors supplemented, stresses applied, and the setup of the *in vitro* system. In this study, it was hypothesised that the improvement in epidermal compartment caused by delayed perfusion can be attributed to two of these factors: an increase in growth factor circulation and uptake, and generation of stresses. In the first case, perfusion enables growth factors required by the keratinocytes to be efficiently circulated, thus improving uptake and cell accessibility; this is in conjunction with improved flow due to disruption of unstirred layers.

Three exogenous molecules were supplemented in this study: KGF, calcium chloride, and AA. Firstly, KGF is reported to induce hyperproliferation, regulate keratinocyte migration from the basal layer up to the *stratum corneum*, and influence the rate of differentiation (64,141). Increased circulation of this growth factor would likely encourage more cells to proliferate in the basal layer and increase turnover of keratinocyte migration across layers; this would have a greater impact on thickening the viable epidermis, rather than increasing terminal differentiation. Secondly, calcium chloride is supplemented at a higher concentration during ALI culture to stimulate a 'calcium switch,' which reportedly turns on calcium-dependent genes and increases expression of keratinocyte differentiation markers such as K1, K10, and K16 (142). Perfusing the skin model would ensure that most keratinocytes in the basal layer can undergo calcium-driven early and mid-differentiation; this can contribute to epidermal

thickness by forming more distinct layers of keratinocytes with specific morphologies, as they migrate. Lastly, AA is a growth factor that can influence both fibroblast and keratinocyte behaviour. In literature, the addition of AA can influence basal keratinocytes to undergo reorganisation, influence fibroblasts to stimulate ECM proteins such as collagen-I and collagen-III, and improve the stability of the DEJ (143). Additionally, AA acts as an antioxidant and has been reported to counter the upregulation of reactive oxygen species (ROS) levels in cells, as a response to shear stress (144). Increased circulation of AA would therefore contribute to stabilising the full thickness model as a whole and facilitate improved development. While the exogenous molecules supplied may influence the morphology and physiology of the epidermal compartment, it is also worth noting that the fibroblasts will secrete additional factors that may contribute to observable changes.

In the second case, improved epidermal compartment development is attributed to the generation of stresses in dynamic culture, similar to *in vivo* conditions. Mechanical forces play a large role in tissue maintenance *in vivo*, at a cellular level, and if stresses are absent, the model will not be representative of *in vivo* conditions; forces can be linked to changes in cell morphology, behaviour, and gene expression (145). Due to the need to create reliable tissue mimics, different types of bioreactors are utilised in literature to incorporate and control shear stress into models (146,147). In a recent study, it has been identified that the thickening of the epidermal layer in full thickness skin models is attributed to dynamic culture's ability to regulate expression of MMPs and TIMPs, which in turn affects the ECM composition and stability in the dermal compartment (145). As previously established, any changes to the dermal compartment can impact the epidermal compartment due to changes in cell-ECM interactions and keratinocyte-fibroblast cross talk. From this perspective, it is to be expected that perfusion would improve the thickness of viable epidermis in full thickness models, since they can benefit from the presence of mechanical stimuli unlike static conditions.

4.2.3 Perfusion can speed up the maturity of the full thickness model, through changes in proliferation and early/mid differentiation

The improved thickness of viable epidermis in our late perfused full thickness skin models from day 7 to day 14 asserts the significance of dynamic culture on proliferation and differentiation during model development. This was to be expected based on previous perfusion studies of full thickness models, which all displayed changes in both physiological processes (100–103). Multiple immunofluorescence analyses were performed to investigate

further. In this study, changes in proliferation, early/mid differentiation, and terminal differentiation were analysed.

Proliferation was observed using Ki-67, which stained positive for proliferating cells in the basal layer of the epidermal compartment. While proliferation has previously been analysed in static Alvetex® Scaffold-grown models, analysing the proliferation of keratinocytes in Alvetex® grown models in perfused conditions is novel for this study. During the development of the full thickness models, static models showed increasing proliferation from day 7 to day 14 of ALI culture (Figure 17A,E, I). This is to be expected, as human skin equivalents tend to be hyperproliferative compared to *in vivo* conditions (148). Quantitative analysis of Ki67 in this study showed that proliferation in the basal layer increased from ~27% to ~38%, which is in excess of the proliferation observed *in vivo* (~10-12%) (149). Additionally, increased proliferation is expected as human skin equivalents are generally physiologically stable at 7 to 14 days (148). A study conducted by Schimek et al. found that the proliferation of basal keratinocytes in static models was highest between day 10 and 17 (150).

However, it was identified that increasing media volume and incorporating delayed perfusion caused a decline in proliferation rate from day 7 to day 14 (Figure 17B,C,F,G,I). At day 14, both conditions had a proliferation rate <20%. Despite this, it does not mean that proliferation is negatively affected, as day 7 static bioreactor models and day 7 delayed perfused models both had an excessive proliferation rate compared to static (~55% for static bioreactor models and ~70% for delayed perfused models). This implies that increasing media volume and incorporating perfusion increases the rate of hyperproliferation and speeds up epidermal development, but proliferative activity is reduced >1 week. Previously, it has been reported that keratinocytes generally proliferated better in the presence of dynamic culture (105), which is representative of day 7 delayed perfused models, but there is no literature which demonstrates a drop in proliferation after a period of hyperproliferation. Glaum et al. conducted a study which investigated time-based changes in the proliferation of keratinocytes during dynamic culture and identified minimal changes from day 7 to day 14, which is contradictory to the results of this study; however, they discussed that if the purpose of skin equivalents is to stimulate and maintain differentiation, proliferation should theoretically drop over time (151). Therefore, it is feasible to believe that perfusion causes hyperproliferation in the first week of culture, which speeds up early development.

Upon analysing differentiation markers, perfusion was found to have a greater influence on early and mid-differentiation at day 14, rather than on proliferation. K10 and K14 were used to mark early/mid differentiation as they were commonly used in prior studies which analyse *in vitro* full thickness models (7,52,152). In this study, I observed K14 structural protein in proliferating keratinocytes within the basal layer and K10 found in migrating cells which are inhibited from further proliferation (153). The previous studies mentioned above provided insight into the localisation of these biomarkers and were used as a reference to determine whether the epidermal compartments formed in this study were physiologically viable. It was identified in this study that the localisation of these biomarkers in both static conditions and the delayed perfused condition were as expected; however, delayed perfusion led to localisation of K14 beyond the basal layer (Figure 18C,G). In this case, broader K14 localisation may be the result of hyperproliferation of basal keratinocytes triggered by mechanotransduction (154). As the keratinocytes above the basal layer still produce K14 filaments, this means that the keratinocytes are likely constrained to early differentiation (155). Since K14 is expressed beyond the basal layer in delayed perfused models, it means that a greater proportion of keratinocytes are yet to inhibit proliferation and express K10.

In terms of terminal differentiation, perfusion did not seem to have a considerable effect. The thickness of the filaggrin band in the delayed perfused model remained similar at day 7 and day 14 and did not have noticeable change compared to static models. Changes in filaggrin expression due to perfusion are unclear in literature. In some cases, filaggrin is upregulated (100), and in others, there is no comparable difference to static (102); the latter being comparable to this study's findings. However, other terminal differentiation biomarkers such as involucrin are consistently upregulated in most perfusion studies (100,102). Therefore, as a more accurate representation of terminal differentiation, other biomarkers such as involucrin should be investigated.

4.2.4 Longevity of full thickness models is not improved post-21 days

As perfusion influenced the development of Alvetex® Scaffold full thickness skin models, it was expected that it would also affect long term maintenance of the models. The optimal duration for *in vitro* skin model development is assumed to be 7 to 14 days, as the epidermal compartment undergoes continuous proliferation and differentiation for the first two weeks (148). Models cultured beyond two weeks may exhibit a loss in viability and structure as skin models are typically generated for short term maintenance; extended culture may result in a halt in proliferation or a loss of fully differentiated cells in the *stratum corneum* (156,157).

A previous study on Alvetex® Scaffold models found that the epidermal compartment thickened from day 7 to day 21, which confirms the typical assertion of short term maintenance. However, it was identified that at day 28, the viable epidermis was considerably reduced, therefore suggesting that the models begin losing viability post-21 days (7). Like the aforementioned paper, the current study also investigates day 21 and day 28 models, but with the inclusion of perfusion.

Similar to the results of Roger et al, the Alvetex® Scaffold full thickness skin models were considerably thick in both static and perfused conditions during day 21 but became thinner at day 28 (Figure 21). The phenomenon of epidermal thinning of the models at day 28 shows that perfusion does not improve the longevity of the full thickness models developed. Regardless of culture conditions, a loss in epidermal thickness is observed, therefore confirming that current models can only be used for short term studies. As previously mentioned, this can be caused by a decrease in proliferation within the basal layer, or a loss of cells.

Further analysis on the day 28 models implies that perfusion may even be detrimental for long term maintenance. Firstly, the Ki67 immunofluorescence analysis for day 28 perfused models shows scarce proliferation in the basal layer (Figure 23F). Secondly, the K10/K14 immunofluorescence analysis shows weaker expression of early and mid-differentiation markers (Figure 24F). Lastly, the filaggrin immunofluorescence analysis does not show a clear filaggrin band (Figure 25F). The trends observed shows that perfusion builds on the argument that proliferation is reduced and differentiated cells are lost in long term models; it does not alleviate it.

Despite this, the thickness of viable epidermis in the perfused model was found to be 50% thicker than their static counterparts (Figure 22). As the epidermal compartment remains thick at day 21, it can be assumed that the models are still developing at this stage, regardless of culture conditions. As delayed perfusion was found to have a beneficial effect on the development of full thickness models at day 7 and day 14, it would be reasonable to assume that the same principles would apply for day 21 models. Only when the models begin to lose viability, do the negative effects of perfusion become clearer.

4.2.5 Perfusion impairs barrier function during the development and long term maintenance of full thickness models

Based on histology and immunofluorescence, it was identified that perfusion had an effect on the structure and function of full thickness models. Therefore, it is inevitable that it would also have an effect on skin function. For full thickness skin models, barrier function is commonly observed, using a variety of approaches such as transepithelial electrical resistance (TEER) (152), permeation assays (158), and TEWL (159). In this study, barrier function was investigated by measuring TEWL. It was understood that an epidermal compartment had good barrier function if TEWL, which is the volume of water that passively evaporates through skin, was minimised (160).

As shown in Figure 20, TEWL decreased in all conditions from day 7 to day 14; therefore, barrier function improves over time. This occurs due to an increased turnover of keratinocytes in longer cultures, which leads to an increase in keratohyalin granules being produced in the *stratum granulosum*, and a denser *stratum corneum;* both are major influences to barrier function (161). On the one hand, keratohyalin granules form a barrier within the epidermis by being water insoluble and cross-linking keratins (162); while on the other hand, corneocytes in the stratum corneum are surrounded by a lipid layer that acts as a barrier on the surface of skin (163). Although the *stratum corneum* can be observed through histology, it is hard to measure and compare, unlike the viable epidermis, as it dissociates during the processing of these models. Therefore, it cannot be a clear indicator in this study to explain the development of barrier function. However, a previous study has managed to quantify the thickness of the stratum corneum and found it increased over time (159).

Perfusion was shown to influence TEWL negatively during full thickness model development, as early and delayed perfused models had a higher TEWL value than both static controls (Figure 20). In the case of early perfusion, this was to be expected as the histology for day 7 showed a thinner epidermal compartment (Figure 15D) and day 14 showed a broken epidermal compartment (Figure 15H). Therefore, it was reasonable to assume that water permeability would increase in this condition. However, high TEWL was not expected for delayed perfusion as it generated the thickest epidermal compartment at both day 7 and day 14 (Figure 15C,G). Fortunately, the TEWL was considerably lower than early perfused models. Based on these observations, it is assumed that perfusion reduces barrier function. It is likely that the shear stress from mixing media is the cause for impairing barrier function and,

although it is flow rate dependent, it has previously been attributed to increasing surface hydration, which is proportional to TEWL (164).

The TEWL was also observed for longer term cultures at day 21 and day 28, as shown in Figure 26. The TEWL for both static controls and delayed perfusion at day 21 had no noticeable difference, which shows that all conditions had a good barrier function between 10-20 $g/m^2/h$. This is representative of the thick viable epidermis observed in all conditions (Figure 21A-C). However, the perfused model had a significantly increased TEWL compared to other conditions at day 28 (Figure 21F). As the models have thinner viable epidermis at day 28, it is expected that all models would have a poorer barrier function. However, the sharp increase in TEWL caused by perfusion implies that shear stress amplifies the drop in function. As day 28 delayed perfused models had poor proliferation, significantly weaker K10/K14 expression based on fluorescence, and an unclear filaggrin band, the drop in barrier function can be attributed to poorer physiology.

In hindsight, TEWL is not the only indicator of barrier function in this study, as the expression of filaggrin can also be used. Filaggrin is usually expressed in the *stratum corneum* and is known to be correlated with good barrier function. It is reported that its degradation products enable the stratum corneum to become more acidic which aid in protecting against irritants (165). Additionally, Scharschmidt et al. found that filaggrin deficiency was linked to increased permeability (166). However, in this study, the filaggrin layer mostly remained consistent, and only barrier to liquid was observed. Therefore, analysis on filaggrin in terms of barrier function is limited in this study. Instead, barrier function can be observed through the continuous permeation of dyes such as lucifer yellow and X-Gal across the upper epidermis (167).

4.3 The bioreactor system directs flow of media towards the base of the full thickness model and stirrer speed affects shear stress and flow rate

Based on the analyses of dermal and full thickness models, perfusion influenced multiple aspects of their development and maintenance, from structure and morphology to function. However, analyses of models alone did not provide insight on how the implementation of dynamic culture in this study was effective. Therefore, analysis of the system was conducted from the following perspectives: direction of flow, velocity, flow rate, and shear stress. Understanding these aspects provided insight into how media is circulated into these models and how the system compares to other models.

The cross section of the bioreactor vessel at the ALI was analysed using direction vectors and velocity gradients (Figure 28). It was identified that the circulation of fluid flow maintained a similar pattern, regardless of stirrer speed, with media being drawn outwards and inwards from the base of the vessel, and subsequently upwards and inwards towards the base of the full thickness model. This pattern asserts why perfusion would have a significant effect on the models as media is constantly being drawn towards the model. Therefore, it is feasible that the exogenous growth factors supplied and the nutrients in the media are continuously being supplied to cells and waste products are being removed. While this circulation pattern is beneficial, it also raises the issue of shear stress. When increasing the stirrer speed, it is shown that the velocity within the system increases; therefore, shear stress should also increase due to a positive correlation (168). A balance must be maintained between stirrer speed and shear stress. In our study, 100 rpm was beneficial to models after delayed incorporation, showing a good compromise of incorporating dynamic culture at a suitable speed.

To further analyse how the bioreactor system affects the model, fluid mechanic simulations focusing on the base of the model were conducted, as this is the interface where the fluid and cells meet. It was identified that as stirrer speed was increased, both shear stress (Table 5) and flow rate increased (Table 6). Since the fluid only came into contact with the dermal compartment, fibroblasts were most affected by shear stress. Previous studies have been conducted on the effects of shear stress on dermal fibroblasts. Yankaskas et al. found that a shear stress of 0.5 dyne/cm^2 was sufficient to influence fibroblast migration (169), while Mackley et al. found that 0.1 dyne/cm^2 was sufficient to cause changes in ECM deposition (170). Additionally, Shi et al. found that α-sma, a marker of tissue damage, was upregulated by double in fibroblasts after applying a shear stress of 8 dyne/cm^2 (171). This would be expected as 8 dyne is comparable to the lower end of approximate shear stress within an artery (172). Based on these comparative studies, shear stress should ideally be <1 dyne/cm^2. The shear stresses acquired in the current study from 0-200 rpm are generally low, compared to the studies outlined above, which means that there should not be a significant effect on fibroblasts. The ranges observed are more likely to affect keratinocytes as it was previously reported that 0.06 dyne/cm^2 could cause changes in keratinocyte morphology and organisation. However, only the dermal compartment was in contact with fluid flow, so if a shear stress was to be imposed indirectly, the overall stress for keratinocytes would be significantly lower than 0.06 dyne/cm^2. It is worth noting that previous studies on fibroblasts were short term studies, while ours involved perfusion over a longer duration of time (≥1

week). Therefore, it is assumed that the lower overall stress over a longer period of time can generate effects similar to higher shear stresses in a short duration of time.

Alongside shear stress, flow rate at the interface also increased as stirrer speed increased (Table 6). However, while flow rate studies are available for comparison, it is difficult to make a direct comparison due to the nature of the bioreactor system used. Most flow studies relating to perfusion of skin models occur in microfluidic systems in which media flows through a constrained space bound by specific parameters, and direction of flow is determined (100,102). In this system, the media is mixed in a large open space within the vessel and there is no flow rate that can be controlled. While the measurements in Table 6 are beneficial for understanding the relationship of flow rate, shear stress, and velocity, shear stress is the best indicator for comparative study.

4.4 Future directions

In general, this study identified that the disruption of unstirred layers caused by perfusion can have a significant effect on both dermal and full thickness models, after an initial period of growth in static conditions. Through histology, improvements in epidermal and dermal compartments were observed in terms of cell nuclear morphology, thicknesses, and compartment structure. Additionally, through immunofluorescence analysis, changes in physiology were observed in terms of ECM deposition, proliferation, and various stages of differentiation. Lastly, through TEWL measurements, changes in barrier function was observed. Although clear observations can be identified, there are several limitations to this study which can be addressed in future studies.

Firstly, in terms of model development, there is high variability that can occur for each replicate due to the process of developing full thickness models over a long duration of time. As all models are manually generated, there are several issues that can be encountered which will lead to variability. Primarily, during the ALI stage, accidental wetting can occur which can influence the development of a stratified epidermal compartment. The dryness of the surface plays a large role in downstream development and can be influenced by the mixing of media in the bioreactor vessel or user handling. Another problem pertaining to the models is that the epidermal surface of the full thickness models can be affected by the processing technique. A major consequence of this is the loss of *stratum corneum* in models, which begins to dissociate and prevents accurate measurements to be taken. As it is

unavoidable to eliminate the risk of handling issues during long term cultures, a greater sample size would help improve the comparability of the models.

Secondly, the expression of ECM deposition, proliferation, and differentiation markers were only qualitatively analysed using immunofluorescence. Conclusions relating to expression were drawn from the intensities of stains, which can be influenced by varying factors such as photobleaching, autofluorescence and non-specific fluorescence (173). In the case of dermal compartments, autofluorescence of the Alvetex® Scaffold is a noticeable issue, which can be problematic if staining is weak relative to it. To improve conclusions pertaining to biomarker expression, quantitative analysis should be undertaken in future studies. The most common technique used to quantify protein expression is Western Blotting, which is a semi-quantitative technique which enables specific proteins to be isolated and identified based on molecular weight, and its abundance compared against a control via band thicknesses (174). Comparing band thicknesses for each protein would provide greater insight on changes in protein levels between conditions; while it does not give absolute measurements, it provides more than the identification of presence and localisation using immunofluorescence.

Thirdly, other biomarkers can be observed to further investigate the effect of disrupting unstirred layers via perfusion on physiology. For dermal models, fibroblast morphology and response to damage can be observed using the biomarkers vimentin and alpha smooth muscle actin (α-sma), respectively. Both of these markers have been used to observe changes in fibroblast morphology and also identify the number of fibroblasts present within a dermal compartment (175,176). For full thickness models, DEJ integrity can be observed using the biomarker integrin-α6, which indicate the attachment of keratinocytes to ECM proteins, and tight junction formation (7). This would aid in further understanding why early perfusion prevents poor growth of fibroblast and keratinocyte layers via changes in adhesion. Other proteins that can be observed include other terminal differentiation biomarkers such as loricrin and involucrin.

Lastly, future studies can investigate further optimisation of the perfusion conditions in this study. Improvements can be made on the parameters already utilised, such as stirrer speed and culture duration. Further research can be more specific, such as investigating a greater range of stirrer speeds and understanding the precise duration in culture when perfusion should be implemented. Additionally, changes in skin model development caused by switching between static and perfused, as a control mechanism, can be investigated. It may

be the case that thickness, and integrity of the models can be controlled by changing culture conditions multiple times during culture.

By successfully optimising these models, it is possible to use them for long term applications which many different skin models aim to tackle. A prominent application would be chronic skin condition studies, such as the investigation of skin irritation and relative inflammation (177). Alternatively, the optimised models would be beneficial for commercial research, in identifying the long term effects of different cosmetic formulations (178). By acknowledging these potential research fields, it is clear that the future directions for these models are significant.

Chapter 5: Conclusion

In this study, it was successfully determined that the disruption of unstirred layers *in vitro* influences the development and maintenance of both dermal models and full thickness models. While an abundance of literature reports that dynamic culture generally improves the structure, physiology, and function of skin models, the results acquired indicate that timing of perfusion, introduced through dynamic culture, is crucial for model development. On the one hand, introducing perfusion at the beginning of model culture hinders the maturation of the dermal compartment and prevents stratification of the epidermal compartment. On the other hand, delayed perfusion improves the thickness of the fibroblast surface layer and ECM deposition in the dermal compartment , as well as the thickness of viable epidermis in the epidermal compartment. It was established that dermal models and full thickness models should be grown in static for a period of time before transferring to dynamic culture, to aid initial cell adhesion and the formation of an epidermis which acts as a foundation for downstream proliferation and differentiation. Whilst delayed perfusion improved structure and physiology, through improved nutrient diffusion resulting from the disruption of unstirred layers, it was surprisingly found that delayed perfusion did not improve the barrier function.

Additionally, for full thickness models, it was identified that perfusion does not improve longevity. Full thickness models grew well from day 7 to day 21 in both static and perfused conditions, with the latter showing increased proliferation and potentially greater differentiation until day 21. However, perfusion did not improve the morphology of more mature models cultured for 28 days at the air-liquid interface. This suggests that the models still require further optimisation for large-scale long-term applications.

Lastly, within the scope of this study, an attempt was made to optimise parameters which could improve development of models in a dynamic culture system. While shear stress is necessary for mimicking *in vivo* conditions, stirrer speed should be minimised, as our fluid mechanics simulations show an exponential increase of shear stress with increasing speed. This will directly or indirectly impact the development of both the dermal compartment and epidermal compartment, respectively. Through histology, stirrer speed was shown to change the nuclear morphology of fibroblasts in the dermal compartment and prevent stratification of the epidermal compartment.

In summary, our attempt to disrupt unstirred layers through the use of a magnetic stirrer-based bioreactor introduces the issue of perfusing skin models too early, and affirms similar

improvements found in other bioreactor systems when a culture shift from static to dynamic is delayed. The result of this study lays the groundwork for future studies in optimising the incorporation of perfusion, from its time-based introduction to the stirrer speed applied. Scholars may be interested in determining the best balance between the disruption of unstirred layers, to maximise nutrient delivery, and shear stress, which can be detrimental to cells at high levels. Additionally, other parameters can be optimised alongside dynamic culture, such as the design of the bioreactor and the exogenous growth factors supplied in the system. By addressing these potential solutions, *in vitro* full thickness skin models can be brought forward for long term experimental studies, beneficial for clinical and commercial purposes.

Bibliography

1. Farage MA, Miller KW, Elsner P, Maibach HI. Characteristics of the Aging Skin. Adv Wound Care. 2013; 2(1): 5–10.

2. Tuckman A. The Potential Psychological Impact of Skin Conditions. Dermatol Ther. Springer Healthcare. 2017; 7: 53–57.

3. Abd E, Yousef SA, Pastore MN, Telaprolu K, Mohammed YH, Namjoshi S, et al. Skin models for the testing of transdermal drugs. Clin Pharmacol. 2016; 8: 163–176.

4. Flaten GE, Palac Z, Engesland A, Filipović-Grčić J, Vanić Ž, Škalko-Basnet N. In vitro skin models as a tool in optimization of drug formulation. Eur J Pharm Sci. 2015; 75: 10–24.

5. Ali N, Hosseini M, Vainio S, Taı A, Cario-Andr M, Rezvani H, et al. Skin equivalents: skin from reconstructions as models to study skin development and diseases. Br J Dermatol. 2015; 173: 391–403.

6. Costello L, Fullard N, Roger M, Bradbury S, Dicolandrea T, Isfort R, et al. Engineering a multilayered skin equivalent: The importance of endogenous extracellular matrix maturation to provide robustness and reproducibility. In: Walker J, editor. Methods Mol Bio. Humana Press Inc.; 2019; 107–122.

7. Roger M, Fullard N, Costello L, Bradbury S, Markiewicz E, O'Reilly S, et al. Bioengineering the microanatomy of human skin. J Anat. 2019; 234(4): 438–455.

8. Rossi A, Appelt-Menzel A, Kurdyn S, Walles H, Groeber F. Generation of a three-dimensional full thickness skin equivalent and automated wounding. J Vis Exp. 2015; (96): 52576.

9. Singh S, Marquardt Y, Rimal R, Nishiguchi A, Huth S, Akashi M, et al. Long-Term and Clinically Relevant Full-Thickness Human Skin Equivalent for Psoriasis. ACS Appl Bio Mater. 2020; 3(10): 6639–6647.

10. Korjamo T, Heikkinen AT, Mönkkönen J. Analysis of Unstirred Water Layer in In Vitro Permeability Experiments. J Pharm Sci. 2009; 98(12): 4469–4479.

11. Ravichandran A, Liu Y, Teoh SH. Review: bioreactor design towards generation of relevant engineered tissues: focus on clinical translation. J Tissue Eng Reg Med. 2018; 12: 7–22.

12. Yousef H, Sharma S. Anatomy, Skin (Integument), Epidermis. StatPearls. 2018.

13. Wickett RR, Visscher MO. Structure and function of the epidermal barrier. Am J Infect Control. 2006; 34(10): S98–110.

14. Michniak-Kohn BB, Wertz PW, Al-Khalili M, Meidan VM. Skin: Physiology and Penetration Pathways. In: Rosen MR, editor. Deliv Syst Handb Pers Care Cosmet Prod Technol Appl Formul. Norwich, NY: William Andrew. 2005; 77–100.

15. Richard Hibbs BG, Clark WH. Electron Microscope Studies of the Human Epidermis The Cell Boundaries and Topography of the Stratum Malpighii. J Biophys Biochem Cytol. 1959; 6(1): 71-76.

16. Selby JC. Mechanobiology of Epidermal Keratinocytes: Desmosomes, Hemidesmosomes, Keratin Intermediate Filaments, and Blistering Skin Diseases. In: Wagoner Johnson A, Harley B, editors. Mechanobiol Cell-Cell Cell-Matrix Interact. Boston, MA: Springer. 2011; 169–210.

17. Fuchs E, Green, H. Changes in keratin gene expression during terminal differentiation of the keratinocyte. Cell. 1980; 19(4): 1033–1042.

18. Fukuyama, Epstein WL. Heterogeneous ultrastructure of keratohyalin granules: a comparative study of adjacent skin and mucous membrane. J Invest Dermatol. 1973; 61(2): 94–100.

19. Hirao T. Corneocyte Analysis. In: Farage, MA, Miller KW, Maibach HI. Textb Aging Ski. 2nd ed. Berlin, Heidelberg: Springer. 2017; 1127–1140.

20. Burgeson RE, Christiano AM. The dermal-epidermal junction. Curr Opin Cell Biol. 1997; 9(5): 651–658.

21. Shirshin EA, Gurfinkel YI, Priezzhev A V., Fadeev V V., Lademann J, Darvin ME. Two-photon autofluorescence lifetime imaging of human skin papillary dermis in vivo: assessment of blood capillaries and structural proteins localization. Sci Reports. 2017; 7(1): 1–10.

22. Tzaphilidou, M. The role of collagen and elastin in aged skin: an image processing approach. Micron. 2004; 35(3): 173–7.

23. Kumar N, Kumar P, Nayak Badagabettu S, Kudva R, Surendran S, Adiga M. Collagen and Elastic Fiber Content Correlation Analysis between Horizontal and Vertical

Orientations of Skin Samples of Human Body. Dermatol Res Pract. 2015; 2015(4): 1-8.

24. Ishida-Yamamoto A, Igawa S, Kishibe M. Molecular basis of the skin barrier structures revealed by electron microscopy. Exp Dermatol. 2018; 27(8): 841–846.

25. Swerlick RA. The Structure and Function of the Cutaneous Vasculature. J Dermatol. 1997; 24(11): 734–8.

26. Carroll RG. The Integument. In: Carroll, R, editor. Elsevier's Integrated Physiology. St Louis, MO: Elsevier. 2007: 11–17.

27. Kapałczyńska M, Kolenda T, Przybyła W, Zajączkowska M, Teresiak A, Filas V, et al. 2D and 3D cell cultures – a comparison of different types of cancer cell cultures. Arch Med Sci. 2018; 14(4): 910–919.

28. Mirbagheri M, Adibnia V, Hughes BR, Waldman SD, Banquy X, Hwang DK. Advanced cell culture platforms: a growing quest for emulating natural tissues. Mater Horiz. 2019; 6: 45–71.

29. Duval K, Grover H, Han LH, Mou Y, Pegoraro AF, Fredberg J, et al. Modeling physiological events in 2D vs. 3D cell culture. Physiology. 2017; 13: 266–277.

30. Białkowska K, Komorowski P, Bryszewska M, Miłowska K. Spheroids as a type of three-dimensional cell cultures—examples of methods of preparation and the most important application. Int J Mol Sci. 2020; 21: 1–17.

31. Lei KF, Lin BY, Tsang NM. Real-time and label-free impedimetric analysis of the formation and drug testing of tumor spheroids formed via the liquid overlay technique. RSC Adv. 2017; 7(23): 13939–13946.

32. Huang S-W, Tzeng S-C, Chen J-K, Sun J-S, Lin F-H. A Dynamic Hanging-Drop System for Mesenchymal Stem Cell Culture. Int J Mol Sci. 2020; 21(12): 4298.

33. Edmondson R, Broglie JJ, Adcock AF, Yang L. Three-dimensional cell culture systems and their applications in drug discovery and cell-based biosensors. Assay Drug Dev Technol. 2014; 12: 207–218.

34. Hoffman AS. Hydrogels for biomedical applications. Adv Drug Deliv Rev. 2002 ;54(1):3–12.

35. Ahmed EM. Hydrogel: Preparation, characterization, and applications: A review. J

Adv Res. 2015; 6: 105–121.

36. Catoira MC, Fusaro L, Di Francesco D, Ramella M, Boccafoschi F. Overview of natural hydrogels for regenerative medicine applications. J Mater Sci Mater Med. 2019; 30(10): 115.

37. Martínez A, Blanco MD, Davidenko N, Cameron RE. Tailoring chitosan/collagen scaffolds for tissue engineering: Effect of composition and different crosslinking agents on scaffold properties. Carbohydr Polym. 2015; 132: 606–619.

38. Lin CC, Anseth KS. PEG hydrogels for the controlled release of biomolecules in regenerative medicine. Pharm Res. 2009; 26: 631–643.

39. Parlato M, Reichert S, Barney N, Murphy WL. Poly(ethylene glycol) hydrogels with adaptable mechanical and degradation properties for use in biomedical applications. Macromol Biosci. 2014; 14(5): 687–698.

40. Utech S, Boccaccini AR. A review of hydrogel-based composites for biomedical applications: enhancement of hydrogel properties by addition of rigid inorganic fillers. J Mat Sci. 2016; 51: 271–310.

41. Akhtar MF, Hanif M, Ranjha NM. Methods of synthesis of hydrogels … A review. Saudi Pharm J. 2016; 24: 554–559.

42. Desai ES, Tang MY, Ross AE, Gemeinhart RA. Critical factors affecting cell encapsulation in superporous hydrogels. Biomed Mater. 2012; 7(2): 024108–024108.

43. Giobbe GG, Crowley C, Luni C, Campinoti S, Khedr M, Kretzschmar K, et al. Extracellular matrix hydrogel derived from decellularized tissues enables endodermal organoid culture. Nat Commun. 2019; 10(1): 1–14.

44. An J, Teoh JEM, Suntornnond R, Chua CK. Design and 3D Printing of Scaffolds and Tissues. Engineering. 2015; 1(2): 261–268.

45. Henkel J, Hutmacher DW. Design and fabrication of scaffold-based tissue engineering. Bionanomaterials. 2013; 14(3–4): 171–193.

46. Marrazzo P, Maccari S, Taddei A, Bevan L, Telford J, Soriani M, et al. 3D Reconstruction of the Human Airway Mucosa In Vitro as an Experimental Model to Study NTHi Infections. PLoS One. 2016; 11(4): e0153985.

47. Terrence Brooks P, Rasmussen MA. Structural Analysis of Three-dimensional Human Neural Tissue derived from Induced Pluripotent Stem Cells. J Stem Cell Res Ther. 2016; 6(4): 1-7.

48. Ryu NE, Lee SH, Park H. Spheroid Culture System Methods and Applications for Mesenchymal Stem Cells. Cells. 2019; 8(12): 1620.

49. Ravi M, Paramesh V, Kaviya SR, Anuradha E, Paul Solomon FD. 3D cell culture systems: Advantages and applications. J Cell Physiol. 2015; 230(1): 16–26.

50. Fang Y, Eglen RM. Three-Dimensional Cell Cultures in Drug Discovery and Development. SLAS Discovery. 2017; 22: 456–472.

51. Zhang Z, Michniak-Kohn BB. Tissue engineered human skin equivalents. Pharmaceutics. 2012; 4: 26–41.

52. Salameh S, Tissot N, Cache K, Lima J, Suzuki I, Marinho PA, et al. A perfusable vascularized full-thickness skin model for potential topical and systemic applications. Biofabrication. 2021; 13(3): 1-17.

53. Li L, Fukunaga-Kalabis M, Herlyn M. The Three-Dimensional Human Skin Reconstruct Model: a Tool to Study Normal Skin and Melanoma Progression. J Vis Exp. 2011; (54): 2937.

54. Schmidt FF, Nowakowski S, Kluger PJ. Improvement of a Three-Layered in vitro Skin Model for Topical Application of Irritating Substances. Front Bioeng Biotechnol. 2020; 8: 388.

55. Bataillon M, Lelièvre D, Chapuis A, Thillou F, Autourde JB, Durand S, et al. Characterization of a new reconstructed full thickness skin model, t-skin™, and its application for investigations of anti-aging compounds. Int J Mol Sci. 2019; 20(9): 2240.

56. Russo B, Brembilla NC, Chizzolini C. Interplay Between Keratinocytes and Fibroblasts: A Systematic Review Providing a New Angle for Understanding Skin Fibrotic Disorders. Front Immunol. 2020; 11: 648.

57. MacNeil S. Progress and opportunities for tissue-engineered skin. Nature. 2007; 445: 874–880.

58. Mewes KR, Raus M, Bernd A, Zöller NN, Sättler A, Graf R. Elastin expression in a

newly developed full-thickness skin equivalent. Skin Pharmacol Physiol. 2007; 20(2): 85–95.

59. Juhl P, Bondesen S, Hawkins CL, Karsdal MA, Bay-Jensen A-C, Davies MJ, et al. Dermal fibroblasts have different extracellular matrix profiles induced by TGF-β, PDGF and IL-6 in a model for skin fibrosis. Sci Rep. 2020; 10(1): 17300.

60. Murad S, Grove D, Lindberg KA, Reynolds G, Sivarajah A, Pinnellt SR. Regulation of collagen synthesis by ascorbic acid (prolyl hydroxylation/lysyl hydroxylation/human skin fibroblasts). Biochemistry. 1981; 78(5): 2879–2882.

61. Prunieras M, Regnier M, Woodley D. Methods for cultivation of keratinocytes with an air-liquid interface. J Invest Dermatol. 1983; 81(1): S28–33.

62. Bikle DD, Xie Z, Tu CL. Calcium regulation of keratinocyte differentiation. Expert Rev Endocrinol Metab. 2012; 7: 461–472.

63. Muroyama A, Lechler T. Polarity and stratification of the epidermis. Semin Cell Dev Biol. 2012; 23: 890–896.

64. Andreadis ST, Hamoen KE, Yarmush ML, Morgan JR. Keratinocyte growth factor induces hyperproliferation and delays differentiation in a skin equivalent model system. FASEB J. 2001; 15(6): 898–906.

65. Blaimauer K, Watzinger E, Erovic BM, Martinek H, Jagersberger T, Thurnher D. Effects of Epidermal Growth Factor and Keratinocyte Growth Factor on the Growth of Oropharyngeal Keratinocytes in Coculture with Autologous Fibroblasts in a Three-Dimensional Matrix. Cells Tissues Organs. 2006; 182(2): 98–105.

66. Diggs J. Accumulative Waste Theory of Aging. In: Loue SJ, Sajatovic M, editors. Encycl Aging Public Heal. Boston, MA: Springer. 2008; 74–75.

67. Fu H, Li J, Du P, Jin W, Cui D. Metabolic wastes are removed by excretosomes, nanotubes and exophers in mouse HT22 cells through an autophagic vesicle clustering mechanism. bioRxiv. 2019; 699405.

68. Weiner ID, Mitch WE, Sands JM. Urea and Ammonia Metabolism and the Control of Renal Nitrogen Excretion. Clin J Am Soc Nephrol. 2015; 10(8): 1444–1458.

69. Tran DH, Wang Z V. Glucose Metabolism in Cardiac Hypertrophy and Heart Failure. J Am Heart Assoc. 2019; 8(12): e012673.

70. Kieninger J, Weltin A, Flamm H, Urban GA. Microsensor systems for cell metabolism-from 2D culture to organ-on-chip. Lab Chip. 2018; 18(9): 1274–1291.

71. Volkmer E, Drosse I, Otto S, Stangelmayer A, Stengele M, Kallukalam BC, et al. Hypoxia in static and dynamic 3D culture systems for tissue engineering of bone. Tissue Eng Part A. 2008; 14(8): 1331–1340.

72. Cueni LN, Detmar M. The Lymphatic System in Health and Disease. Lymphat Res Biol. 2008; 6(3–4): 109.

73. Intaglietta M, Johnson PC, Winslow RM. Microvascular and tissue oxygen distribution. Cardiovasc Res. 1996; 32: 632–643.

74. Jacob M, Chappell D, Becker BF. Regulation of blood flow and volume exchange across the microcirculation. Crit Care. 2016; 20(1): 319.

75. Ng CP, Hinz B, Swartz MA. Interstitial fluid flow induces myofibroblast differentiation and collagen alignment in vitro. J Cell Sci. 2005; 118(20): 4731–4739.

76. Fagerholm U, Lennernäs H. Experimental estimation of the effective unstirred water layer thickness in the human jejunum, and its importance in oral drug absorption. Eur J Pharm Sci. 1995; 3(5): 247–253.

77. Levitt MD, Strocchi A, Levitt DG. Human jejunal unstirred layer: evidence for extremely efficient luminal stirring. Am J Physiol. 1992; 262(3 Pt 1): G593-596.

78. Avdeef A, Nielsen PE, Tsinman O. PAMPA--a drug absorption in vitro model 11. Matching the in vivo unstirred water layer thickness by individual-well stirring in microtitre plates. Eur J Pharm Sci. 2004; 22(5): 365–374.

79. Itano T, Konno K, Inagaki T, Sugihara-Seki M. Estimating timescale of unstirred layer formation in osmotically driven flow. J Phys Commun. 2019; 3(1): 015007.

80. Thomson ABR, Dietschy JM. The Role of the Unstirred Water Layer in Intestinal Permeation. In: Csáky TZ, editor. Pharm Instest Perm II: Handb Exp Pharm. Berlin, Heidelberg: Springer. 1984; 165–269.

81. Schafer JA, Andreoli TE. Principles of Water and Nonelectrolyte Transport across Membranes. In: Andreoli TE, Hoffman JF, Fanestil DD, Schultz SG. Physiol Membr Disord. Boston, MA: Springer. 1986; 177–190.

82. Moradkhani H, Izadkhah MS, Anarjan N, Abdi A. Oxygen mass transfer and shear

stress effects on Pseudomonas putida BCRC 14365 growth to improve bioreactor design and performance. Environ Sci Pollut Res. 2017; 24(28): 22427–22441.

83. Zhiwei Z, Boyan S, Yang W. Mass transfer and shear stress in stirred bioreactor: A parameter method. Adv Sci Lett. 2012; 5(2): 701–704.

84. Rouwkema J, Koopman BFJM, Blitterswijk CAV, Dhert WJA, Malda J. Supply of nutrients to cells in engineered tissues. Biotechnol Genet Eng Rev. 2009; 26(1): 163–178.

85. Tramper J. Oxygen gradients in animal-cell bioreactors. Cytotechnology. 1995; 18(1–2): 27–34.

86. Alberti M, Dancik Y, Sriram G, Wu B, Teo YL, Feng Z, et al. Multi-chamber microfluidic platform for high-precision skin permeation testing. Lab Chip. 2017; 17(9): 1625–1634.

87. Zhong J-J, Fujiyama K, Seki T, Yoshida T. A quantitative analysis of shear effects on cell suspension and cell culture ofperilla frutescens in bioreactors. Biotechnol Bioeng. 1994; 44(5): 649–654.

88. Grein TA, Loewe D, Dieken H, Weidner T, Salzig D, Czermak P. Aeration and Shear Stress Are Critical Process Parameters for the Production of Oncolytic Measles Virus. Front Bioeng Biotechnol. 2019; 7: 78.

89. Dong X, Wang K. Prediction and simulation on the shear stress and mass transfer in perfused bioreactors I: Circular bioreactors. In: Chinese Control and Decision Conference 2008. CCDC. 2008; 4237–4242.

90. Schmid J, Schwarz S, Meier-Staude R, Sudhop S, Clausen-Schaumann H, Schieker M, et al. A perfusion bioreactor system for cell seeding and oxygen-controlled cultivation of three-dimensional cell cultures. Tissue Eng - Part C Methods. 2018; 24(10): 585–595.

91. Pedersen JM, Shim Y-S, Hans V, Phillips MB, Macdonald JM, Walker G, et al. Fluid Dynamic Modeling to Support the Development of Flow-Based Hepatocyte Culture Systems for Metabolism Studies. Front Bioeng Biotechnol. 2016; 4(SEP): 72.

92. Grayson W, Stephenson M. Recent advances in bioreactors for cell-based therapies. Research. 2018; 7: F1000.

93. Ahmed S, Chauhan VM, Ghaemmaghami AM, Aylott JW. New generation of bioreactors that advance extracellular matrix modelling and tissue engineering. Biotechnol Lett. 2019; 41: 1–25.

94. Mekala NK, Raju R. Review on bioreactors in tissue engineering. Biotechnol An Indian J. 2018; 5(4): 246-253.

95. Lei XH, Ning LN, Cao YJ, Liu S, Zhang SB, Qiu ZF, et al. Nasa-approved rotary bioreactor enhances proliferation of human epidermal stem cells and supports formation of 3d epidermis-like structure. PLoS One. 2011; 6(11): e26603.

96. Kim W-S. Cell Culture Bioreactors: Controls, Measurements, and Scale-Down Model. In: Manual of Industrial Microbiology and Biotechnology. ASM Press. 2014; 676–684.

97. O'Grady BJ, Wang JX, Faley SL, Balikov DA, Lippmann ES, Bellan LM. A Customizable, Low-Cost Perfusion System for Sustaining Tissue Constructs. SLAS Technol. 2018; 23(6): 592–598.

98. Huh D, Hamilton GA, Ingber DE. From 3D cell culture to organs-on-chips. Trends Cell Biol. 2011; 21: 745–754.

99. Wufuer M, Lee GH, Hur W, Jeon B, Kim BJ, Choi TH, et al. Skin-on-a-chip model simulating inflammation, edema and drug-based treatment. Sci Rep. 2016; 6(1): 1–12.

100. Strüver K, Friess W, Hedtrich S. Development of a Perfusion Platform for Dynamic Cultivation of in vitro Skin Models. Skin Pharmacol Physiol. 2017; 30(4): 180–189.

101. Helmedag MJ, Weinandy S, Marquardt Y, Baron JM, Pallua N, Suschek C V., et al. The effects of constant flow bioreactor cultivation and keratinocyte seeding densities on prevascularized organotypic skin grafts based on a fibrin scaffold. Tissue Eng - Part A. 2015; 21(1–2): 343–352.

102. Sriram G, Alberti M, Dancik Y, Wu B, Wu R, Feng Z, et al. Full-thickness human skin-on-chip with enhanced epidermal morphogenesis and barrier function. Mater Today. 2018; 21(4): 326–340.

103. Mori N, Morimoto Y, Takeuchi S. Perfusable and stretchable 3D culture system for skin-equivalent. Biofabrication. 2019; 11(1): 011001.

104. Luo HY, Ding CM, Zhou Y, Ye ZY. Effect of perfusion rate on growth and collagen production of human dermal fibroblasts in 3D scaffold. J East China Univ Sci Technol. 2012; 38(4): 465–471.

105. Hagedorn GM, Blank A, Mai R, Weiland B, Spassov A, Lauer G. Perfusion culture promotes differentiation of oral keratinocytes in vitro. J Physiol Pharmacol. 2009; 60(8): 25–29.

106. Liu JY, Hafner J, Dragieva G, Burg G. A Novel Bioreactor Microcarrier Cell Culture System for High Yields of Proliferating Autologous Human Keratinocytes. Cell Transplant. 2006; 15: 435–443.

107. Stoker M, O'Neill C, Berryman S, Waxman V. Anchorage and growth regulation in normal and virus-transformed cells. Int J Cancer. 1968; 3(5): 683–693.

108. Korin N, Bransky A, Dinnar U, Levenberg S. A parametric study of human fibroblasts culture in a microchannel bioreactor. Lab Chip. 2007; 7(5): 611–617.

109. Urbaczek AC, Leão PAGC, De Souza FZR, Afonso A, Vieira Alberice J, Cappelini LTD, et al. Endothelial Cell Culture Under Perfusion On A Polyester-Toner Microfluidic Device. Sci Reports. 2017; 7(1): 1–12.

110. Garziano A, Urciuolo F, Imparato G, Martorina F, Corrado B, Netti P. A micro-perfusion bioreactor for on line investigation of ECM remodeling under hydrodynamic and biochemical stimulation. Lab Chip. 2016; 16(5): 855–867.

111. Pfenniger A, Wong C, Sutter E, Cuhlmann S, Dunoyer-Geindre S, Mach F, et al. Shear stress modulates the expression of the atheroprotective protein Cx37 in endothelial cells. J Mol Cell Cardiol. 2012; 53(2): 299–309.

112. Mammoto A, Mammoto T, Ingber DE. Mechanosensitive mechanisms in transcriptional regulation. J Cell Sci. 2012; 125(13): 3061–3073.

113. Mackley JR, Ando J, Herzyk P, Winder SJ. Phenotypic responses to mechanical stress in fibroblasts from tendon, cornea and skin. Biochem J. 2006; 396(2): 307.

114. Ng CP, Swartz MA. Fibroblast alignment under interstitial fluid flow using a novel 3-D tissue culture model. Am J Physiol - Hear Circ Physiol. 2003; 284(5 53-5): 1771–1777.

115. Liass LA, Vasil'ev IM. Changes in the morphology and cytoskeleton of cultured

fibroblasts as a result of raised osmotic pressure. Bull Exp Biol Med. 1981; 92(8): 93-96.

116. Kimura S, Tsuchiya A, Ogawa M, Ono M, Suda N, Sekimoto K, et al. Tissue-scale tensional homeostasis in skin regulates structure and physiological function. Commun Biol. 2020; 3(1): 1–14.

117. Michels AJ, Frei B. Myths, artifacts, and fatal flaws: Identifying limitations and opportunities in vitamin C research. Nutrients. 2013; 5(12): 5161–5192.

118. Wilson JX. The physiological role of dehydroascorbic acid. FEBS Letters. 2002; 527: 5–9.

119. Pedraza CE, Chien YC, McKee MD. Calcium oxalate crystals in fetal bovine serum: Implications for cell culture, phagocytosis and biomineralization studies in vitro. J Cell Biochem. 2008; 103(5): 1379–1393.

120. Kwack M-H, Ahn J-S, Kim M-K, Kim J-C, Sung Y-K. Preventable effect of L-threonate, an ascorbate metabolite, on androgen-driven balding via repression of dihydrotestosteroneinduced dickkopf-1 expression in human hair dermal papilla cells. BMB Rep. 2010; 43(10): 688–692.

121. Robins SP, Milne G, Duncan A, Davies C, Butt R, Greiling D, et al. Increased skin collagen extractability and proportions of collagen type III are not normalized after 6 months healing of human excisional wounds. J Invest Dermatol. 2003; 121(2): 267–272.

122. Volk SW, Wang Y, Mauldin EA, Liechty KW, Adams SL. Diminished Type III Collagen Promotes Myofibroblast Differentiation and Increases Scar Deposition in Cutaneous Wound Healing. Cells Tissues Organs. 2011; 194(1): 25–37.

123. Abe S, Steinmann BU, Wahl LM, Martin GR. High cell density alters the ratio of type III to I collagen synthesis by fibroblasts. Nature. 1979; 279(5712): 442–444.

124. Eidet JR, Pasovic L, Maria R, Jackson CJ, Utheim TP. Objective assessment of changes in nuclear morphology and cell distribution following induction of apoptosis. Diagn Pathol. 2014;9 (1): 92.

125. Khatau SB, Hale CM, Stewart-Hutchinson PJ, Patel MS, Stewart CL, Searson PC, et al. A perinuclear actin cap regulates nuclear shape. Proc Natl Acad Sci U S A. 2009; 106(45): 19017.

126. Dahl KN, Kalinowski A, Pekkan K. Mechanobiology and the microcirculation: cellular, nuclear and fluid mechanics. Microcirculation. 2010; 17(3): 179.

127. Dalby MJ, Riehle MO, Yarwood SJ, Wilkinson CDW, Curtis ASG. Nucleus alignment and cell signaling in fibroblasts: Response to a micro-grooved topography. Exp Cell Res. 2003; 284(2): 272–280.

128. Kim JK, Louhghalam A, Lee G, Schafer BW, Wirtz D, Kim DH. Nuclear lamin A/C harnesses the perinuclear apical actin cables to protect nuclear morphology. Nat Commun. 2017; 8(1): 1–13.

129. Pfisterer K, Shaw LE, Symmank D, Weninger W. The Extracellular Matrix in Skin Inflammation and Infection. Front Cell Dev Biol. 2021; 9: 1578.

130. Tasanen K, Varpuluoma O, Nishie W. Dipeptidyl peptidase-4 inhibitor-associated bullous pemphigoid. Front Immunol. 2019; 10: 1238.

131. Gilchrest BA, Calhoun JK, Maciag T. Attachment and growth of human keratinocytes in a serum-free environment. J Cell Physiol. 1982; 112(2): 197–206.

132. Dawson RA, Goberdhan NJ, Freedlander E, MacNeil S. Influence of extracellular matrix proteins on human keratinocyte attachment, proliferation and transfer to a dermal wound model. Burns. 1996; 22(2): 93–100.

133. Bush KA, Downing BR, Walsh SE, Pins GD. Conjugation of extracellular matrix proteins to basal lamina analogs enhances keratinocyte attachment. J Biomed Mater Res A. 2007; 80(2): 444–452.

134. Ngo MA, Sinitsyna NN, Qin Q, Rice RH. Oxygen-Dependent Differentiation of Human Keratinocytes. J Invest Dermatol. 2007; 127(2): 354–361.

135. Breitkrutz, D., Boukamp, P., Lueder, M., Fusenig NE. Morphological and biochemical criteria for keratinization in primary and permanent mouse epidermal cell cultures. Front Matrix Biol. 1981; 9: 57–82.

136. Florin L, Maas-Szabowski N, Werner S, Szabowski A, Angel P. Increased keratinocyte proliferation by JUN-dependent expression of PTN and SDF-1 in fibroblasts. J Cell Sci. 2005; 118(9): 1981–1989.

137. Smola H, Thiekotter G, Fusenig NE. Mutual induction of growth factor gene expression by epidermal-dermal cell interaction. J Cell Biol. 1993; 122(2): 417–429.

138. Bernard FX, Morel F, Camus M, Pedretti N, Barrault C, Garnier J, et al. Keratinocytes under Fire of Proinflammatory Cytokines: Bona Fide Innate Immune Cells Involved in the Physiopathology of Chronic Atopic Dermatitis and Psoriasis. J Allergy. 2012;2012: 718725.

139. Jevtić M, Löwa A, Nováčková A, Kováčik A, Kaessmeyer S, Erdmann G, et al. Impact of intercellular crosstalk between epidermal keratinocytes and dermal fibroblasts on skin homeostasis. Biochim Biophys Acta - Mol Cell Res. 2020; 1867(8): 118722.

140. Puccinelli TJ, Bertics PJ, Masters KS. Regulation of keratinocyte signaling and function via changes in epidermal growth factor presentation. Acta Biomater. 2010; 6(9): 3415–3425.

141. Bernstam LI, Vaughan FL, Bernstein IA. Keratinocytes grown at the air-liquid interface. In Vitro Cell Dev Biol. 1986; 22(12): 695–705.

142. Borowiec AS, Delcourt P, Dewailly E, Bidaux G. Optimal Differentiation of In Vitro Keratinocytes Requires Multifactorial External Control. PLoS One. 2013; 8(10): e77507.

143. Marionnet C, Vioux-Chagnoleau C, Pierrard C, Sok J, Asselineau D, Bernerd F. Morphogenesis of dermal–epidermal junction in a model of reconstructed skin: beneficial effects of vitamin C. Exp Dermatol. 2006; 15(8): 625–633.

144. Bagi Z, Csekó C, Tóth E, Koller A. Oxidative stress-induced dysregulation of arteriolar wall shear stress and blood pressure in hyperhomocysteinemia is prevented by chronic vitamin C treatment. Am J Physiol Heart Circ Physiol. 2003; 285(6): H2277-2283.

145. Biggs LC, Kim CS, Miroshnikova YA, Wickström SA. Mechanical Forces in the Skin: Roles in Tissue Architecture, Stability, and Function. J Invest Dermatol. 2020; 140(2): 284–290.

146. Bhatia SN, Ingber DE. Microfluidic organs-on-chips. Nat Biotechnol. 2014; 32(8): 760–772.

147. Rothbauer M, Zirath H, Ertl P. Recent advances in microfluidic technologies for cell-to-cell interaction studies. Lab Chip. 2018; 18(2): 249–270.

148. Carlson MW, Alt-Holland A, Egles C, Garlick JA. Three-Dimensional Tissue Models of Normal and Diseased Skin. Curr Protoc Cell Biol. 2008; 19(1):Unit 19.9.

149. Gibbs S, Pinto ANS, Murli S, Huber M, Hohl D, Ponec M. Epidermal growth factor and keratinocyte growth factor differentially regulate epidermal migration, growth, and differentiation. Wound Repair Regen. 2000; 8(3): 192–203.

150. Schimek K, Hsu HH, Boehme M, Kornet JJ, Marx U, Lauster R, et al. Bioengineering of a full-thickness skin equivalent in a 96-well insert format for substance permeation studies and organ-on-a-chip applications. Bioengineering. 2018; 5(2): 43.

151. Glaum R, Wiedmann-Al-Ahmad M, Huebner U, Schmelzeisen R. Tissue engineering of composite grafts: Cocultivation of human oral keratinocytes and human osteoblast-like cells on laminin-coated polycarbonate membranes and equine collagen membranes under different culture conditions. J Biomed Mater Res - Part A. 2010; 93(2): 704–715.

152. Zoio P, Ventura S, Leite M, Oliva A. Pigmented Full-Thickness Human Skin Model Based on a Fibroblast-Derived Matrix for Long-Term Studies. Tissue Eng - Part C Methods. 2021; 27(7): 433–443.

153. Zhang L. Keratins in Skin Epidermal Development and Diseases. In: Blumenberg M, editor. Keratin. London: IntechOpen. 2018.

154. Reichelt J. Mechanotransduction of keratinocytes in culture and in the epidermis. Eur J Cell Bio. 2007; 86(11–12): 807–816.

155. Alam H, Sehgal L, Kundu ST, Dalal SN, Vaidya MM. Novel function of keratins 5 and 14 in proliferation and differentiation of stratified epithelial cells. Mol Biol Cell. 2011; 22(21): 4068.

156. Stark HJ, Boehnke K, Mirancea N, Willhauck MJ, Pavesio A, Fusenig NE, et al. Epidermal Homeostasis in Long-Term Scaffold-Enforced Skin Equivalents. J Investig Dermatology Symp Proc. 2006; 11(1): 93–105.

157. Van Gele M, Geusens B, Brochez L, Speeckaert R, Lambert J. Three-dimensional skin models as tools for transdermal drug delivery: Challenges and limitations. Expert Opin Drug Deliv. 2011; 8(6): 705–720.

158. Yeste J, Illa X, Alvarez M, Villa R. Engineering and monitoring cellular barrier models. J Biol Eng. 2018; 12: 18.

159. Mieremet A, Rietveld M, Absalah S, Van Smeden J, Bouwstra JA, El Ghalbzouri A. Improved epidermal barrier formation in human skin models by chitosan modulated

dermal matrices. PLoS One. 2017; 12(3): e0174478.

160. Honari G, Maibach H. Skin Structure and Function. Appl Dermatotoxic. 2014; 1–10.

161. Madison KC. Barrier Function of the Skin: “La Raison d’Être” of the Epidermis. J Invest Dermatol. 2003; 121(2): 231–241.

162. Freeman SC, Sonthalia S. Histology, Keratohyalin Granules. StatPearls. 2021.

163. Akiyama M. Corneocyte lipid envelope (CLE), the key structure for skin barrier function and ichthyosis pathogenesis. J Dermatol Sci. 2017; 88(1): 3–9.

164. Kalyanaraman B, Supp DM, Boyce ST. Medium flow rate regulates viability and barrier function of engineered skin substitutes in perfusion culture. Tissue Eng Part A. 2008; 14(5): 583–593.

165. Mildner M, Jin J, Eckhart L, Kezic S, Gruber F, Barresi C, et al. Knockdown of filaggrin impairs diffusion barrier function and increases UV sensitivity in a human skin model. J Invest Dermatol. 2010; 130(9): 2286–2294.

166. Scharschmidt TC, Man MQ, Hatano Y, Crumrine D, Gunathilake R, Sundberg JP, et al. Filaggrin deficiency confers a paracellular barrier abnormality that reduces inflammatory thresholds to irritants and haptens. J Allergy Clin Immunol. 2009; 124(3): 496-506.

167. Indra AK, Leid M. Epidermal Permeability Barrier Measurement in Mammalian Skin. Methods Mol Biol. 2011; 763: 73–81.

168. Rosser J, Thomas DJ. Bioreactor processes for maturation of 3D bioprinted tissue. 3D Bioprinting Reconstr Surg Tech Appl. 2018; 191–215.

169. Yankaskas CL, Bera K, Stoletov K, Serra SA, Carrillo-Garcia J, Tuntithavornwat S, et al. The fluid shear stress sensor TRPM7 regulates tumor cell intravasation. Sci Adv. 2021; 7(28): eabh3457.

170. Mackley JR, Ando J, Herzyk P, Winder SJ. Phenotypic responses to mechanical stress in fibroblasts from tendon, cornea and skin. Biochem J. 2006; 396(2): 307.

171. Shi ZD, Mathura RA, Garanich JS, Abraham G, Tarbell JM. Shear stress plays a role in differentiation and migration of adventitial fibroblasts. Proc IEEE Annu Northeast Bioeng Conf NEBEC. 2007; 205–206.

172. Roux E, Bougaran P, Dufourcq P, Couffinhal T. Fluid Shear Stress Sensing by the Endothelial Layer. Front Physiol. 2020; 11: 861.

173. Kawamura A, Aoyama Y. Immunofluorescence in medical science. Berlin: Springer. 1983; 262.

174. Mahmood T, Yang PC. Western blot: Technique, theory, and trouble shooting. N Am J Med Sci. 2012; 4(9): 429.

175. Karl F, Wußmann M, Kreß L, Malzacher T, Fey P, Groeber-Becker F, et al. Patient-derived in vitro skin models for investigation of small fiber pathology. Ann Clin Transl Neurol. 2019; 6(9): 1797–1806.

176. Nomura S. Identification, Friend or Foe: Vimentin and α-Smooth Muscle Actin in Cancer-Associated Fibroblasts. Ann Surg Oncol 2019 2613. 2019; 26(13): 4191–4192.

177. De Brugerolle De Fraissinette A, Picarles V, Chibout S, Kolopp M, Medina J, Burtin P, et al. Predictivity of an in vitro model for acute and chronic skin irritation (SkinEthic) applied to the testing of topical vehicles. Cell Biol Toxicol. 1999; 15(2): 121–135.

178. Schlotmann K, Kaeten M, Black AF, Damour O, Waldmann-Laue M, Förster T. Cosmetic efficacy claims in vitro using a three-dimensional human skin model. Int J Cosmet Sci. 2001; 23(5): 309–318.